

Copyright
by
Ion Garate
2009

The Dissertation Committee for Ion Garate
certifies that this is the approved version of the following dissertation:

**Nonequilibrium Order Parameter Dynamics in Spin
and Pseudospin Ferromagnets**

Committee:

Allan H. MacDonald, Supervisor

James Chelikowsky

Alex Demkov

Gregory Fiete

Maxim Tsoi

**Nonequilibrium Order Parameter Dynamics in Spin
and Pseudospin Ferromagnets**

by

Ion Garate, B.S.

DISSERTATION

Presented to the Faculty of the Graduate School of

The University of Texas at Austin

in Partial Fulfillment

of the Requirements

for the Degree of

DOCTOR OF PHILOSOPHY

THE UNIVERSITY OF TEXAS AT AUSTIN

August 2009

Dedicated to cancer survivors and their caregivers.

*Oh heart, if one should say to you that the soul perishes like the body, answer
that the flower withers, but the seed remains. (Khalil Gibran)*

Acknowledgments

It was Spring 2006 and as a newly diagnosed cancer patient I was harboring serious doubts on whether I would ever resume my work towards a doctorate. Three years later I am elated to bring this dissertation to completion. Yet above all I am grateful that I have had the opportunity to live and enjoy life as never before.

On the academic side, I first and foremost thank my advisor Allan MacDonald. His insightful thinking, sharp intuition and encyclopedic knowledge are all the more inspiring as he delivers them with his signature modesty and generosity.

I have been fortunate to collaborate with and learn from Keith Gilmore, Tomas Jungwirth, Jairo Sinova and Mark Stiles. Visits to beautiful Prague and Washington D.C. were pleasant byproducts of our scientific overlaps.

Throughout the years, my education in condensed matter physics has benefited enormously from courses taught by James Chelikowsky, James Erskine, Gregory Fiete, Allan MacDonald, Qian Niu, Maxim Tsoi and Emanuel Tutuc. I also acknowledge Alex Demkov for taking the time to join my dissertation committee.

I am grateful to my numerous groupmates for their collegiality over the last six years. I have been honored by Hongki Min's brotherly advice

and friendship. Joseph Wang's perennial smile and open spirit are infectious. It was always a pleasure to discuss physics with the omniscient Wei-Cheng Lee. Jeil Jung has been a companion for interesting philosophical dialogue and sweaty squash games.

Becky Drake is not only the most competent secretary I know, but also the nicest. Likewise Annie Harding, Carol Noriega and Olga Vorloou have provided crucial assistance with paperwork.

Aitor Bergara was largely responsible for my coming to Texas as an undergraduate exchange student in Summer 2002. He was a gentle and encouraging guide during the bureaucratic difficulties that plagued my first months here. Mina Dadgar was the irresistibly sassy girl who catalyzed my decision to pursue graduate studies in Austin. While our paths have diverged since then, our friendship shall live on. I thank Bahniman Ghosh for distracting me from my problems by presenting his. At times we were two broken branches that supported each other with dignity and humor. I retain very fond memories of the daily, shine-or-rain walks that I shared with Hyojin Han during Summer 2006. Anukal Chiralaksanakul, Abe Dunn, Mukremin Kilic, Khalid Miah, Jennifer Ramirez and Dave Yong are some of the fellow College Houses co-ops who unbeknownst to them have shaped my views of the world in the course of joyful conversations and meals. Azkenik, ezin ditxut ahaztu Euskal Herriko Unibertsitateko ikaskidiak, Elgoibarko lagunak, ta bereziki hurbileko senidiak: lan hau zuek ereindako hazixan fruitua da.

Nonequilibrium Order Parameter Dynamics in Spin and Pseudospin Ferromagnets

Publication No. _____

Ion Garate, Ph.D.

The University of Texas at Austin, 2009

Supervisor: Allan H. MacDonald

Research on spintronics has galvanized the design of new devices that exploit the electronic spin in order to augment the performance of current microelectronic technologies. The successful implementation of these devices is largely contingent on a quantitative understanding of nonequilibrium magnetism in conducting ferromagnets. This thesis is largely devoted to expanding the microscopic theory of magnetization relaxation and current-induced spin torques in transition metals ferromagnets as well as in (III,Mn)V dilute magnetic semiconductors.

We start with two theoretical studies of the Gilbert damping in electric equilibrium, which treat disorder exactly and include atomic-scale spatial inhomogeneities of the exchange field. These studies enable us to critically review the accuracy of the conventional expressions used to evaluate the Gilbert damping in transition metals.

We follow by generalizing the calculation of the Gilbert damping to current-carrying steady states. We find that the magnetization relaxation changes in presence of an electric current. We connect this change with the non-adiabatic spin transfer torque parameter, which is an elusive yet potentially important quantity of nonequilibrium magnetism. This connection culminates in a concise analytical expression that will lead to the first *ab initio* estimates of the non-adiabatic spin transfer torque in real materials.

Subsequently we predict that in gyrotropic ferromagnets the magnetic anisotropy can be altered by a *dc* current. In these systems spin-orbit coupling, broken inversion symmetry and chirality conspire to yield current-induced spin torques even for uniform magnetic textures. We thus demonstrate that a transport current can switch the magnetization of strained (Ga,Mn)As.

This thesis concludes with the transfer of some fundamental ideas from nonequilibrium magnetism into the realm of superconductors, which may be viewed as easy-plane ferromagnets in the particle-hole space. We emphasize on the analogies between nonequilibrium magnetism and superconductivity, which have thus far been studied as completely separate disciplines. Our approach foreshadows potentially new effects in superconductors.

Table of Contents

Acknowledgments	v
Abstract	vii
List of Figures	xii
Chapter 1. Introduction	1
1.1 Equilibrium Magnetism and Superconductivity	4
1.2 Nonequilibrium Magnetism and Superconductivity	7
1.3 Outline	9
Chapter 2. Theory of Gilbert Damping in Conducting Ferromagnets I: Kohn-Sham Theory.	12
2.1 Introduction	13
2.2 Many-Body Transverse Response Function and the Gilbert Damping Parameter	15
2.3 SDF-Stoner Theory Expression for Gilbert Damping	19
2.4 Discussion	25
2.5 Conclusions	28
Chapter 3. Theory of Gilbert Damping in Conducting Ferromagnets II: Disorder Vertex Corrections	29
3.1 Introduction	29
3.2 Gilbert Damping and Transverse Spin Response Function	31
3.2.1 Realistic SDFT <i>vs.</i> s-d and p-d models	31
3.2.2 Disorder Perturbation Theory	33
3.2.3 Evaluation of Impurity Vertex Corrections for Multi-Band Models	35
3.3 Gilbert Damping for a Magnetic 2DEG	37
3.4 Gilbert Damping for (Ga,Mn)As	45

3.5	Assessment of the torque-correlation formula	49
3.6	Conclusions	57
Chapter 4. Non-Adiabatic Spin Transfer Torque in Real Materials		58
4.1	Introduction	59
4.2	Microscopic Theory of α , β and v_s	64
4.3	Non-Adiabatic STT for the Parabolic Two-Band Ferromagnet	76
4.4	Non-Adiabatic STT for a Magnetized Two-Dimensional Electron Gas	79
4.5	Non-Adiabatic STT for (Ga,Mn)As	80
4.6	α/β in real materials	82
4.7	Torque-Correlation Formula for the Non-Adiabatic STT . .	88
4.8	Connection to the Effective Field Model	92
4.9	Summary and Conclusions	99
Chapter 5. Influence of a Transport Current on Magnetic Anisotropy in Gyrotropic Ferromagnets		101
5.1	Introduction	101
5.2	Theory of the Ferromagnetic Inverse Spin-Galvanic Effect . .	104
5.3	Current-Driven Magnetization Reversal in Monodomain (Ga,Mn)As	121
5.4	Summary and Conclusions	132
Chapter 6. Landau-Lifshitz-Slonczewski Equation Approach to Nonequilibrium Superconductivity		135
6.1	Basics of Nonequilibrium Superconductivity	136
6.2	Theories of Nonequilibrium Superconductivity	142
6.2.1	Time-Dependent Ginzburg-Landau Theory	142
6.2.2	Kinetic Equation Approach	144
6.2.3	Keldysh Green's Function Method	145
6.3	LLS Equation Approach to Superconductivity	148
6.4	Adiabatic Pseudospin Transfer Torques	160
6.5	Pseudospin Relaxation in Superconductors	164
6.6	Non-Adiabatic Pseudospin Transfer Torque	170

6.7	Thermal Doppler Shift of Pseudospin Waves	171
6.8	Thermal Pseudospin-Galvanic Effects	175
6.9	“Quasiparticle Spin Imbalance” in Spiral Magnets	180
6.10	Summary and Conclusions	183
Chapter 7. Conclusions		185
Appendices		188
Appendix A.	Quadratic Spin Response to an Electric and Mag-	
	netic Field	189
Appendix B.	First order impurity vertex correction	192
Appendix C.	Derivation of Eq. (4.26)	195
Bibliography		198
Vita		212

List of Figures

3.1	Dyson equation for the renormalized vertex of the transverse spin-spin response function. The dotted line denotes impurity scattering.	34
3.2	M2DEG: Gilbert damping in the absence of spin-orbit coupling. When the intrinsic spin-orbit interaction is small, the 1st vertex correction is sufficient for the evaluation of Gilbert damping, provided that the ferromagnet’s exchange splitting is large compared to the lifetime-broadening of the quasiparticle energies. For more disordered ferromagnets ($E_F\tau_0 < 5$ in this figure) higher order vertex corrections begin to matter. In either case vertex corrections are significant. In this figure $1/\tau_0$ stands for the scattering rate off spin-independent impurities, defined as a two-band average at the Fermi energy, and the spin-dependent and spin-independent impurity strengths are chosen to satisfy $u^0 = 3u^z$	40
3.3	M2DEG: Gilbert damping for strong SO interactions ($\lambda k_F = 1.2E_F \simeq 4\Delta_0$). In this case higher order vertex corrections matter (up to 20 %) even at low disorder. This suggests that higher order vertex corrections will be important in real ferromagnetic semiconductors because their intrinsic SO interactions are generally stronger than their exchange splittings.	41
3.4	M2DEG: Gilbert damping for moderate SO interactions ($\lambda k_F = 0.2\Delta_0$). In this case there is a crossover between the intra-band dominated and the inter-band dominated regimes, which gives rise to a non-monotonic dependence of Gilbert damping on disorder strength. The stronger the intrinsic SO relative to the exchange field, the higher the value of disorder at which the crossover occurs. This is why the damping is monotonically increasing with disorder in Fig. (3.2) and monotonically decreasing in Fig. (3.3).	42

3.5	<p>GaMnAs: Higher order vertex corrections make a significant contribution to Gilbert damping, due to the prominent spin-orbit interaction in the band structure of GaAs. x is the Mn fraction, and p is the hole concentration that determines the Fermi energy E_F. In this figure, the spin-independent impurity strength u^0 was taken to be 3 times larger than the magnetic impurity strength u^z. $1/\tau_0$ corresponds to the scattering rate off Coulomb impurities and is evaluated as a four-band average at the Fermi energy.</p>	47
3.6	<p>GaMnAs: When the spin-orbit splitting is reduced (in this case by reducing the hole density to $0.2nm^{-3}$ and artificially taking $\gamma_3 = 0.5$), the crossover between inter- and intra-band dominated regimes produces a non-monotonic shape of the Gilbert damping, much like in Fig. (3.4). When either γ_2 or p is made larger or x is reduced, we recover the monotonic decay of Fig.(3.5).</p>	48
3.7	<p>M2DEG: Comparison of Gilbert damping predicted using spin-flip and torque matrix element formulas, as well as the exact vertex corrected result. In this figure the intrinsic spin-orbit interaction is relatively weak ($\lambda k_F = 0.05E_F \simeq 0.06\Delta_0$) and we have taken $u^z = 0$. The torque correlation formula does not distinguish between spin-dependent and spin-independent disorder.</p>	52
3.8	<p>M2DEG: Comparison of Gilbert damping predicted using spin-flip and torque matrix element formulas, as well as the exact vertex corrected result. In this figure the intrinsic spin-orbit interaction is relatively strong ($\lambda k_F = 0.5E_F = 5\Delta_0$) and we have taken $u^z = 0$</p>	53
3.9	<p>GaMnAs: Comparison of Gilbert damping predicted using spin-flip and torque matrix element formulas, as well as the exact vertex corrected result. p is the hole concentration that determines the Fermi energy E_F and x is the Mn fraction. Due to the strong intrinsic SO, this figure shows similar features as Fig.(3.8).</p>	55
3.10	<p>GaMnAs: Comparison of Gilbert damping predicted using spin-flip and torque matrix element formulas, as well as the exact vertex corrected result. In relation to Fig. (3.9) the effective spin-orbit interaction is stronger, due to a larger p and a smaller x.</p>	56

4.1	Feynman diagrams for (a) α and (b) $\beta(\mathbf{q} \cdot \mathbf{v}_s)$, the latter with a heuristic consideration of the electric field (for a more rigorous treatment see Appendix A). Solid lines correspond to Green's functions of the band quasiparticles in the Born approximation, dashed lines stand for the magnon of frequency ω and wavevector \mathbf{q} , ω_n is the Matsubara frequency and $eV_{a,b}$ is the difference in the transport deviation energies.	75
4.2	M2DEG : inter-band contribution, intra-band contribution and the total non-adiabatic STT for a magnetized two-dimensional electron gas (M2DEG). In this figure the exchange field dominates over the spin-orbit splitting. At higher disorder the inter-band part (proportional to resistivity) dominates, while at low disorder the inter-band part (proportional to conductivity) overtakes. For simplicity, the scattering time τ is taken to be the same for all sub-bands.	81
4.3	GaMnAs : $\beta^{(0)}$ for \mathbf{E} perpendicular to the easy axis of magnetization (\hat{z}). x and p are the Mn fraction and the hole density, respectively. The intra-band contribution is considerably larger than the inter-band contribution, due to the strong intrinsic spin-orbit interaction. Since the 4-band model typically overestimates the influence of intrinsic spin-orbit interaction, it is likely that the dominion of intra-band contributions be reduced in the more accurate 6-band model. By evaluating β for $\mathbf{E} \parallel \hat{z}$ (not shown) we infer that it does not depend significantly on the relative direction between the magnetic easy axis and the electric field.	83
4.4	Comparison of α and β in (Ga,Mn)As for $x = 0.08$ and $p = 0.4nm^{-3}$. It follows that $\beta/\alpha \simeq 8$, with a weak dependence on the scattering rate off impurities. If we use the torque correlation formula (Section VII), we obtain $\beta/\alpha \simeq 10$	87
4.5	M2DEG : comparing S and K matrix element expressions for the non-adiabatic STT formula in the weakly spin-orbit coupled regime. Both formulations agree in the clean limit, where the intra-band contribution is dominant. In more disordered samples inter-band contributions become more visible and S and K begin to differ; the latter is known to be more accurate in the weakly spin-orbit coupled regime.	89
4.6	M2DEG : In the strongly spin-orbit coupled limit the intra-band contribution reigns over the inter-band contribution and accordingly S and K matrix element expressions display a good (excellent in this figure) agreement. Nevertheless, this agreement does not guarantee quantitative reliability, because for strong spin-orbit interactions impurity vertex corrections may play an important role.	90

4.7	<p>GaMnAs: comparison between S and K matrix element expressions for $\mathbf{E} \perp \hat{z}$. The disagreement between both formulations stems from inter-band transitions, which are less important as τ increases. Little changes when $\mathbf{E} \parallel \hat{z}$.</p>	92
5.1	<p>Feynman diagram that encodes the transverse spin density induced by a current (ferromagnetic ISGE effect) which results in a change in the steady-state magnetization direction. a and b are band labels for the quasiparticle and the quasihole.</p>	107
5.2	<p>Cartoon of a magnetic thin film (shaded area). The exchange field Δ is an effective magnetic field which is parallel to the magnetization only when it points along easy or hard crystalline directions. The orientation of Δ can be specified by the polar and azimuthal angles θ and ϕ. The relationship between the direction of Δ and the direction of magnetization is altered by an electric current in gyrotropic ferromagnets.</p>	111
5.3	<p>Spin response to a transverse magnetic field \mathbf{B}_\perp in the presence of a current: perturbation theory to all orders in \mathbf{B}_\perp. The quasiparticles (quasiholes) in these diagrams diagonalize a Hamiltonian whose exchange field is pointing along an easy direction and \mathbf{B}_\perp is by definition perpendicular to this easy direction. Provided that in Eq. (5.10) we take the exact eigenstates of the mean field Hamiltonian (within which the exchange field need not be pointing along an easy direction), all the diagrams of this figure are implicit in the diagram of Fig. (5.1). In particular, the ferromagnetic ISGE captures the influence of currents on ferromagnetic resonance.</p>	116
5.4	<p>Equilibrium anisotropy field (meV per spin) in (Ga,Mn)As for $\phi = 0$, and $\theta \in (0, \pi)$. The parameters used for this calculation were: Mn fraction $x = 0.08$, hole concentration $p \simeq 0.15\text{nm}^{-3}$, $\epsilon_{F\tau} = 3$, and axial strain $\epsilon_{\text{ax}} = -0.5\%$. These anisotropy field results were evaluated using the model explained in the text.</p>	122
5.5	<p>Equilibrium anisotropy field (meV per spin) in (Ga,Mn)As for $\theta = \pi/2$ and $\phi \in (0, \pi)$. The parameters are: Mn fraction $x = 0.08$, hole concentration $p \simeq 0.15\text{nm}^{-3}$, $\epsilon_{F\tau} = 3$, and axial strain $\epsilon_{\text{ax}} = -0.5\%$. These results were evaluated using the model explained in the text. Due to strain, the in-plane anisotropy is notably weaker than the out-of-plane anisotropy represented in the previous figure.</p>	123

- 5.6 Change in the magnetic anisotropy field of (Ga,Mn)As (in meV per spin) due to the inverse spin-galvanic effect, for an electric field of 1mV/nm along [010]. The parameters are: Mn fraction $x = 0.08$, hole concentration $\simeq 0.25\text{nm}^{-3}$, $\epsilon_F\tau = 2$, and axial strain $\epsilon_{\text{ax}} = -1\%$. We compare between interband and intraband contributions: in contrast to the case of good metals, the interband contributions are not negligible in (Ga,Mn)As. For the present case, had we neglected the interband contribution the minimum electric field needed to reorient the magnetization by 90° would be off by approximately 20 %. The sum of interband and intraband pieces gives rise to a smooth curve that reflects the Dresselhaus symmetry of the axial strain. Reversing the sign of the axial strain (i.e. making it tensile) leads to a sign reversal of δH_ϕ 124
- 5.7 Reorientation of the magnetization due to an electric current. An initial magnetization along [100] can be rotated (assisted by damping) into [010] by applying a sufficiently strong electric field with a nonzero projection along the [010] direction (a current along [100] would not destabilize the [100] easy axis). For the parameters of this figure ($x = 0.08$, $p \simeq 0.15\text{nm}^{-3}$, $\epsilon_F\tau = 3$, $\epsilon_{\text{ax}} = -0.5\%$) the critical electric field is $\simeq 5\text{mV/nm}$, which corresponds roughly to a critical current density of $5 \times 10^7\text{A/cm}^2$. 125
- 5.8 Dependence of the critical electric field (at which the magnetization gets reoriented by 90°) on (compressive) axial strain. The critical current is (roughly) inversely proportional to ϵ_{ax} . The reason behind this relationship is that the equilibrium, *azimuthal* anisotropy is largely indifferent to ϵ_{ax} . For $x = 0.04$ and $\epsilon_{\text{ax}} = -2\%$ we find $E_c \simeq 0.25\text{mV/nm}$, which corresponds to a critical current on the order of 10^6A/cm^2 . These results are for a (Ga,Mn)As model with carrier density $p \simeq 0.15\text{nm}^{-3}$ and $\epsilon_F\tau = 3$ 128
- 6.1 Two superconducting wires are separated by a thin insulating layer. One of the wires is placed under a uniform temperature gradient. According to Eq. (6.53), biasing this wire with a current I is akin to applying an electrochemical potential difference between the two wires, which will spearhead *ac* Josephson currents between them. 163

6.2	Integration contours in the complex plane for the Matsubara summations required by the microscopic evaluation of transverse spin response functions. In normal metals (a), the disorder self energy is given by $i/(2\tau)Im[z]$, where z stand for the complex frequency. This leads to a branch cut for $Im[z] = 0$ (there is an additional cut at $Im[z] = -i\omega$ where ω is the frequency of the external perturbation). In a superconductor (b), the disorder self energy has an additional factor of $1/\sqrt{z^2 - \Delta^2}$, which alters the structure of the branches.	166
6.3	Gilbert damping for a pseudospin ferromagnet as a function of the non-magnetic impurity scattering rate. We take a temperature that is a third of the superconducting gap, and for simplicity we consider a one-dimensional superconductor. For $\alpha_{z,z}$, we find breathing-Fermi-surface type behavior with the damping decreasing monotonically as disorder becomes more pronounced. While we expect $\alpha_{y,y} = 0$ on physical grounds, our numerical results show that $\alpha_{y,y}$ has a residual nonzero value that originates from interband transitions (it is easy to see that intraband contributions vanish); these residual terms remain even when we include impurity vertex corrections. We thus associate the numerical value of $\alpha_{y,y}$ with the uncertainty/error of our calculation.	167
6.4	Non-adiabatic pseudospin transfer torque coefficient as a function of disorder. We take $T = \Delta/3$. The intraband contributions dominate over interband contributions and accordingly β grows linearly with the quasiparticle lifetime. We find that β is several orders of magnitude larger than α	170
6.5	Quasiparticle charge imbalance induced by a temperature gradient in a current-carrying superconductor, as a function of the scattering rate from impurities.	180
A.1	Feynman diagram for $\chi_{S,S,j}$. The dashed lines correspond to magnons, whereas the wavy line represents a photon.	191
B.1	Feynman diagram for the first order vertex correction. The dotted line with a cross represents the particle-hole correlation mediated by impurity scattering.	192

Chapter 1

Introduction

In principle, all physical properties of solids are determined by the behavior of their fundamental constituents, namely ions ¹ and valence electrons. ² This reductionist viewpoint has been vindicated by the fruitful characterization of condensed matter systems gained from studying the correlations ³ between the elementary constituents. In crystalline solids, ions optimize Coulomb interactions by arranging themselves in predictable periodic arrays. Their small but inevitable excursions away from equilibrium positions are likewise readily described in terms of spinless harmonic modes (phonons). ⁴ In contrast, valence electrons are organized in relatively intricate patterns that are sensitive to their spins by virtue of Pauli's exclusion principle. ⁵ In fact, understanding the behavior of these electrons along with the exotic phenomena they give rise to is the most challenging quest of quantum condensed matter

¹Ions consist of atomic nuclei plus some tightly bound core electrons that do not change appreciably when atoms are brought together to form a solid

²These electrons are relatively delocalized and not attached to any particular ion. Unless otherwise stated valence electrons will be referred to simply as electrons

³The sources of the correlations are the charge and spin of the ions and electrons.

⁴Provided that the temperature is low compared to the melting temperature of the crystal.

⁵Ions too may have half-integer spins; however, the Pauli exclusion principle plays no role in determining their equilibrium configuration because the wavefunctions of different ions do not overlap significantly.

physics.

The quantum mechanical equation of motion for 10^{23} interacting electrons in a periodic lattice of ions is simple to write, yet impossible to solve exactly. Fortunately, insofar as low-temperature electronic properties are concerned, ⁶ it is often possible[1] to map the insoluble problem of interacting electrons into a soluble problem of nearly-independent *elementary excitations*. Elementary excitations are grouped into quasiparticles and collective modes. A quasiparticle can be viewed as a fictitious particle which consists of an electron coupled to a cloud of other electrons or ions; this cloud renormalizes the effective mass of the original electron and makes its lifetime finite. Collective modes such as plasmons (charge oscillations) and magnons (spin precession) describe the synchronized motion or dynamics of a group of quasiparticles. ⁷ The description of an interacting electron system in terms of elementary excitations requires that the latter be sufficiently long-lived. Landau's Fermi liquid theory guarantees the fulfillment of this requirement for most common materials. Nevertheless, there exist interesting systems[2] where the concept of elementary excitation is altogether ill-defined; these *strongly correlated* systems lie beyond the scope of this thesis.

The residual interactions between elementary excitations can be treated

⁶The low-temperature requirement is normally not stringent because the characteristic electronic energy scale (the Fermi energy) is typically about $10^4 K$. Hence even at room temperature only the few energy levels closest to the ground state matter.

⁷The harmonic vibrations of the lattice are also collective modes, yet they do not have an electronic origin.

perturbatively borrowing methods from quantum many-body physics, which have revolutionized the predictive power of condensed matter theorists in the past 50 years. While unimportant for most non-magnetic metals and semiconductors, these residual interactions are crucial for systems that exhibit magnetism or superconductivity. In magnets and superconductors perturbative calculations diverge, thus revealing the emergence of ground states that differ qualitatively from the ground state of a non-interacting system. For instance, an infinite spin susceptibility is a signature of incipient ferromagnetism: the interacting electron system develops a macroscopic magnetic moment even under an infinitesimal external field. Similarly, the divergence of the two-particle scattering amplitude indicates an instability of electrons towards the formation of bound pairs, which subsequently lead to superconductivity. The magnetization of a ferromagnet and the binding energy of the electron pairs in superconductors are examples of physical quantities that become nonzero under certain environmental conditions; they are called *order parameters*. The simplest way to characterize the order parameter of these interacting systems involves the use of a *mean-field approximation*. In this approximation, each quasiparticle interacts with a self-consistent average potential involving every other quasiparticle. As a result, the interacting quasiparticle problem is cast into a single-particle problem.⁸ Standard (time-independent) as well

⁸Note that there is a hierarchy of transformations. First, we mapped the original electron system into a collection of weakly interacting elementary excitations. Afterwards, we invoked mean-field theory in order to transform the system of weakly interacting quasiparticles into a new set of non-interacting quasiparticles.

as generalized (time-dependent) mean-field theories form the backbone of this thesis.

1.1 Equilibrium Magnetism and Superconductivity

Ferromagnetism[3] constitutes the core subject of this thesis. In a ferromagnet, the vector sum of the electrons' spin is nonzero and points in a direction determined by the shape of the sample as well as the spin-orbit interactions.⁹ A precondition for ferromagnetism is the existence of permanent magnetic moments, which most often originate from incompletely filled $3d$ and $4f$ atomic orbitals in transition metals and rare earth metals, respectively.

On one hand, the f -electrons in rare earths are tightly bound to their ions and form localized magnetic moments. Mn-doped GaAs is another important example where the local moment picture is accurate to a good approximation. In these systems the ferromagnetic alignment between local moments is mediated by the itinerant s or p electrons, which are coupled to the local moments through Coulomb interactions. Due to this *exchange coupling*, the Fermi surface constructed from itinerant bands is split into a spin-up and a spin-down surface; however, the difference in volume between these two Fermi surfaces accounts for only a fraction of the total magnetic moment per atom. Consequently, the magnetism of these systems may be studied by concentrating solely on the local moments.¹⁰

⁹See chapter 5 and references therein.

¹⁰Heisenberg Hamiltonians are especially popular in studies of local-moment ferromag-

On the other hand, the d electrons responsible for magnetism in transition metals such as Co, Ni, or Fe are partially mobile because the width of the d -like bands is comparable to the characteristic strength of Coulomb interactions. In this case the splitting between spin-up and spin-down Fermi surfaces accounts for a significant portion of the magnetization, and one may no longer ignore translational degrees of freedom. Conventional wisdom portrays the ferromagnetism in transition metals as the outcome of various competing tendencies. Certainly, electrons with parallel spin experience less Coulomb repulsion than electrons with antiparallel spin as they are kept further apart from each other due to Pauli's exclusion principle. Nevertheless, keeping electrons further from each other incurs in a larger relative angular momentum and hence a higher kinetic energy for the parallel spin configuration. Ferromagnetism follows when the gain in Coulomb correlations exceeds the cost in kinetic energy.

From a quantitative standpoint, the most successful theory for the ground state of transition metals[4] has been based on the Kohn-Sham equations of spin-density functional theory. Solving these equations is tantamount to diagonalizing a mean-field Hamiltonian of non interacting quasiparticles placed in an effective, self-consistent potential. The spin-dependent part of such potential is called the *exchange field*, which acts as a magnetic field on the quasiparticles' spins. Provided that the effective potential is chosen appropriately, the solution of the Kohn-Sham equations leads to the ground state

netism.

charge- and spin-density of the original interacting problem.

Another striking manifestation of electron-electron interactions is superconductivity,[5] which will be the subject of the last part of this thesis. Whenever the effective electron-electron interaction is attractive ¹¹ the Fermi sea becomes unstable under the formation of Cooper pairs. At sufficiently low temperatures these pairs Bose condense into a macroscopic quantum state whose phase breaks the gauge symmetry. ¹² The low energy elementary excitations of bulk superconductors are quasiparticles that arise as a consequence of breaking Cooper pairs. ¹³ Since the binding energy of the Cooper pairs is finite, the quasiparticle spectrum is gapped near the Fermi surface. This energy gap is due to electron-electron interactions and has profound implications, such as perfect diamagnetism (Meissner effect), superfluidity (zero electrical resistance), flux quantization and the Josephson effect (quantum interference). The microscopic physics of conventional superconductors is described by the mean field theory ¹⁴ of Bardeen, Cooper and Schrieffer.[6] The BCS theory explains the thermodynamic properties[5] of low-temperature superconductors

¹¹In conventional superconductors the attractive interaction originates from the electron-phonon coupling.

¹²Unlike in a ferromagnet, where weak but nonzero relativistic effects (spin-orbit interactions) favor a particular direction for the equilibrium magnetization, in a superconductor the phase of the Cooper pairs' wave function is a true example of a *spontaneously* broken symmetry.

¹³Collective modes in *bulk* superconductors involve high energies (except in the immediate vicinity of the transition temperature) and thus they are irrelevant for thermodynamic properties. We shall revisit this topic in chapter 6.

¹⁴The mean field theory works very well in bulk samples, where the energy barriers for fluctuations are large.

with remarkable success.¹⁵ Another widely employed theory[7] is that of Ginzburg and Landau, where a complex-valued order parameter is introduced along with various phenomenological parameters. Gorkov showed that the Ginzburg-Landau equations may be derived from the BCS theory and furthermore identified the Ginzburg-Landau order parameter with the wavefunction of the Bose-condensed Cooper pairs.

1.2 Nonequilibrium Magnetism and Superconductivity

Much of the modern research conducted in magnetism concentrates on ferromagnets that are perturbed away from thermodynamic equilibrium. The blossoming of nonequilibrium magnetism has been partly stimulated by the advent of *spintronics*, a new technology¹⁶ that exploits the spin of the electron in order to store and process information.¹⁷

In metals, the landmark spintronics phenomena arise from the quantum mechanical interplay¹⁸ between transport currents and the magnetization. An iconic example of this interplay is the giant magnetoresistance (GMR),¹⁹ *i.e.* the high sensitivity of the electrical resistance with respect to the magnetic

¹⁵The microscopic aspects of non-conventional superconductors such as cuprates or iron pnictides are not fully understood yet.

¹⁶For a recent overview see *e.g.* Ref. [8].

¹⁷“Traditional” electronics harnesses only the charge degree of freedom of electrons.

¹⁸Ampere’s law and Biot-Savart’s law also describe the relationship between currents and magnetic fields. However, spintronics focuses on the electronic spin, which is a quantum mechanical attribute that lies beyond Maxwell’s equations.

¹⁹GMR is exploited in all modern computer hard drives and its discoverers have been awarded the 2007 Nobel Prize in physics.

configuration in ferromagnet/paramagnet/ferromagnet heterostructures. This phenomenon occurs because in a ferromagnet the density of states (and thereby the electrical conductivity) is spin-dependent.

Another emblematic example of the interplay between transport currents and the magnetic order parameter is the *spin transfer torque* (STT). STT arises when a spin polarized current is applied along a non-collinear magnetic configuration. The exchange coupling aligns the spins of the injected quasiparticles with the local magnetization, which translates into a torque on the carriers' spins as they traverse the inhomogeneous magnetic landscape. Conversely, the carriers produce a reciprocal torque (STT)²⁰ on the underlying magnetic texture, leading to current-induced magnetization dynamics. STTs are important in prototypes such as the magnetic random access memory and the magnetic race track memory.

The optimal implementation of STT devices requires a detailed understanding of magnetization relaxation,^[9] namely of dissipative processes that bring the magnetization back to equilibrium. From a microscopic standpoint, damping may be understood in terms of the decay of magnons. In conducting ferromagnets magnons are exchange-coupled to particle-hole excitations, which in turn scatter off phonons and/or impurities.²¹ Throughout this process the spin information of the quasiparticles is lost by way of spin-orbit interactions,

²⁰In absence of spin-orbit interactions and magnetic impurities, the counter-torque is equal in magnitude and opposite in sign to the original torque.

²¹The relevant quasiparticles are those located in the vicinity of the Fermi surface. The Pauli principle limits the scattering phase space for states away from the Fermi energy.

which results in an overall magnetization relaxation.

In superconductors, nonequilibrium states[10,11] are achieved by applying electromagnetic fields as well as by injecting phonons or quasiparticles. These states are characterized by the departures from equilibrium of any (or all) components of superconductors: the order parameter, the quasiparticle excitations and the phonons. Problems of nonequilibrium superconductivity are interesting from both theoretical and experimental perspectives. On the theoretical front, the remarkable success of the BCS theory makes of superconductors an ideal testbed for ideas concerning nonequilibrium many-body systems. On the experimental side, integrated circuits made from Josephson junctions are a leading candidate[12] for scalable quantum information processing. The control of these systems with voltages and magnetic fluxes involves perturbing the order parameter out of equilibrium. Other phenomena of longstanding interest include the microwave-induced enhancement of the superconducting gap and thermoelectric effects.

Notwithstanding their common challenges and objectives, nonequilibrium superconductivity and nonequilibrium magnetism have developed independently. In the last chapter of this thesis we shall advocate for a theoretical approach that cross-fertilizes these two fields.

1.3 Outline

This thesis is organized in two blocks. The first block (chapters 2-5) focuses on nonequilibrium magnetism, while the second block (chapter 6)

concentrates on nonequilibrium superconductivity from the vantage point of nonequilibrium magnetism.

Chapters 2 and 3 describe the microscopic theory of magnetic relaxation in monodomain, conducting ferromagnets. In chapter 2 we allow for spatial inhomogeneities in the magnitude of the exchange-field at the atomic scale. We subsequently derive expressions for damping that are closely related to the ones used in contemporary electronic structure calculations. In chapter 3 we present an exact treatment of disorder, which is a key ingredient of the magnetization relaxation. While our exact results are derived for simple models, they are able to shed light on the reliability of state-of-the-art spin-density functional theory calculations.

Chapter 4 explores the magnetization relaxation in a inhomogeneous ferromagnet under the flow of an electric current. We identify the change in damping induced by the current with the non-adiabatic spin transfer torque, a potentially important yet little understood parameter in spintronics. We then construct an analytical expression for the non-adiabatic spin transfer torque that will enable its first realistic estimate in transition metal ferromagnets.

Chapter 5 unveils a novel nonequilibrium effect in ferromagnets. We find that by applying a current in a special kind of ferromagnet with a single magnetic domain, the magnetization may be reoriented by 180° . We relate this effect to the change in anisotropy field due to a transport current, and estimate its importance in technologically important materials.

In chapter 6 we translate the knowledge acquired in the previous chapters to the realm of superconductivity. Interpreting superconductivity as easy-plane ferromagnetism in the particle-hole space, we compute superconducting counterparts of magnetization relaxation and STTs. We suggest a number of potentially novel thermal effects that may be experimentally verified.

Chapter 7 summarizes this thesis and presents the conclusions.

Chapter 2

Theory of Gilbert Damping in Conducting Ferromagnets I: Kohn-Sham Theory.

In this chapter we derive an approximate expression for the Gilbert damping coefficient α_G of itinerant electron ferromagnets which is based on their description in terms of spin-density-functional-theory (SDFT) and Kohn-Sham quasiparticle orbitals. We argue for an expression in which the coupling of magnetization fluctuations to particle-hole transitions is weighted by the spin-dependent part of the theory's exchange-correlation potential, a quantity which has large spatial variations on an atomic length scale. Our SDFT result for α_G is closely related to the previously proposed spin-torque correlation-function expression.¹

This is the first of three chapters related to damping of collective magnetization dynamics in metallic ferromagnets. Chapter 3 will report on *exact* calculations for two different toy model systems, with and without intrinsic spin-orbit interactions and with various spin-independent and spin-dependent disorder models. These model calculations shed light on the the absolute and

¹The contents of this chapter are based on the article: Ion Garate and A.H. MacDonald, *Gilbert Damping in Conducting Ferromagnets I: Kohn-Sham Theory and Atomic-Scale Inhomogeneity*, Phys. Rev. B **79**, 064403 (2009).

relative reliability of the two different formulas for α_G discussed in the present chapter. Chapter 3 will additionally highlight the importance of higher order diffusive particle-hole correlations in strongly spin-orbit coupled systems like (Ga,Mn)As. On the other hand, chapter 4 will concentrate on how the Gilbert damping coefficient changes when a current traverses an inhomogeneously magnetized ferromagnet.

2.1 Introduction

The Gilbert parameter α_G characterizes the damping of collective magnetization dynamics.[13] The key role of α_G in current-driven[14] and precessional[9] magnetization reversal has renewed interest in the microscopic physics of this important material parameter. It is generally accepted that in metals the damping of magnetization dynamics is dominated[9] by particle-hole pair excitation processes. The main ideas which arise in the theory of Gilbert damping have been in place for some time.[15, 16] It has however been difficult to apply them to real materials with the precision required for confident predictions which would allow theory to play a larger role in designing materials with desired damping strengths. Progress has recently been achieved in various directions, both through studies[17–23] of simple models for which the damping can be evaluated exactly and through analyses[24–27] of transition metal ferromagnets that are based on realistic electronic structure calculations. Evaluation of the torque correlation formula[26, 27] for α_G used in the later calculations requires knowledge only of a ferromagnet’s mean-field electronic

structure and of its Bloch state lifetime, which makes this approach practical.

Realistic *ab initio* theories normally employ spin-density-functional theory[28] which has a mean-field theory structure. In this chapter we use time-dependent spin-density functional theory[29, 30] to derive an explicit expression for the Gilbert damping coefficient in terms of Kohn-Sham theory eigenvalues and eigenvectors. Our final result is essentially equivalent to the torque-correlation formula[16] for α_G , but has the advantages that its derivation is fully consistent with density functional theory, that it allows for a consistent microscopic treatments of both dissipative and reactive coefficients in the Landau-Liftshitz Gilbert (LLG) equations, and that it helps establish relationships between different theoretical approaches to the microscopic theory of magnetization damping.

This chapter is organized as follows. In Section II we relate the Gilbert damping parameter α_G of a ferromagnet to the low-frequency limit of its transverse spin response function. Since ferromagnetism is due to electron-electron interactions, theories of magnetism are always many-electron theories, and it is necessary to evaluate the many-electron response function. In time-dependent spin-density functional theory the transverse response function is calculated using a time-dependent self-consistent-field calculation in which quasiparticles respond both to external potentials and to changes in the interaction-induced effective potential. In Section III we use perturbation theory and time-dependent mean-field theory to express the coefficients which appear in the LLG equations in terms of the Kohn-Sham eigenstates and eigenvalues

of the ferromagnet's ground state. These formal expressions are valid for arbitrary spin-orbit coupling, arbitrary atomic length scale spin-dependent and scalar potentials, and arbitrary disorder. By treating disorder approximately, in Section IV we derive and compare two commonly used formulas for Gilbert damping. Finally, in Section V we summarize our results.

2.2 Many-Body Transverse Response Function and the Gilbert Damping Parameter

The Gilbert damping parameter α_G appears in the Landau-Lifshitz-Gilbert expression for the collective magnetization dynamics of a ferromagnet:

$$\frac{\partial \hat{\Omega}}{\partial t} = \hat{\Omega} \times \mathcal{H}_{eff} - \alpha_G \hat{\Omega} \times \frac{\partial \hat{\Omega}}{\partial t}. \quad (2.1)$$

In Eq.(2.1) \mathcal{H}_{eff} is an effective magnetic field which we comment on further below and $\hat{\Omega} \simeq (\Omega_x, \Omega_y, 1 - (\Omega_x^2 + \Omega_y^2)/2)$ is the direction of the magnetization.

² This equation describes the slow dynamics of smooth magnetization textures and is formally the first term in an expansion in time-derivatives.

The damping parameter α_G can be measured by performing ferromagnetic resonance (FMR) experiments in which the magnetization direc-

²Here we assume that the dependence of energy on magnetization direction which determines \mathcal{H}_{eff} is specified as a function of Ω_x and Ω_y only with Ω_z implicitly fixed by the constraint $\Omega_z = [1 - \Omega_x^2 - \Omega_y^2]^{1/2}$. If the free energy was expressed in a form with explicit Ω_z dependence we would find $\mathcal{H}_{eff,x} = -\partial F/\partial \Omega_x - (\partial F/\partial \Omega_z)(\partial \Omega_z/\partial \Omega_x) = -\partial F/\partial \Omega_x + (\partial F/\partial \Omega_z)\Omega_x$, where F is the free energy of the ferromagnet. Similarly we would find $\mathcal{H}_{eff,y} = -\partial F/\partial \Omega_y + (\partial F/\partial \Omega_z)\Omega_y$. The terms which arise from the Ω_z dependence of the free energy would more commonly be regarded as contributions to $\mathcal{H}_{eff,z}$. The difference is purely a matter of convention since both results would give the same value for $\hat{\Omega} \times \mathcal{H}_{eff}$.

tion is driven weakly away from an easy direction (which we take to be the \hat{z} -direction.). To relate this phenomenological expression formally to microscopic theory we consider a system in which external magnetic fields couple only [31, 32] to the electronic spin degree of freedom³ and associate the magnetization direction $\hat{\Omega}$ with the direction of the total electron spin. For small deviations from the easy direction, Eq.(2.1) reads

$$\begin{aligned}\mathcal{H}_{eff,x} &= +\frac{\partial\hat{\Omega}_y}{\partial t} + \alpha_G\frac{\partial\hat{\Omega}_x}{\partial t} \\ \mathcal{H}_{eff,y} &= -\frac{\partial\hat{\Omega}_x}{\partial t} + \alpha_G\frac{\partial\hat{\Omega}_y}{\partial t}.\end{aligned}\tag{2.2}$$

The gyromagnetic ratio has been absorbed into the units of the field \mathcal{H}_{eff} so that this quantity has energy units and we set $\hbar = 1$ throughout. The corresponding formal linear response theory expression is an expansion of the long wavelength transverse total spin response function to first order ⁴ in frequency ω :

$$S_0\hat{\Omega}_\alpha = \sum_\beta [\chi_{\alpha,\beta}^{st} + \omega\chi'_{\alpha,\beta}] \mathcal{H}_{ext,\beta}\tag{2.3}$$

where $\alpha, \beta \in \{x, y\}$, $\omega \equiv i\partial_t$ is the frequency, S_0 is the total spin of the ferromagnet, \mathcal{H}_{ext} is the external magnetic field and χ is the transverse spin-

³In doing so we dodge the subtle difficulties which complicate theories of orbital magnetism in bulk metals. This simplification should have little influence on the theory of damping because the orbital contribution to the magnetization is relatively small in systems of interest and because it in any event tends to be collinear with the spin magnetization.

⁴For most materials the FMR frequency is by far the smallest energy scale in the problem.

spin response function:

$$\begin{aligned}\chi_{\alpha,\beta}(\omega) &= i \int_0^\infty dt \exp(i\omega t) \langle [S_\alpha(t), S_\beta(0)] \rangle \\ &= \sum_n \left[\frac{\langle \Psi_0 | S_\alpha | \Psi_n \rangle \langle \Psi_n | S_\beta | \Psi_0 \rangle}{\omega_{n,0} - \omega - i\eta} + \frac{\langle \Psi_0 | S_\beta | \Psi_n \rangle \langle \Psi_n | S_\alpha | \Psi_0 \rangle}{\omega_{n,0} + \omega + i\eta} \right] \end{aligned} \quad (2.4)$$

Here $|\Psi_n\rangle$ is an exact eigenstate of the many-body Hamiltonian and $\omega_{n,0}$ is the excitation energy for state n . We use this formal expression below to make some general comments about the microscopic theory of α_G . In Eq.(2.3) $\chi_{\alpha,\beta}^{st}$ is the static ($\omega = 0$) limit of the response function, and $\chi'_{\alpha,\beta}$ is the first derivative with respect to ω evaluated at $\omega = 0$. Notice that we have chosen the normalization in which χ is the total spin response to a transverse field; χ is therefore extensive.

The key step in obtaining the Landau-Liftshitz-Gilbert form for the magnetization dynamics is to recognize that in the static limit the transverse magnetization responds to an external magnetic field by adjusting orientation to minimize the total energy including the internal energy E_{int} and the energy due to coupling with the external magnetic field,

$$E_{ext} = -S_0 \hat{\Omega} \cdot \mathcal{H}_{ext}. \quad (2.5)$$

It follows that

$$\chi_{\alpha,\beta}^{st} = S_0^2 \left[\frac{\partial^2 E_{int}}{\partial \hat{\Omega}_\alpha \partial \hat{\Omega}_\beta} \right]^{-1}. \quad (2.6)$$

We obtain a formal equation for H_{eff} corresponding to Eq.(2.2) by multiplying Eq.(2.3) on the left by $[\chi_{\alpha,\beta}^{st}]^{-1}$ and recognizing

$$\mathcal{H}_{int,\alpha} = -\frac{1}{S_0} \sum_\beta \frac{\partial^2 E_{int}}{\partial \hat{\Omega}_\alpha \partial \hat{\Omega}_\beta} \hat{\Omega}_\beta = -\frac{1}{S_0} \frac{\partial E_{int}}{\partial \hat{\Omega}_\alpha} \quad (2.7)$$

as the internal energy contribution to the effective magnetic field $\mathcal{H}_{eff} = \mathcal{H}_{int} + \mathcal{H}_{ext}$. With this identification Eq.(2.3) can be written in the form

$$H_{eff,\alpha} = \sum_{\beta} \mathcal{L}_{\alpha,\beta} \partial_t \hat{\Omega}_{\beta} \quad (2.8)$$

where

$$\mathcal{L}_{\alpha,\beta} = -S_0 [i(\chi^{st})^{-1} \chi' (\chi^{st})^{-1}]_{\alpha,\beta} = iS_0 \partial_{\omega} \chi_{\alpha,\beta}^{-1}. \quad (2.9)$$

According to the Landau-Liftshitz Gilbert equation then $\mathcal{L}_{x,y} = -\mathcal{L}_{y,x} = 1$ and

$$\mathcal{L}_{x,x} = \mathcal{L}_{y,y} = \alpha_G. \quad (2.10)$$

Explicit evaluation of the off-diagonal components of \mathcal{L} will in general yield very small deviation from the unit result assumed by the Landau-Liftshitz-Gilbert formula. The deviation reflects mainly the fact that the magnetization magnitude varies slightly with orientation. We do not comment further on this point because it is of little consequence. Similarly $\mathcal{L}_{x,x}$ is not in general identical to $\mathcal{L}_{y,y}$, although the difference is rarely large or important when the magnetization is aligned with a high symmetry direction of a hexagonal or cubic crystal.[24, 25] Eq.(2.10) is the starting point we use later to derive approximate expressions for α_G .

In Eq.(2.9) $\chi_{\alpha,\beta}(\omega)$ is the correlation function for an interacting electron system with arbitrary disorder and arbitrary spin-orbit coupling. In the absence of spin-orbit coupling, but still with arbitrary spin-independent periodic and disorder potentials, the ground state of a ferromagnet is coupled by

the total spin-operator only to states in the same total spin multiplet. In this case it follows from Eq.(2.4) that

$$\chi_{\alpha,\beta}^{st} = 2 \sum_n \frac{\text{Re}[\langle \Psi_0 | S_\alpha | \Psi_n \rangle \langle \Psi_n | S_\beta | \Psi_0 \rangle]}{\omega_{n,0}} = \delta_{\alpha,\beta} \frac{S_0}{H_0} \quad (2.11)$$

where H_0 is a static external field, which is necessary in the absence of spin-orbit coupling to pin the magnetization to the \hat{z} direction and splits the ferromagnet's ground state many-body spin multiplet. Similarly

$$\chi'_{\alpha,\beta} = 2i \sum_n \frac{\text{Im}[\langle \Psi_0 | S_\alpha | \Psi_n \rangle \langle \Psi_n | S_\beta | \Psi_0 \rangle]}{\omega_{n,0}^2} = i\epsilon_{\alpha,\beta} \frac{S_0}{H_0^2}. \quad (2.12)$$

where $\epsilon_{x,x} = \epsilon_{y,y} = 0$ and $\epsilon_{x,y} = -\epsilon_{y,x} = 1$, yielding $\mathcal{L}_{x,y} = -\mathcal{L}_{y,x} = 1$ and $\mathcal{L}_{x,x} = \mathcal{L}_{y,y} = 0$. Spin-orbit coupling is required for magnetization damping.⁵

2.3 SDF-Stoner Theory Expression for Gilbert Damping

Approximate formulas for α_G in metals are inevitably based on a self-consistent mean-field theory (Stoner) description of the magnetic state. Our goal is to derive an approximate expression for α_G when the adiabatic local spin-density approximation[28] is used for the exchange correlation potential in spin-density-functional theory. The effective Hamiltonian which describes the Kohn-Sham quasiparticle dynamics therefore has the form

$$\mathcal{H}_{KS} = \mathcal{H}_P - \Delta(n(\vec{r}), |\vec{s}(\vec{r})|) \hat{\Omega}(\vec{r}) \cdot \vec{s}, \quad (2.13)$$

⁵For zero spin-orbit coupling α_G vanishes even in presence of magnetic impurities, provided that their spins follow the dynamics of the magnetization adiabatically.

where \mathcal{H}_P is the Kohn-Sham Hamiltonian of a paramagnetic state in which $|\vec{s}(\vec{r})|$ (the local spin density) is set to zero, \vec{s} is the spin-operator, and

$$\Delta(n, s) = -\frac{d [n\epsilon_{xc}(n, s)]}{ds} \quad (2.14)$$

is the magnitude of the spin-dependent part of the exchange-correlation potential. In Eq.(2.14) $\epsilon_{xc}(n, s)$ is the exchange-correlation energy per particle in a uniform electron gas with density n and spin-density s . We assume that the ferromagnet is described using some semi-relativistic approximation to the Dirac equation like those commonly used[33] to describe magnetic anisotropy or X-ray magnetic circular dichroism, even though these approximations are not strictly consistent with spin-density-functional theory. Within this framework electrons carry only a two-component spin-1/2 degree of freedom and spin-orbit coupling terms are included in \mathcal{H}_P . Since $n\epsilon_{xc}(n, s) \sim [(n/2 + s)^{4/3} + (n/2 - s)^{4/3}]$,

$\Delta(n, s) \sim n^{1/3}$ is larger closer to atomic centers and far from spatially uniform on atomic length scales. ⁶ This property figures prominently in the considerations explained below.

In SDFT the transverse spin-response function is expressed in terms of Kohn-Sham quasiparticle response to both external and induced magnetic fields:

$$s_0(\vec{r}) \Omega_\alpha(\vec{r}) = \int \frac{d\vec{r}'}{V} \chi_{\alpha,\beta}^{QP}(\vec{r}, \vec{r}') [\mathcal{H}_{ext,\beta}(\vec{r}') + \Delta(\vec{r}') \Omega_\beta(\vec{r}')]. \quad (2.15)$$

⁶While $\Delta(n, s) \sim n^{1/3}$ is no longer valid when correlation is included, even in this case Δ is inhomogeneous at the atomic lengthscale.

In Eq.(2.15) V is the system volume, $s_0(\vec{r})$ is the magnitude of the ground state spin density, $\Delta(\vec{r})$ is the magnitude of the spin-dependent part of the ground state exchange-correlation potential and

$$\chi_{\alpha,\beta}^{QP}(\vec{r}, \vec{r}') = \sum_{i,j} \frac{f_j - f_i}{\omega_{i,j} - \omega - i\eta} \langle i|\vec{r}\rangle s_\alpha \langle \vec{r}|j\rangle \langle j|\vec{r}'\rangle s_\beta \langle \vec{r}'|i\rangle, \quad (2.16)$$

where f_i is the ground state Kohn-Sham occupation factor for eigenspinor $|i\rangle$ and $\omega_{ij} \equiv \epsilon_i - \epsilon_j$ is a Kohn-Sham eigenvalue difference. $\chi^{QP}(\vec{r}, \vec{r}')$ has been normalized so that it returns the spin-density rather than total spin. Like the Landau-Liftshitz-Gilbert equation itself, Eq.(2.15) assumes that only the direction of the magnetization, and not the magnitudes of the charge and spin-densities, varies in the course of smooth collective magnetization dynamics.⁷ This property should hold accurately as long as magnetic anisotropies and external fields are weak compared to Δ . We are able to use this property to avoid solving the position-space integral equation implied by Eq.(2.15). Multiplying by $\Delta(\vec{r})$ on both sides and integrating over position we find⁸ that

$$S_0\Omega_\alpha = \sum_{\beta} \frac{1}{\bar{\Delta}} \tilde{\chi}_{\alpha,\beta}^{QP}(\omega) \left[\Omega_\beta + \frac{\mathcal{H}_{ext,\beta}}{\bar{\Delta}} \right] \quad (2.17)$$

where we have taken advantage of the fact that in FMR experiments $\mathcal{H}_{ext,\beta}$ and $\hat{\Omega}$ are uniform. $\bar{\Delta}$ is a spin-density weighted average of $\Delta(\vec{r})$,

$$\bar{\Delta} = \frac{\int d\vec{r} \Delta(\vec{r}) s_0(\vec{r})}{\int d\vec{r} s_0(\vec{r})}, \quad (2.18)$$

⁷This approximation does not preclude strong spatial variations of $|s_0(\vec{r})|$ and $|\Delta(\vec{r})|$ at atomic lengthscales; rather it is assumed that such spatial profiles will remain unchanged in the course of the magnetization dynamics.

⁸For notational simplicity we assume that all magnetic atoms are identical. Generalizations to magnetic compounds are straight forward.

and

$$\tilde{\chi}_{\alpha,\beta}^{QP}(\omega) = \sum_{ij} \frac{f_j - f_i}{\omega_{ij} - \omega - i\eta} \langle j|s_\alpha\Delta(\vec{r})|i\rangle \langle i|s_\beta\Delta(\vec{r})|j\rangle \quad (2.19)$$

is the transverse-part of the quasiparticle exchange-correlation effective field response function, *not* the transverse-part of the quasiparticle spin response function. In Eq.(2.19), $\langle i|O(\vec{r})|j\rangle = \int d\vec{r}\langle i|\vec{r}|O(\vec{r})\langle\vec{r}|j\rangle$ denotes a single-particle matrix element. Solving Eq.(2.17) for the many-particle transverse susceptibility (the ratio of $S_0\hat{\Omega}_\alpha$ to $H_{ext,\beta}$) and inserting the result in Eq.(2.9) yields

$$\mathcal{L}_{\alpha,\beta} = iS_0\partial_\omega\chi_{\alpha,\beta}^{-1} = -S_0\bar{\Delta}^2\partial_\omega\text{Im}[\tilde{\chi}_{\alpha,\beta}^{QP-1}]. \quad (2.20)$$

Our microscopic theory of the LLG damping parameter helps explain the relationship between a variety of similar but distinct formulas which appear in the literature in either *ab initio* theory or model calculations. As we have explained, α_G is fundamentally related to the full many-body transverse-spin response function to smooth external magnetic fields. In SDFT and other theories with a similar mean-field structure, this translates not into the transverse-spin response function of quasiparticles but instead into the quasiparticle response function for changes in the orientation of the spin-dependent part of the exchange-correlation potential. Spin-flip operators in this response function are therefore weighted by the local spin-splitting which varies considerably within each unit cell of a magnetic metal. In our formulation, as in some others[24, 25] both reactive and dissipative terms in the LLG equation are understood in a consistent fashion. In addition, as we discuss in

greater detail later, our approach treats the breathing Fermi surface contribution to damping[16, 24, 25] and the inter-band spin-relaxation contribution on the same footing. Using our formulation we are able below to address the relationship between torque-correlation formulas for the magnetization damping and other spin-oriented formulas which arise more naturally in Kubo response function theories for model systems.

Comparing Eq.(2.15) and Eq.(2.7) we find that the internal anisotropy field can also be expressed in terms of $\tilde{\chi}^{QP}$:

$$\mathcal{H}_{int,\alpha} = -\bar{\Delta}^2 S_0 \sum_{\beta} \left[\tilde{\chi}_{\alpha,\beta}^{QP-1}(\omega = 0) - \frac{\delta_{\alpha,\beta}}{S_0 \bar{\Delta}} \right] \Omega_{\beta}. \quad (2.21)$$

Eq.(2.20) and Eq.(2.21) provide microscopic expressions for all ingredients that appear in the LLG equations linearized for small transverse excursions. It is generally assumed that the damping coefficient α_G is independent of orientation; if so, the present derivation is sufficient. The anisotropy-field at large transverse excursions normally requires additional information about magnetic anisotropy. We remark that if the Hamiltonian does not include a spin-dependent mean-field dipole interaction term, as is usually the case, the above quantity will return only the magnetocrystalline anisotropy field. Since the magnetostatic contribution to anisotropy is always well described by mean-field-theory it can be added separately.

We conclude this section by demonstrating that the Stoner theory equations proposed here recover the exact results mentioned at the end of the previous section for the limit in which spin-orbit coupling is neglected. We

consider a SDF theory ferromagnet with arbitrary scalar and spin-dependent effective potentials. Since the spin-dependent part of the exchange correlation potential is then the only spin-dependent term in the Hamiltonian it follows that

$$[\mathcal{H}_{KS}, s_\alpha] = -i \epsilon_{\alpha,\beta} \Delta(\vec{r}) s_\beta \quad (2.22)$$

and hence that

$$\langle i | s_\alpha \Delta(\vec{r}) | j \rangle = -i \epsilon_{\alpha,\beta} \omega_{ij} \langle i | s_\beta | j \rangle. \quad (2.23)$$

Inserting Eq.(2.23) in one of the matrix elements of Eq.(2.19) yields for the no-spin-orbit-scattering case

$$\tilde{\chi}_{\alpha,\beta}^{QP}(\omega = 0) = \delta_{\alpha,\beta} S_0 \bar{\Delta}. \quad (2.24)$$

The internal magnetic field $\mathcal{H}_{int,\alpha}$ is therefore identically zero in the absence of spin-orbit coupling and only external magnetic fields will yield a finite collective precession frequency. Inserting Eq.(2.23) in both matrix elements of Eq.(2.19) yields

$$\partial_\omega \text{Im}[\tilde{\chi}_{\alpha,\beta}^{QP}] = \epsilon_{\alpha,\beta} S_0. \quad (2.25)$$

Using both Eq.(2.24) and Eq.(2.25) to invert $\tilde{\chi}^{QP}$ we recover the results proved previously for the no-spin-orbit case using a many-body argument: $\mathcal{L}_{x,y} = -\mathcal{L}_{y,x} = 1$ and $\mathcal{L}_{x,x} = \mathcal{L}_{y,y} = 0$. The Stoner-theory equations derived here allow spin-orbit interactions, and hence magnetic anisotropy and Gilbert damping, to be calculated consistently from the same quasiparticle response function $\tilde{\chi}^{QP}$.

2.4 Discussion

As long as magnetic anisotropy and external magnetic fields are weak compared to the exchange-correlation splitting in the ferromagnet we can use Eq.(2.24) to approximate $\tilde{\chi}_{\alpha,\beta}^{QP}(\omega = 0)$. Using this approximation and assuming that damping is isotropic we obtain the following explicit expression for temperature $T \rightarrow 0$:

$$\begin{aligned}
\alpha_G &= \mathcal{L}_{x,x} \\
&= -S_0 \bar{\Delta}^2 \partial_\omega \text{Im}[\tilde{\chi}_{x,x}^{QP-1}] \\
&= \frac{\pi}{S_0} \sum_{ij} \delta(\epsilon_j - \epsilon_F) \delta(\epsilon_i - \epsilon_F) \langle j | s_x \Delta(\vec{r}) | i \rangle \langle i | s_x \Delta(\vec{r}) | j \rangle \\
&= \frac{\pi}{S_0} \sum_{ij} \delta(\epsilon_j - \epsilon_F) \delta(\epsilon_i - \epsilon_F) \langle j | [\mathcal{H}_P, s_y] | i \rangle \langle i | [\mathcal{H}_P, s_y] | j \rangle. \quad (2.26)
\end{aligned}$$

The second form for α_G is equivalent to the first and follows from the observation that for matrix elements between states that have the same energy

$$\langle i | [\mathcal{H}_{KS}, s_\alpha] | j \rangle = -i \epsilon_{\alpha,\beta} \langle i | \Delta(\vec{r}) s_\beta | j \rangle + \langle i | [\mathcal{H}_P, s_\alpha] | j \rangle = 0 \quad (\text{for } \omega_{ij} = 0). \quad (2.27)$$

Eq. (2.26) is valid for any scalar and any spin-dependent potential. It is clear however that the numerical value of α_G in a metal is very sensitive to the degree of disorder in its lattice. To see this we observe that for a perfect crystal the Kohn-Sham eigenstates are Bloch states. Since the operator $\Delta(\vec{r}) s_\alpha$ has the periodicity of the crystal its matrix elements are non-zero only between states with the same Bloch wavevector label \vec{k} . For the case of a perfect crystal

then

$$\begin{aligned}
\alpha_G &= \frac{\pi}{s_0} \int_{BZ} \frac{d\vec{k}}{(2\pi)^3} \sum_{nn'} \delta(\epsilon_{\vec{k}n'} - \epsilon_F) \delta(\epsilon_{\vec{k}n} - \epsilon_F) |\langle \vec{k}n' | s_x \Delta(\vec{r}) | \vec{k}n \rangle|^2 \\
&= \frac{\pi}{s_0} \int_{BZ} \frac{d\vec{k}}{(2\pi)^3} \sum_{nn'} \delta(\epsilon_{\vec{k}n'} - \epsilon_F) \delta(\epsilon_{\vec{k}n} - \epsilon_F) |\langle \vec{k}n' | [\mathcal{H}_P, s_y] | \vec{k}n \rangle|^2 \quad (2.28)
\end{aligned}$$

where nn' are band labels and s_0 is the ground state spin per unit volume and the integral over \vec{k} is over the Brillouin-zone (BZ).

Clearly α_G diverges⁹ in a perfect crystal since $\langle \vec{k}n' | s_x \Delta(\vec{r}) | \vec{k}n \rangle$ is generically non-zero. A theory of α_G must therefore always account for disorder in a crystal.¹⁰ The easiest way to account for disorder is to replace the $\delta(\epsilon_{\vec{k}n} - \epsilon_F)$ spectral function of a Bloch state by a broadened spectral function evaluated at the Fermi energy $A_{\vec{k}n}^-(\epsilon_F)$. If disorder is treated perturbatively this simple *ansatz* can be augmented[34] by introducing impurity vertex corrections in Eq. (2.28). Provided that the quasiparticle lifetime is computed via Fermi's golden rule, these vertex corrections restore Ward identities and yield an exact treatment of disorder in the limit of dilute impurities. Nevertheless, this approach is rarely practical outside the realm of toy models, because the sources of disorder are rarely known with sufficient precision.

Although appealing in its simplicity, the $\delta(\epsilon_{\vec{k}n} - \epsilon_F) \rightarrow A_{\vec{k}n}^-(\epsilon_F)$ substitution is prone to ambiguity because it gives rise to qualitatively different

⁹Eq. (2.26) is valid provided that $\omega\tau \ll 1$, where τ is the quasiparticle lifetime. While this condition is normally satisfied in cases of practical interest, it invariably breaks down as $\tau \rightarrow \infty$. Hence the divergence of Eq. (2.26) in *perfect* crystals is spurious.

¹⁰In most systems of interest the main contribution to damping originates from a combination of intrinsic spin-orbit interactions and spin-independent disorder.

outcomes depending on whether it is applied to the first or second line of Eq.

(2.28):

$$\begin{aligned}
\alpha_G^{(TC)} &= \frac{\pi}{s_0} \int_{BZ} \frac{d\vec{k}}{(2\pi)^3} \sum_{nn'} A_{\vec{k},n}(\epsilon_F) A_{\vec{k},n'}(\epsilon_F) \langle \vec{k}n' | [\mathcal{H}_P, s_y] | \vec{k}n \rangle \langle \vec{k}n | [\mathcal{H}_P, s_y] | \vec{k}n' \rangle, \\
\alpha_G^{(SF)} &= \frac{\pi}{s_0} \int_{BZ} \frac{d\vec{k}}{(2\pi)^3} \sum_{nn'} A_{\vec{k},n}(\epsilon_F) A_{\vec{k},n'}(\epsilon_F) \langle \vec{k}n' | s_x \Delta(\vec{r}) | \vec{k}n \rangle \langle \vec{k}n | s_x \Delta(\vec{r}) | \vec{k}n' \rangle.
\end{aligned}
\tag{2.29}$$

$\alpha_G^{(TC)}$ is the torque-correlation (TC) formula used in realistic electronic structure calculations[26, 27] and $\alpha_G^{(SF)}$ is the spin-flip (SF) formula used in certain toy model calculations[35]. The discrepancy between TC and SF expressions stems from inter-band ($n \neq n'$) contributions to damping, which may now connect states with *different* band energies due to the disorder broadening of the spectral functions. Therefore, $\langle \vec{k}n | [\mathcal{H}_{KS}, s_\alpha] | \vec{k}n' \rangle$ no longer vanishes for $n \neq n'$ and Eq. (2.27) indicates that $\alpha_G^{(TC)} \simeq \alpha_G^{(SF)}$ only if the Gilbert damping is dominated by intra-band contributions and/or if the energy difference between the states connected by inter-band transitions is small compared to Δ . When $\alpha_G^{(TC)} \neq \alpha_G^{(SF)}$, it is *a priori* unclear which approach is the most accurate. One obvious flaw of the SF formula is that it produces a spurious damping in absence of spin-orbit interactions; this unphysical contribution originates from inter-band transitions and may be cancelled out by adding the leading order impurity vertex correction.[21] In contrast, $[\mathcal{H}_P, s_y] = 0$ in absence of spin-orbit interaction and hence the TC formula vanishes identically, even without vertex corrections. From this analysis, TC appears to have a pragmatic edge over SF in materials with weak spin-orbit interaction. However, insofar as

it allows inter-band transitions that connect states with $\omega_{i,j} > \Delta$, TC is not quantitatively reliable. Furthermore, it can be shown[34] that when the intrinsic spin-orbit coupling is significant (e.g. in ferromagnetic semiconductors), the advantage of TC over SF (or vice versa) is marginal, and impurity vertex corrections play a significant role.

2.5 Conclusions

Using spin-density functional theory we have derived a Stoner model expression for the Gilbert damping coefficient in itinerant ferromagnets. This expression accounts for atomic scale variations of the exchange self energy, as well as for arbitrary disorder and spin-orbit interaction. By treating disorder approximately, we have derived the spin-flip and torque-correlation formulas previously used in toy-model and *ab-initio* calculations, respectively. We have traced the discrepancy between these equations to the treatment of inter-band transitions that connect states which are not close in energy. A better treatment of disorder, which requires the inclusion of impurity vertex corrections, will be the ultimate judge on the relative reliability of either approach. When damping is dominated by intra-band transitions, a circumstance which we believe is common, the two formulas are identical and both are likely to provide reliable estimates.

Chapter 3

Theory of Gilbert Damping in Conducting Ferromagnets II: Disorder Vertex Corrections

In this chapter we report on a study of Gilbert damping due to particle-hole pair excitations in conducting ferromagnets. We focus on a toy two-band model and on a four-band spherical model which provides an approximate description of ferromagnetic (Ga,Mn)As. These models are sufficiently simple that disorder-ladder-sum vertex corrections to the long-wavelength spin-spin response function can be summed to all orders. An important objective of this study is to assess the reliability of practical approximate expressions introduced in chapter 2 which can be combined with electronic structure calculations to estimate Gilbert damping in more complex systems.¹

3.1 Introduction

The key role of the Gilbert parameter α_G in current-driven[14] and precessional[9] magnetization reversal has led to a renewed interest in this important magnetic material parameter. The theoretical foundations which relate

¹The contents of this chapter are based on the article: Ion Garate and A.H. MacDonald, *Gilbert Damping in Conducting Ferromagnets II: Model Tests of the Torque-Correlation Formula*, Phys. Rev. B 79, 064404 (2009).

Gilbert damping to the transverse spin-spin response function of the ferromagnet have been in place for some time.[15, 16] It has nevertheless been difficult to predict trends as a function of temperature and across materials systems, partly because damping depends on the strength and nature of the disorder in a manner that requires a more detailed characterization than is normally available. Two groups have recently[26, 27] reported successful applications to transition metal ferromagnets of the *torque-correlation* formula[16, 26, 27, 36] for α_G . This formula has the important advantage that its application requires knowledge only of the band structure, including its spin-orbit coupling, and of Bloch state lifetimes. The torque-correlation formula is physically transparent and can be applied with relative ease in combination with modern spin-density-functional-theory[28] (SDFT) electronic structure calculations. In this chapter we compare the predictions of the torque correlation formula with Kubo-formula self-consistent-Born-approximation results for two different relatively simple model systems, an artificial two-band model of a ferromagnet with Rashba spin-orbit interactions and a four-band model which captures the essential physics of (III,Mn)V ferromagnetic semiconductors.[37, 38] The self-consistent Born approximation theory for α_G requires that ladder-diagram vertex corrections be included in the transverse spin-spin response function. Since the Born approximation is exact² for weak scattering, we can use this comparison to assess the reliability of the simpler and more practical torque-

²The Born approximation is no longer accurate at high impurity concentrations in which electron localization plays a role; however, localization effects are weak in transition metal ferromagnets and metallic (Ga,Mn)As .

correlation formula. We conclude that the torque-correlation formula is accurate when the Gilbert damping is dominated by intra-band excitations of the transition metal Fermi sea, but that it can be inaccurate when it is dominated by inter-band excitations.

This chapter is organized as follows. In Section II we explain how we evaluate the transverse spin-spin response function for simple model ferromagnets. Section III discusses our result for the two-band Rashba model while Section IV summarizes our findings for the four-band (III,Mn)V model. We conclude in Section V with a summary of our results and recommended *best practices* for the use of the torque-correlation formula.

3.2 Gilbert Damping and Transverse Spin Response Function

3.2.1 Realistic SDFT *vs.* *s-d* and *p-d* models

We view the two-band *s-d* and four band *p-d* models studied in this paper as toy models which capture the essential features of metallic magnetism in systems that are, at least in principle,³ more realistically described using SDFT. The *s-d* and *p-d* models correspond to the limit of *ab initio* SDFT in which i) the majority spin *d*-bands are completely full and the minority

³These simplified models sometimes have the advantage that their parameters can be adjusted phenomenologically to fit experiments, compensating for inevitable inaccuracies in *ab initio* electronic structure calculations. This advantage makes *p-d* models of (III,Mn)V ferromagnets particularly useful. *s-d* models of transition elements are less realistic from the start because they do not account for the minority-spin hybridized *s-d* bands which are present at the Fermi energy.

spin d -bands completely empty, ii) hybridization between s or p and d -bands is relatively weak, and iii) there is exchange coupling between d and s or p moments. In chapter 2 we have proposed the following expression for the Gilbert-damping contribution from particle-hole excitations in SDFT bands:

$$\alpha_G = \frac{1}{S_0} \partial_\omega \text{Im}[\tilde{\chi}_{x,x}^{QP}] \quad (3.1)$$

where $\tilde{\chi}_{x,x}^{QP}$ is a response-function which describes how the quasiparticle bands change in response to a spatially smooth variation in magnetization orientation and S_0 is the total spin. Specifically,

$$\tilde{\chi}_{\alpha,\beta}^{QP}(\omega) = \sum_{ij} \frac{f_j - f_i}{\omega_{ij} - \omega - i\eta} \langle j | s^\alpha \Delta_0(\vec{r}) | i \rangle \langle i | s^\beta \Delta_0(\vec{r}) | j \rangle. \quad (3.2)$$

where α and β label the x and y transverse spin directions and the easy direction for the magnetization is assumed to be the \hat{z} direction. In Eq.(3.2) $|i\rangle$, f_i and ω_{ij} are Kohn-Sham eigenspinors, Fermi factors, and eigenenergy differences respectively, s_α is a spin operator, and $\Delta_0(\vec{r})$ is the difference between the majority spin and minority spin exchange-correlation potential. In the $s-d$ and $p-d$ models $\Delta_0(\vec{r})$ is replaced by a phenomenological constant, which we denote by Δ_0 below. With $\Delta_0(\vec{r})$ replaced by a constant $\tilde{\chi}_{x,x}^{QP}$ reduces to a standard spin-response function for non-interacting quasiparticles in a possibly spin-dependent random static external potential. The evaluation of this quantity, and in particular the low-frequency limit in which we are interested, is non-trivial only because disorder plays an essential role.

3.2.2 Disorder Perturbation Theory

We start by writing the transverse spin response function of a disordered metallic ferromagnet in the Matsubara formalism,

$$\tilde{\chi}_{xx}^{QP}(i\omega) = -V \frac{\Delta_0^2}{\beta} \sum_{\omega_n} P(i\omega_n, i\omega_n + i\omega) \quad (3.3)$$

where the minus sign originates from fermionic statistics, V is the volume of the system and

$$P(i\omega_n, i\omega_n + i\omega) \equiv \int \frac{d^D k}{(2\pi)^D} \Lambda_{\alpha,\beta}(i\omega_n, i\omega_n + i\omega; \mathbf{k}) G_{\beta}(i\omega_n + i\omega, \mathbf{k}) s_{\beta,\alpha}^x(\mathbf{k}) G_{\alpha}(i\omega_n, \mathbf{k}). \quad (3.4)$$

In Eq. (3.4) $|\alpha\mathbf{k}\rangle$ is a band eigenstate at momentum \mathbf{k} , D is the dimensionality of the system, $s_{\alpha,\beta}^x(\mathbf{k}) = \langle \alpha\mathbf{k} | s^x | \beta\mathbf{k} \rangle$ is the spin-flip matrix element, $\Lambda_{\alpha,\beta}(\mathbf{k})$ is its vertex-corrected counterpart (see below), and

$$G_{\alpha}(i\omega_n, \mathbf{k}) = \left[i\omega_n + E_F - E_{\mathbf{k},\alpha} + i \frac{1}{2\tau_{\mathbf{k},\alpha}} \text{sign}(\omega_n) \right]^{-1}. \quad (3.5)$$

We have included disorder within the Born approximation by incorporating a finite lifetime τ for the quasiparticles and by allowing for vertex corrections at one of the spin vertices.

The vertex function in Eq.(3.4) obeys the Dyson equation (Fig. (3.1)):

$$\begin{aligned} \Lambda_{\alpha,\beta}(i\omega_n, i\omega_n + i\omega; \mathbf{k}) &= s_{\alpha,\beta}^x(\mathbf{k}) + \\ &+ \int \frac{d^D k'}{(2\pi)^D} u^a(\mathbf{k} - \mathbf{k}') s_{\alpha,\alpha'}^a(\mathbf{k}, \mathbf{k}') G_{\alpha'}(i\omega_n, \mathbf{k}') \Lambda_{\alpha',\beta'}(i\omega_n, i\omega_n + i\omega; \mathbf{k}') \\ &\quad \times G_{\beta'}(i\omega_n + i\omega, \mathbf{k}') s_{\beta',\beta}^a(\mathbf{k}', \mathbf{k}), \end{aligned} \quad (3.6)$$

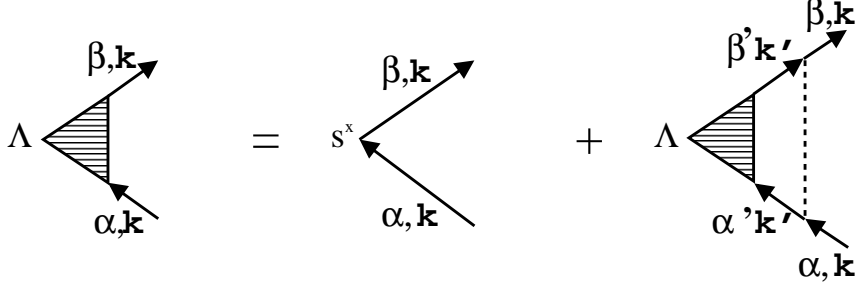


Figure 3.1: Dyson equation for the renormalized vertex of the transverse spin-spin response function. The dotted line denotes impurity scattering.

where $u^a(\mathbf{q}) \equiv n_a \overline{V_a^2}(\mathbf{q})$ ($a = 0, x, y, z$), n_a is the density of scatterers, $V_a(\mathbf{q})$ is the scattering potential (dimensions: (energy) \times (volume)) and the overline stands for disorder[21] averaging.⁴ Ward's identity requires that $u^a(\mathbf{q})$ and $\tau_{\mathbf{k},\alpha}$ be related via the Fermi's golden rule:

$$\frac{1}{\tau_{\alpha\mathbf{k}}} = 2\pi \int_{\mathbf{k}'} u^a(\mathbf{k} - \mathbf{k}') \sum_{\alpha'} s_{\alpha,\alpha'}^a s_{\alpha',\alpha}^a \delta(E_{\mathbf{k}\alpha} - E_{\mathbf{k}'\alpha'}), \quad (3.7)$$

where $\int_{\mathbf{k}} \equiv \int d^D k / (2\pi)^D$. In this paper we restrict ourselves to spin-independent ($a = 0$) disorder and spin-dependent disorder oriented along the equilibrium-exchange-field direction ($a = z$).⁵ Performing the conventional[39] integration around the branch cuts of P , we obtain

$$\begin{aligned} \tilde{\chi}_{xx}^{QP}(i\omega) &= V \Delta_0^2 \int_{-\infty}^{\infty} \frac{d\epsilon}{2\pi i} f(\epsilon) [P(\epsilon + i\delta, \epsilon + i\omega) - P(\epsilon - i\delta, \epsilon + i\omega)] \\ &+ V \Delta_0^2 \int_{-\infty}^{\infty} \frac{d\epsilon}{2\pi i} f(\epsilon) [P(\epsilon - i\omega, \epsilon + i\delta) - P(\epsilon - i\omega, \epsilon - i\delta)] \end{aligned} \quad (3.8)$$

⁴This is not the most general type of disorder for quasiparticles with spin $> 1/2$, but it will be sufficient for the purpose of this work.

⁵We assume that the spins of magnetic impurities are *frozen* along the *static* part of the exchange field. In reality, the direction of the impurity spins is a dynamical variable that is influenced by the magnetization precession.

where $f(\epsilon)$ is the Fermi function. Next, we perform an analytical continuation $i\omega \rightarrow \omega + i\eta$ and take the imaginary part of the resulting retarded response function. Assuming low temperatures, this yields

$$\begin{aligned}\alpha_G &= \frac{\Delta_0^2}{2\pi s_0} \{ \text{Re} [P(-i\delta, i\delta)] - \text{Re} [P(i\delta, +i\delta)] \} \\ &= \frac{\Delta_0^2}{2\pi s_0} \text{Re}(P^{A,R} - P^{R,R})\end{aligned}\quad (3.9)$$

where $s_0 = S_0/V$,

$$P^{R(A),R} = \int_{\mathbf{k}} \Lambda_{\alpha,\beta}^{R(A),R}(\mathbf{k}) G_{\beta}^R(0, \mathbf{k}) s_{\beta,\alpha}^x(\mathbf{k}) G_{\alpha}^{R(A)}(0, \mathbf{k}) \quad (3.10)$$

and $G^{R(A)}(0, \mathbf{k})$ is the retarded (advanced) Green's function at the Fermi energy. The principal difficulty of Eq.(3.9) resides in solving the Dyson equation for the vertex function. We first discuss our method of solution in general terms before turning in Sections III and IV to its application to the $s - d$ and $p - d$ models.

3.2.3 Evaluation of Impurity Vertex Corrections for Multi-Band Models

Eq.(6.20) encodes disorder-induced diffusive correlations between itinerant carriers, and is an integral equation of considerable complexity. Fortunately, it is possible to transform it into a relatively simple algebraic equation, provided that the impurity potentials are short-ranged in real space.

Referring back at Eq.(6.20) it is clear that the solution of the Dyson equation would be trivial if the vertex function was independent of momentum. That is certainly not the case in general, because the matrix elements of the

spin operators may be momentum dependent. Yet, for short-range scatterers the entire momentum dependence of the vertex matrix elements comes from the eigenstates alone:

$$s_{\alpha,\alpha'}^a(\mathbf{k}, \mathbf{k}') = \sum_{m,m'} \langle \alpha \mathbf{k} | m \rangle \langle m' | \alpha' \mathbf{k}' \rangle s_{m,m'}^a \quad (3.11)$$

This property motivates our solution strategy which characterizes the momentum dependence of the vertex function by expanding it in terms of the eigenstates of s^z (s^x or s^y bases would work equally well):

$$\begin{aligned} \Lambda_{\alpha,\beta}(\mathbf{k}) &= \langle \alpha \mathbf{k} | \Lambda | \beta \mathbf{k} \rangle \\ &= \sum_{m,m'} \langle \alpha \mathbf{k} | m \rangle \Lambda_{m,m'} \langle m' | \beta \mathbf{k} \rangle \end{aligned} \quad (3.12)$$

where $|m\rangle$ is an eigenstate of s^z , with eigenvalue m . Plugging Eqs.(3.11) and (3.12) into Eq.(6.20) demonstrates that, as expected, $\Lambda_{m,m'}$ is *independent* of momentum. After cancelling common factors from both sides of the resulting expression and using $\partial_{\mathbf{q}} u^a(\mathbf{q}) = 0$ ($a = 0, z$) we arrive at

$$\Lambda_{m,m'}^{R(A),R} = s_{m,m'}^x + \sum_{l,l'} U_{m,m':l,l'}^{R(A),R} \Lambda_{l,l'}^{R(A),R} \quad (3.13)$$

where

$$U_{m,m':l,l'}^{R(A),R} \equiv (u^0 + u^z m m') \int_{\mathbf{k}} \langle m | \alpha \mathbf{k} \rangle G_{\alpha}^{R(A)}(0, \mathbf{k}) \langle \alpha \mathbf{k} | l \rangle \langle l' | \beta \mathbf{k} \rangle G_{\beta}^R(0, \mathbf{k}) \langle \beta \mathbf{k} | m' \rangle \quad (3.14)$$

Eqs. (3.12),(3.13) and (3.14) provide a solution for the vertex function that is significantly easier to analyse than the original Dyson equation.

3.3 Gilbert Damping for a Magnetic 2DEG

The first model we consider is a two-dimensional electron gas (2DEG) model with ferromagnetism and Rashba spin-orbit interactions. We refer to this as the magnetic 2DEG (M2DEG) model. This toy model is almost never even approximately realistic,[40] but a theoretical study of its properties will prove useful in a number of ways. First, it is conducive to a fully analytical evaluation of the Gilbert damping, which will allow us to precisely understand the role of different actors. Second, it enables us to explain in simple terms why higher order vertex corrections are significant when there is spin-orbit interaction in the band structure. Third, as we demonstrate below the Gilbert damping of a M2DEG has qualitative features similar to those of (Ga,Mn)As.

The band Hamiltonian of the M2DEG model is

$$H = \frac{k^2}{2m} + \mathbf{b}_{\mathbf{k}} \cdot \boldsymbol{\sigma} \quad (3.15)$$

where $\mathbf{b}_{\mathbf{k}} = (-\lambda k_y, \lambda k_x, \Delta_0)$, Δ_0 is the difference between majority and minority spin exchange-correlation potentials, λ is the strength of the Rashba SO coupling and $\vec{\sigma} = 2\vec{s}$ is a vector of Pauli matrices. The corresponding eigenvalues and eigenstates are

$$E_{\pm, \mathbf{k}} = \frac{k^2}{2m} \pm \sqrt{\Delta_0^2 + \lambda^2 k^2} \quad (3.16)$$

$$|\alpha \mathbf{k}\rangle = e^{-is^z \phi} e^{-is^y \theta} |\alpha\rangle \quad (3.17)$$

where $\phi = -\tan^{-1}(k_x/k_y)$ and $\theta = \cos^{-1}(\Delta_0/\sqrt{\Delta_0^2 + \lambda^2 k^2})$ are the spinor

angles and $\alpha = \pm$ is the band index. It follows that

$$\begin{aligned}\langle m|\alpha, \mathbf{k}\rangle &= \langle m|e^{-is^z\phi}e^{-is^y\theta}|\alpha\rangle \\ &= e^{-im\phi}d_{m,\alpha}(\theta)\end{aligned}\quad (3.18)$$

where $d_{m,\alpha} = \langle m|e^{-is^y\theta}|\alpha\rangle$ is a Wigner function for $J=1/2$ angular momentum[41]. With these simple spinors, the azimuthal integral in Eq.(3.14) can be performed analytically to obtain

$$U_{m,m':l,l'}^{R(A),R} = \delta_{m-m',l-l'}(u^0+u^zmm') \sum_{\alpha,\beta} \int \frac{dkk}{2\pi} d_{m\alpha}G_{\alpha}^{R(A)}(k)d_{l\alpha}(\theta)d_{m'\beta}(\theta)G_{\beta}^R(k)d_{l'\beta}(\theta), \quad (3.19)$$

where the Kronecker delta reflects the conservation of the angular momentum along z , owing to the azimuthal symmetry of the problem. In Eq.(3.19)

$$d_{m,m'} = \begin{pmatrix} \cos(\theta/2) & -\sin(\theta/2) \\ \sin(\theta/2) & \cos(\theta/2) \end{pmatrix}, \quad (3.20)$$

and the retarded and advanced Green's functions are

$$\begin{aligned}G_{+}^{R(A)} &= \frac{1}{-\xi_k - b_k + (-)i\gamma_{+}} \\ G_{-}^{R(A)} &= \frac{1}{-\xi_k + b_k + (-)i\gamma_{-}},\end{aligned}\quad (3.21)$$

where $\xi_k = \frac{k^2 - k_F^2}{2m}$, $b_k = \sqrt{\Delta_0^2 + \lambda^2 k^2}$, and γ_{\pm} is (half) the golden-rule scattering rate of the band quasiparticles. In addition, Eq. (3.13) is readily inverted to yield

$$\begin{aligned}\Lambda_{+,+}^{R(A),R} &= \Lambda_{-,-}^{R(A),R} = 0 \\ \Lambda_{+,-}^{R(A),R} &= \frac{1}{2} \frac{1}{1 - U_{+,-;+,-}^{R(A),R}} \\ \Lambda_{-,+}^{R(A),R} &= \frac{1}{2} \frac{1}{1 - U_{-,+;-,+}^{R(A),R}}\end{aligned}\quad (3.22)$$

In order to make further progress analytically we assume that $(\Delta_0, \lambda k_F, \gamma) \ll E_F = k_F^2/2m$. It then follows that $\gamma_+ \simeq \gamma_- \equiv \gamma$ and that $\gamma = \pi N_{2D} u^0 + \pi N_{2D} \frac{u^z}{4} \equiv \gamma_0 + \gamma_z$. Eqs. (3.19) and (3.20) combine to give

$$\begin{aligned}
U_{-,+;-,+}^{R,R} &= U_{+,-;+,-}^{R,R} = 0 \\
U_{-,+;-,+}^{A,R} &= (\gamma_0 - \gamma_z) \left[\frac{i}{-b + i\gamma} \cos^4 \left(\frac{\theta}{2} \right) + \frac{i}{b + i\gamma} \sin^4 \left(\frac{\theta}{2} \right) + \frac{2}{\gamma} \cos^2 \left(\frac{\theta}{2} \right) \sin^2 \left(\frac{\theta}{2} \right) \right] \\
U_{+,-;+,-}^{A,R} &= (U_{-,+;-,+}^{A,R})^*
\end{aligned} \tag{3.23}$$

where $b \simeq \sqrt{\lambda^2 k_F^2 + \Delta_0^2}$ and $\cos \theta \simeq \Delta_0/b$. The first and second terms in square brackets in Eq.(3.23) emerge from inter-band transitions ($\alpha \neq \beta$ in Eq. (3.19)), while the last term stems from intra-band transitions ($\alpha = \beta$). Amusingly, U vanishes when the spin-dependent scattering rate equals the Coulomb scattering rate ($\gamma_z = \gamma_0$); in this particular instance vertex corrections are completely absent. On the other hand, when $\gamma_z = 0$ and $b \ll \gamma$ we have $U_{-,+;-,+}^{A,R} \simeq U_{+,-;+,-}^{A,R} \simeq 1$, implying that vertex corrections strongly enhance Gilbert damping (recall Eq. (3.22)). We will discuss the role of vertex corrections more fully below.

After evaluating $\Lambda(\mathbf{k})$ from Eqs. (3.12),(3.22)and (3.23), the last step is to compute

$$P^{R(A),R} = \int_{\mathbf{k}} \Lambda_{\alpha,\beta}^{R(A),R}(\mathbf{k}) s_{\beta,\alpha}^x(\mathbf{k}) G_{\alpha}^{R(A)}(\mathbf{k}) G_{\beta}^R(\mathbf{k}). \tag{3.24}$$

Since we are assuming that the Fermi energy is the largest energy scale, the integrand in Eq. (3.24) is sharply peaked at the Fermi surface, leading to $P^{R,R} \simeq 0$. In the case of spin-independent scatterers ($\gamma_z = 0 \rightarrow \gamma = \gamma_0$),

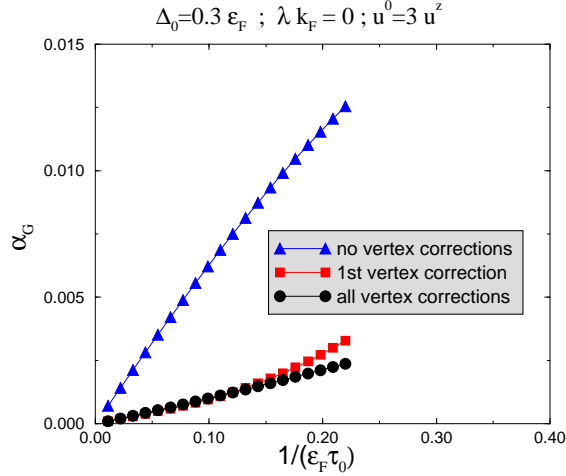


Figure 3.2: **M2DEG**: Gilbert damping in the absence of spin-orbit coupling. When the intrinsic spin-orbit interaction is small, the 1st vertex correction is sufficient for the evaluation of Gilbert damping, provided that the ferromagnet's exchange splitting is large compared to the lifetime-broadening of the quasiparticle energies. For more disordered ferromagnets ($E_F\tau_0 < 5$ in this figure) higher order vertex corrections begin to matter. In either case vertex corrections are significant. In this figure $1/\tau_0$ stands for the scattering rate off spin-independent impurities, defined as a two-band average at the Fermi energy, and the spin-dependent and spin-independent impurity strengths are chosen to satisfy $u^0 = 3u^z$.

tedious but straightforward algebra takes us to

$$\alpha_G(u^z = 0) = \frac{N_{2D}\Delta_0^2}{4s_0\gamma_0} \frac{(\lambda^2 k_F^2)(b^2 + \Delta_0^2 + 2\gamma_0^2)}{(b^2 + \Delta_0^2)^2 + 4\Delta_0^2\gamma_0^2}. \quad (3.25)$$

Eq. (29) agrees⁶ with results published in the recent literature.[18] We note that $\alpha_G(u^z = 0)$ vanishes in the absence of SO interactions, as expected. It is

⁶In Ref.[18] the inter-band splitting in the Green's function is Ω , while in our case it is $2b$. In addition, we neglect interactions between band quasiparticles.

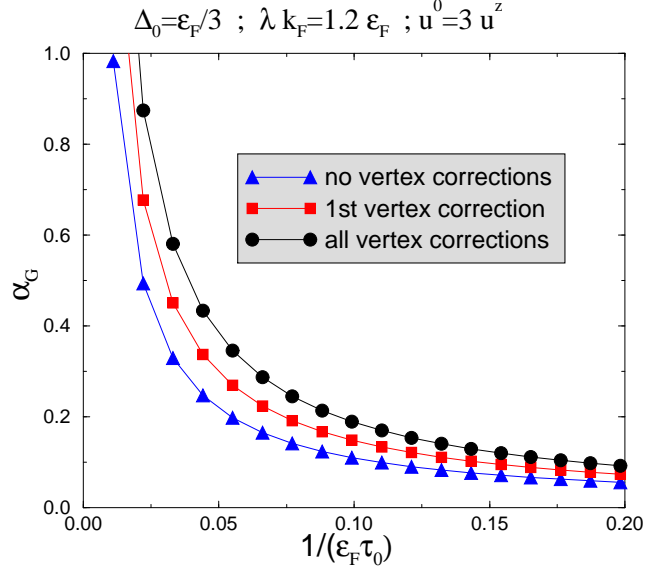


Figure 3.3: **M2DEG**: Gilbert damping for strong SO interactions ($\lambda k_F = 1.2 E_F \simeq 4 \Delta_0$). In this case higher order vertex corrections matter (up to 20 %) even at low disorder. This suggests that higher order vertex corrections will be important in real ferromagnetic semiconductors because their intrinsic SO interactions are generally stronger than their exchange splittings.

illustrative to expand Eq. (3.25) in the $b \gg \gamma_0$ regime:

$$\alpha_G(u^z = 0) \simeq \frac{N_{2D} \Delta_0^2}{2s_0} \left[\frac{\lambda^2 k_F^2}{2(b^2 + \Delta_0^2)} \frac{1}{\gamma_0} + \frac{\lambda^4 k_F^4}{(b^2 + \Delta_0^2)^3} \gamma_0 \right] \quad (3.26)$$

which displays intra-band ($\sim \gamma_0^{-1}$) and inter-band ($\sim \gamma_0$) contributions separately. The intra-band damping is due to the dependence of band eigenenergies on magnetization orientation, the *breathing Fermi surface* effect[16] which produces more damping when the band-quasiparticles scatter infrequently because the population distribution moves further from equilibrium. The intra-band contribution to damping therefore tends to scale with the conductivity.

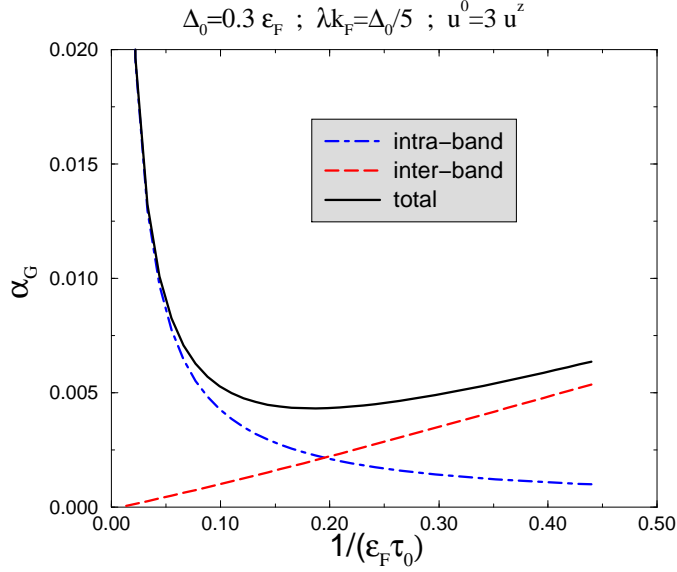


Figure 3.4: **M2DEG**: Gilbert damping for moderate SO interactions ($\lambda k_F = 0.2\Delta_0$). In this case there is a crossover between the intra-band dominated and the inter-band dominated regimes, which gives rise to a non-monotonic dependence of Gilbert damping on disorder strength. The stronger the intrinsic SO relative to the exchange field, the higher the value of disorder at which the crossover occurs. This is why the damping is monotonically increasing with disorder in Fig. (3.2) and monotonically decreasing in Fig. (3.3).

For stronger disorder, the inter-band term in which scattering relaxes spin-orientations takes over and α_G is proportional to the resistivity. Insofar as phonon-scattering can be treated as elastic, the Gilbert damping will often show a non-monotonic temperature dependence with the intra-band mechanism dominating at low-temperatures when the conductivity is large and the inter-band mechanism dominating at high-temperatures when the resistivity is large.

For completeness, we also present analytic results for the case $\gamma = \gamma_z$ in the $b \gg \gamma_z$ regime:

$$\alpha_G(u^0 = 0) \simeq \frac{N_{2D}\Delta_0^2}{2s_0} \left[\frac{1}{\gamma_z} \frac{\lambda^2 k_F^2}{6b^2 - 2\Delta_0^2} + \gamma_z \frac{3b^4 + 6b^2\Delta_0^2 - \Delta_0^4}{(3b^2 - \Delta_0^2)^3} \right] \quad (3.27)$$

This expression illustrates that spin-orbit (SO) interactions in the band structure are a necessary condition for the intra-band transition contribution to α_G . The interband contribution survives in absence of SO as long as the disorder potential is spin-dependent. Interband scattering is possible for spin-dependent disorder because majority and minority spin states on the Fermi surface are not orthogonal when their potentials are not identical. Note incidentally the contrast between Eq.(3.26) and Eq. (3.27): in the former the inter-band coefficient is most suppressed at weak intrinsic SO interaction while in the latter it is the intra-band coefficient which gets weakest for small λk_F .

More general cases relaxing the $(\Delta_0, \lambda k_F, \gamma) \ll E_F$ assumption must be studied numerically; the results are collected in Figs. (3.2), (3.3) and (3.4). Fig (3.2) highlights the inadequacy of completely neglecting vertex corrections in the limit of weak spin-orbit interaction; the inclusion of the the leading order vertex correction largely solves the problem. However, Fig. (3.2) and (3.3) together indicate that higher order vertex corrections are noticeable when disorder or spin-orbit coupling is strong. In the light of the preceding discussion the monotonic decay in Fig.(3.3) may appear surprising because the inter-band contribution presumably increases with γ . Yet, this argument is strictly correct only for weakly spin-orbit coupled systems, where the crossover

between inter-band and intra-band dominated regimes occurs at low disorder. For strongly spin-orbit coupled systems the crossover may take place at a scattering rate that is (i) beyond experimental relevance and/or (ii) larger than the band-splitting, in which case the inter-band contribution behaves much like its intra-band partner, i.e. $O(1/\gamma)$. Non-monotonic behavior is restored when the spin-orbit splitting is weaker, as shown in Fig. (3.4).

Finally, our analysis opens an opportunity to quantify the importance of higher order impurity vertex-corrections. Kohno, Shibata and Tatara [21] claim that the bare vertex along with the *first* vertex correction fully captures the Gilbert damping of a ferromagnet, provided that $\Delta_0\tau \gg 1$. To first order in U the vertex function is

$$\Lambda_{m,m'}^{R(A),R} = s_{m,m'}^x + \sum_{l'} U_{m,m':l,l'}^{R(A),R} s_{l,l'}^x \quad (3.28)$$

Taking $\gamma = \gamma_z$ for simplicity, we indeed get

$$\begin{aligned} \lim_{\lambda \rightarrow 0} \alpha_G &\simeq A\gamma + O(\gamma^2) \\ \frac{A(1)}{A(\infty)} &= 1 \end{aligned} \quad (3.29)$$

where $A(1)$ contains the first vertex correction only, and $A(\infty)$ includes all vertex corrections. However, the state of affairs changes after turning on the intrinsic SO interaction, whereupon Eq. (3.29) transforms into

$$\begin{aligned} \alpha_G(\lambda \neq 0) &\simeq B\gamma + C\frac{1}{\gamma} \\ \frac{B(1)}{B(\infty)} &= \frac{\Delta_0^2(3b^2 - \Delta_0^2)^3(3b^2 + \Delta_0^2)}{4b^6(3b^4 + 6b^2\Delta_0^2 - \Delta_0^4)} \\ \frac{C(1)}{C(\infty)} &= \frac{(b^2 + \Delta_0^2)(3b^2 - \Delta_0^2)}{4b^4} \end{aligned} \quad (3.30)$$

When $\Delta_0 \ll \lambda k_F$, both intra-band and inter-band ratios show a significant deviation from unity,⁷ to which they converge as $\lambda \rightarrow 0$. In order to understand this behavior, let us look back at Eq. (3.22). There, we can formally expand the vertex function as $\Lambda = \frac{1}{2} \sum_{n=0}^{\infty} U^n$, where the n -th order term stems from the n -th vertex correction. From Eq. (3.23) we find that when $\lambda = 0$, $U^n \sim O(\gamma^n)$ and thus $n \geq 2$ vertex corrections will not matter for the Gilbert damping, which is $O(\gamma)$ ⁸ when $E_F \gg \gamma$. In contrast, when $\lambda \neq 0$ the intra-band term in Eq. (3.23) is no longer zero, and consequently *all* powers of U contain $O(\gamma^0)$ and $O(\gamma^1)$ terms. In other words, all vertices contribute to $O(1/\gamma)$ and $O(\gamma)$ in the Gilbert damping, especially if $\lambda k_F/\Delta_0$ is not small. This conclusion should prove valid beyond the realm of the M2DEG because it relies only on the mantra “intra-band $\sim O(1/\gamma)$; inter-band $\sim O(\gamma)$ ”. Our expectation that higher order vertex corrections be important in (Ga,Mn)As will be confirmed numerically in the next section.

3.4 Gilbert Damping for (Ga,Mn)As

(Ga,Mn)As and other (III,Mn)V ferromagnets are like transition metals in that their magnetism is carried mainly by d-orbitals, but unlike transition metals in that neither majority nor minority spin d-orbitals are present at the

⁷ $C(1)$ and $C(\infty)$ differ by as much as 25%; the disparity between $B(1)$ and $B(\infty)$ may be even larger.

⁸The disorder dependence in α_G originates not only from the vertex part, but from the Green’s functions as well. It is useful to recall that $\int G_{\sigma} G_{-\sigma} \propto 1/(b + i\text{sg}(\sigma)\gamma)$ and $\int G_{\sigma} G_{\sigma} \propto 1/\gamma$.

Fermi energy. The orbitals at the Fermi energy are very similar to the states near the top of the valence band of the host (III,V) semiconductor, although they are of course weakly hybridized with the minority and majority spin d-orbitals. For this reason the electronic structure of (III,Mn)V ferromagnets is extremely simple and can be described reasonably accurately with the phenomenological model which we employ in this section. Because the top of the valence band in (III,V) semiconductors is split by spin-orbit interactions, spin-orbit coupling plays a dominant role in the bands of these ferromagnets. An important consequence of the strong SO interaction in the band structure is that diffusive vertex corrections influence α_G significantly at *all* orders; this is the central idea of this section.

Using a p-d mean-field theory model[37, 38] for the ferromagnetic ground state and a four-band spherical model[42] for the host semiconductor band structure, $\text{Ga}_{1-x}\text{Mn}_x\text{As}$ may be described by

$$H = \frac{1}{2m} \left[\left(\gamma_1 + \frac{5}{2}\gamma_2 \right) k^2 - 2\gamma_3(\mathbf{k} \cdot \mathbf{s})^2 \right] + \Delta_0 s^z, \quad (3.31)$$

where \mathbf{s} is the spin operator projected onto the $J=3/2$ total angular momentum subspace at the top of the valence band and $\{\gamma_1 = 6.98, \gamma_2 = \gamma_3 = 2.5\}$ are the Luttinger parameters for the spherical-band approximation to GaAs. In addition, $\Delta_0 = J_{pd}SN_{Mn}$ is the exchange field, $J_{pd} = 55\text{meVnm}^3$ is the p-d exchange coupling, $S = 5/2$ is the spin of the Mn ions, $N_{Mn} = 4x/a^3$ is the density of Mn ions, and $a = 0.565\text{nm}$ is the lattice constant of GaAs.

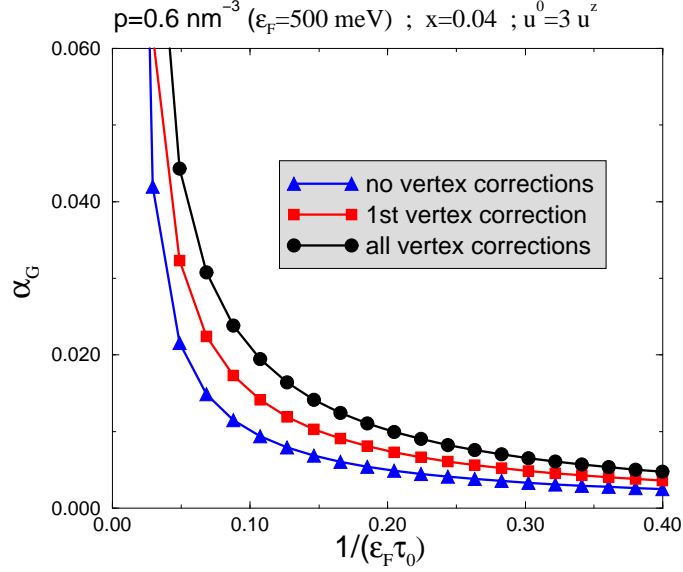


Figure 3.5: **GaMnAs**: Higher order vertex corrections make a significant contribution to Gilbert damping, due to the prominent spin-orbit interaction in the band structure of GaAs. x is the Mn fraction, and p is the hole concentration that determines the Fermi energy E_F . In this figure, the spin-independent impurity strength u^0 was taken to be 3 times larger than the magnetic impurity strength u^z . $1/\tau_0$ corresponds to the scattering rate off Coulomb impurities and is evaluated as a four-band average at the Fermi energy.

The $\Delta_0 = 0$ eigenstates of this model are

$$|\tilde{\alpha}, \mathbf{k}\rangle = e^{-is^z\phi} e^{-is^y\theta} |\tilde{\alpha}\rangle \quad (3.32)$$

where $|\tilde{\alpha}\rangle$ is an eigenstate of s^z with eigenvalue $\tilde{\alpha}$. Unfortunately, the analytical form of the $\Delta_0 \neq 0$ eigenstates is unknown. Nevertheless, since the exchange field preserves the azimuthal symmetry of the problem, the ϕ -dependence of the full eigenstates $|\alpha\mathbf{k}\rangle$ will be identical to that of Eq. (3.32). This observation leads to $U_{m,m':l,l'} \propto \delta_{m-m',l-l'}$, which simplifies Eq. (3.14). α_G can be

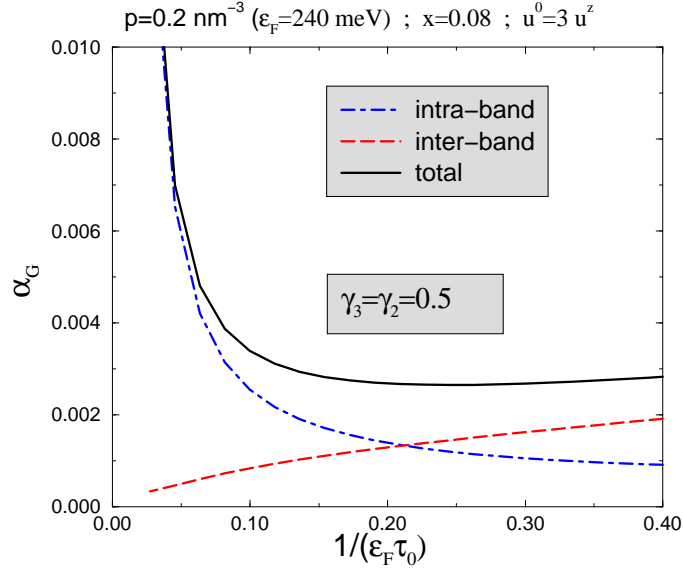


Figure 3.6: **GaMnAs**: When the spin-orbit splitting is reduced (in this case by reducing the hole density to 0.2 nm^{-3} and artificially taking $\gamma_3 = 0.5$), the crossover between inter- and intra-band dominated regimes produces a non-monotonic shape of the Gilbert damping, much like in Fig. (3.4). When either γ_2 or p is made larger or x is reduced, we recover the monotonic decay of Fig.(3.5).

calculated numerically following the steps detailed in the previous sections; the results are summarized in Figs. (3.5) and (3.6). Note that vertex corrections moderately increase the damping rate, as in the case of a M2DEG model with strong spin-orbit interactions. Fig. (3.5) underlines both the importance of higher order vertex corrections in (Ga,Mn)As and the monotonic decay of the damping as a function of scattering rate. The latter signals the supremacy of the intra-band contribution to damping, accentuated at larger hole concen-

trations. Had the intrinsic spin-orbit interaction been substantially weaker,⁹ α_G would have traced a non-monotonic curve as shown in Fig. (3.6). The degree to which the intraband *breathing Fermi surface* model effect dominates depends on the details of the band-structure and can be influenced by corrections to the spherical model which we have adopted here to simplify the vertex-correction calculation. The close correspondence between Figs. (3.5)-(3.6) and Figs. (3.3)-(3.4) reveals the success of the M2DEG as a versatile gateway for realistic models and justifies the extensive attention devoted to it in this paper and elsewhere.

3.5 Assessment of the torque-correlation formula

Thus far we have evaluated the Gilbert damping for a M2DEG model and a (Ga,Mn)As model using the (bare) spin-flip vertex $\langle\alpha, \mathbf{k}|s^x|\beta, \mathbf{k}\rangle$ and its renormalized counterpart $\langle\alpha, \mathbf{k}|\Lambda|\beta, \mathbf{k}\rangle$. The vertex corrected results are expected to be exact for $1/\tau$ small compared to the Fermi energy. For practical reasons, state-of-the-art band-structure calculations[26, 27] forgo impurity vertex corrections altogether and instead employ the *torque-correlation* matrix element, which we shall denote as $\langle\alpha, \mathbf{k}|K|\beta, \mathbf{k}\rangle$ (see below for an explicit expression). In this section we compare damping rates calculated using $s_{\alpha,\beta}^x$ vertices with those calculated using $K_{\alpha,\beta}$ vertices. We also compare both results with the exact damping rates obtained by using $\Lambda_{\alpha,\beta}$. The ensuing

⁹Notwithstanding that the four-band model is a $SO \rightarrow \infty$ limit of the more general six-band model, we shall tune the effective spin-orbit strength via p (hole concentration) and γ_3 .

discussion overlaps with and extends chapter 2.

We shall begin by introducing the following identity:[16]

$$\begin{aligned}
\langle \alpha, \mathbf{k} | s^x | \beta, \mathbf{k} \rangle &= i \langle \alpha, \mathbf{k} | [s^z, s^y] | \beta, \mathbf{k} \rangle \\
&= \frac{i}{\Delta_0} (E_{\mathbf{k},\alpha} - E_{\mathbf{k},\beta}) \langle \alpha, \mathbf{k} | s^y | \beta, \mathbf{k} \rangle \\
&\quad - \frac{i}{\Delta_0} \langle \alpha, \mathbf{k} | [H_{so}, s^y] | \beta, \mathbf{k} \rangle.
\end{aligned} \tag{3.33}$$

In Eq. (4.36) we have decomposed the mean-field quasiparticle Hamiltonian into a sum of spin-independent, exchange spin-splitting, and other spin-dependent terms: $H = H_{kin} + H_{so} + H_{ex}$, where H_{kin} is the kinetic (spin-independent) part, $H_{ex} = \Delta_0 s^z$ is the exchange spin-splitting term and H_{so} is the piece that contains the intrinsic spin-orbit interaction. The last term on the right hand side of Eq. (4.36) is the torque-correlation matrix element used in band structure computations:

$$\langle \alpha, \mathbf{k} | K | \beta, \mathbf{k} \rangle \equiv -\frac{i}{\Delta_0} \langle \alpha, \mathbf{k} | [H_{so}, s^y] | \beta, \mathbf{k} \rangle. \tag{3.34}$$

Eq. (4.36) allows us to make a few general remarks on the relation between the spin-flip and torque-correlation matrix elements. For intra-band matrix elements, one immediately finds that $s_{\alpha,\alpha}^x = K_{\alpha,\alpha}$ and hence the two approaches agree. For inter-band matrix elements the agreement between $s_{\alpha,\beta}^x$ and $K_{\alpha,\beta}$ should be nearly identical when the first term in the final form of Eq.(4.36) is small, *i.e.* when¹⁰ $(E_{\mathbf{k},\alpha} - E_{\mathbf{k},\beta}) \ll \Delta_0$. Since this requirement cannot

¹⁰Strictly speaking, it is $|s_{\alpha,\beta}^x|^2 \simeq |K_{\alpha,\beta}|^2$ what is needed, rather than $s_{\alpha,\beta}^x \simeq K_{\alpha,\beta}$. The former condition is less demanding, and can occasionally be satisfied when $E_\alpha - E_\beta$ is of the order of the exchange splitting.

be satisfied in the M2DEG, we expect that the inter-band contributions from K and s^x will always differ significantly in this model. More typical models, like the four-band model for (Ga,Mn)As, have band crossings at a discrete set of k-points, in the neighborhood of which $K_{\alpha,\beta} \simeq s_{\alpha,\beta}^x$. The relative weight of these crossing points in the overall Gilbert damping depends on a variety of factors. First, in order to make an impact they must be located within a shell of thickness $1/\tau$ around the Fermi surface. Second, the contribution to damping from those special points must outweigh that from the remaining k-points in the shell; this might be the case for instance in materials with weak spin-orbit interaction and weak disorder, where the contribution from the crossing points would go like τ (large) while the contribution from points far from the crossings would be $\sim 1/\tau$ (small). Only if these two conditions are fulfilled should one expect good agreement between the inter-band contribution from spin-flip and torque-correlation formulas. When vertex corrections are included, of course, the same result should be obtained using either form for the matrix element, since all matrix elements are between essentially degenerate electronic states when disorder is treated non-perturbatively.[18, 36]

In the remaining part of this section we shall focus on a more quantitative comparison between the different formulas. For the M2DEG it is straightforward to evaluate α_G analytically using K instead of s^x and neglecting vertex

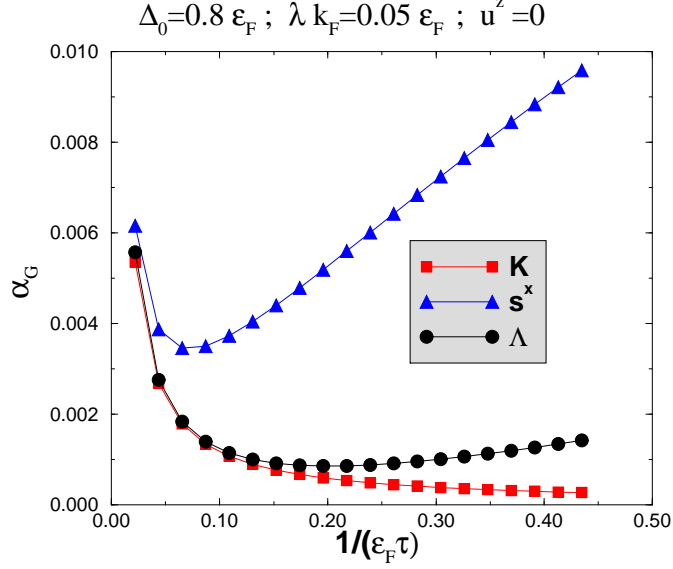


Figure 3.7: **M2DEG**: Comparison of Gilbert damping predicted using spin-flip and torque matrix element formulas, as well as the exact vertex corrected result. In this figure the intrinsic spin-orbit interaction is relatively weak ($\lambda k_F = 0.05 E_F \simeq 0.06 \Delta_0$) and we have taken $u^z = 0$. The torque correlation formula does not distinguish between spin-dependent and spin-independent disorder.

corrections; we obtain

$$\alpha_G^K = \frac{N_{2D} \Delta_0}{8s_0} \left[\frac{\lambda^2 k_F^2 \Delta_0}{b^2 \gamma} + \left(\frac{\lambda^2 k_F^2}{\Delta_0 b} \right)^2 \frac{\gamma \Delta_0}{\gamma^2 + b^2} \right] \quad (3.35)$$

where we assumed $(\gamma, \lambda k_F, \Delta_0) \ll \epsilon_F$. By comparing Eq. (3.35) with the exact expression Eq. (3.25), we find that the intra-band parts are in excellent agreement when $\Delta_0 \ll \lambda k_F$, i.e. when vertex corrections are relatively unimportant. In contrast, the inter-band parts differ markedly regardless of the vertex corrections. These trends are captured by Figs. (3.7) and (3.8), which compare the Gilbert damping obtained from s^x , K and Λ matrix elements.

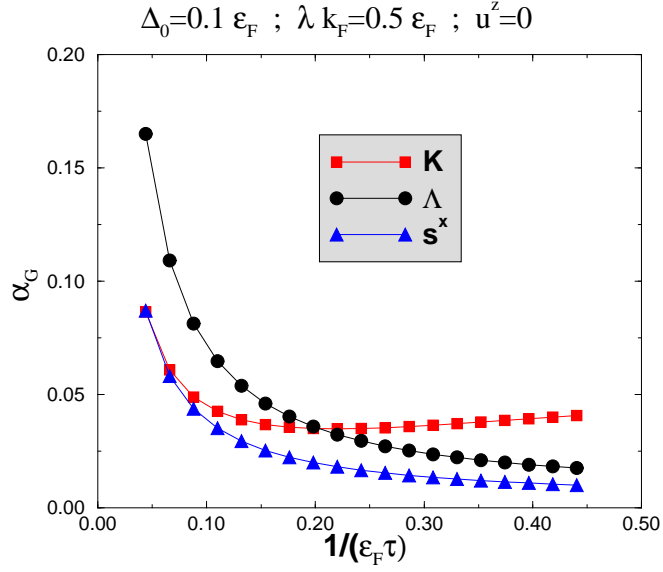


Figure 3.8: **M2DEG**: Comparison of Gilbert damping predicted using spin-flip and torque matrix element formulas, as well as the exact vertex corrected result. In this figure the intrinsic spin-orbit interaction is relatively strong ($\lambda k_F = 0.5 E_F = 5 \Delta_0$) and we have taken $u^z = 0$

Fig. (3.7) corresponds to the weak spin-orbit limit, where it is found that in disordered ferromagnets s^x may grossly overestimate the Gilbert damping because its inter-band contribution does not vanish even as SO tends to zero. As explained in Section III, this flaw may be repaired by adding the leading order impurity vertex correction. The torque-correlation formula is free from such problem because K vanishes identically in absence of SO interaction. Thus the main practical advantage of K is that it yields a physically sensible result without having to resort to vertex corrections. Continuing with Fig.(3.7), at weak disorder the intra-band contributions dominate and therefore s^x and K

coincide; even Λ agrees, because for intra-band transitions at weak spin-orbit interaction the vertex corrections are unimportant. Fig. (3.8) corresponds to the strong spin-orbit case. In this case, at low disorder s^x and K agree well with each other, but differ from the exact result because higher order vertex corrections alter the intra-band part substantially. For a similar reason, neither s^x nor K agree with the exact Λ at higher disorder. Based on these model calculations, we do not believe that there are any objective grounds to prefer either the K torque-correlation or the s^x spin-flip formula estimate of α_G when spin-orbit interactions are strong and α_G is dominated by inter-band relaxation. A precise estimation of α_G under these circumstances appears to require that the character of disorder, including its spin-dependence, be accounted for reliably and that the vertex-correction Dyson equation be accurately solved. Carrying out this program remains a challenge both because of technical complications in performing the calculation for general band structures and because disorder may not be sufficiently well characterized.

Analogous considerations apply for Figs. (3.9) and (3.10), which show results for the four-band model related to (Ga,Mn)As. These figures show results similar to those obtained in the strong spin-orbit limit of the M2DEG (Fig. 3.8). Overall, our study indicates that the *torque-correlation* formula captures the intra-band contributions accurately when the vertex corrections are unimportant, while it is less reliable for inter-band contributions unless the predominant inter-band transitions connect states that are close in energy. The torque-correlation formula has the practical advantage that it correctly

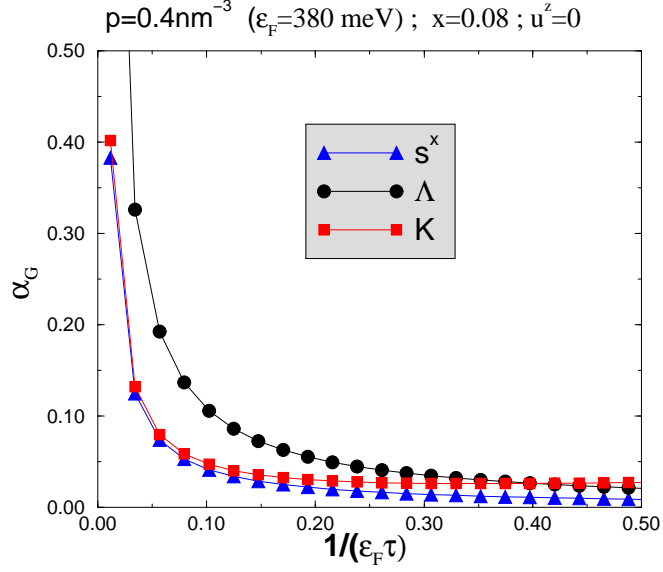


Figure 3.9: **GaMnAs**: Comparison of Gilbert damping predicted using spin-flip and torque matrix element formulas, as well as the exact vertex corrected result. p is the hole concentration that determines the Fermi energy E_F and x is the Mn fraction. Due to the strong intrinsic SO, this figure shows similar features as Fig.(3.8).

gives a zero spin relaxation rate when there is no spin-orbit coupling in the band structure and spin-independent disorder. The damping it captures derives entirely from spin-orbit coupling in the bands. It therefore incorrectly predicts, for example, that the damping rate vanishes when spin-orbit coupling is absent in the bands and the disorder potential is spin-dependent. Nevertheless, assuming that the dominant disorder is normally spin-independent, the K -formula may have a pragmatic edge over the s^x -formula in weakly spin-orbit coupled systems. In strongly spin-orbit coupled systems there appears to be little advantage of one formula over the other. We recommend that

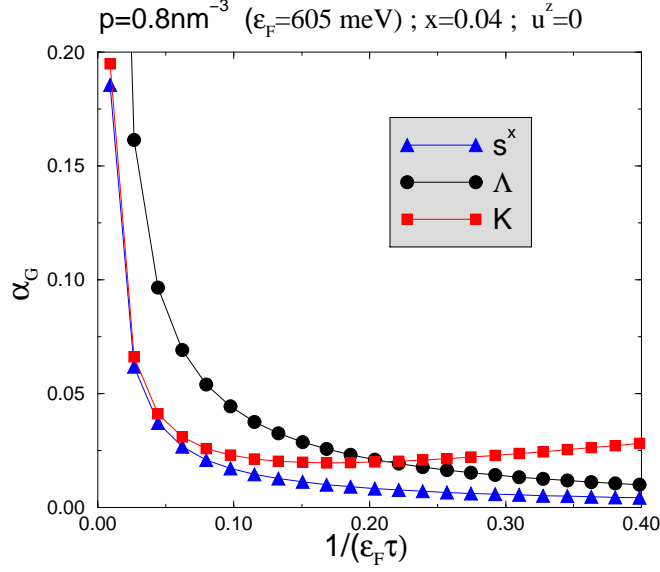


Figure 3.10: **GaMnAs**: Comparison of Gilbert damping predicted using spin-flip and torque matrix element formulas, as well as the exact vertex corrected result. In relation to Fig. (3.9) the effective spin-orbit interaction is stronger, due to a larger p and a smaller x .

inter-band and intra-band contributions be evaluated separately when α_G is evaluated using the torque-correlation formula. For the intra-band contribution the s^x and K life-time formulas are identical. The model calculations reported here suggest that vertex corrections to the intra-band contribution do not normally have an overwhelming importance. We conclude that α_G can be evaluated relatively reliably when the intra-band contribution dominates. When the inter-band contribution dominates it is important to assess whether or not the dominant contributions are coming from bands that are nearby in momentum space, or equivalently whether or not the matrix elements which contribute originate from pairs of bands that are energetically spaced by much

less than the exchange spin-splitting at the same wavevector. If the dominant contributions are from nearby bands, the damping estimate should have the same reliability as the intra-band contribution. If not, we conclude that the α_G estimate should be regarded with caution.

3.6 Conclusions

To summarize, this chapter has described an evaluation of Gilbert damping for two simple models, a two-dimensional electron-gas ferromagnet model with Rashba spin-orbit interactions and a four-band model which provides an approximate description of (III, Mn)V of ferromagnetic semiconductors. Our results are exact in the sense that they combine time-dependent mean field theory[36] with an impurity ladder-sum to all orders, hence giving us leverage to make the following statements. First, previously neglected higher order vertex corrections become quantitatively significant when the intrinsic spin-orbit interaction is larger than the exchange splitting. Second, strong intrinsic spin-orbit interaction leads to the the supremacy of intra-band contributions in (Ga,Mn)As, with the corresponding monotonic decay of the Gilbert damping as a function of disorder. Third, the spin-torque formalism used in *ab-initio* calculations of the Gilbert damping is quantitatively reliable as long as the intra-band contributions dominate *and* the exchange field is weaker than the spin-orbit splitting; if these conditions are not met, the use of the spin-torque matrix element in a life-time approximation formula offers no significant improvement over the original spin-flip matrix element.

Chapter 4

Non-Adiabatic Spin Transfer Torque in Real Materials

This chapter completes our studies of magnetization relaxation in conducting ferromagnets. It differs from and complements with the previous chapters by analyzing an inhomogeneously magnetized ferromagnet which is connected to a source and a drain. The motion of simple domain walls and of more complex magnetic textures in the presence of a transport current is described by the Landau-Lifshitz-Slonczewski (LLS) equations. Predictions of the LLS equations depend sensitively on the ratio between the dimensionless material parameter β which characterizes non-adiabatic spin-transfer torques and the Gilbert damping parameter¹ α . This ratio has been variously estimated to be close to zero, close to one, and large compared to one. By identifying β as the influence of a transport current on α , we derive a concise, explicit and relatively simple expression which relates β to the band structure and Bloch state lifetimes of a magnetic metal. Using this expression we demonstrate that intrinsic spin-orbit interactions lead to intra-band contributions to β which are often dominant and can be (i) estimated with some confidence

¹For ease of notation, in this chapter we denote the Gilbert damping as α rather than as α_G .

and (ii) interpreted using the “breathing Fermi surface” model.²

4.1 Introduction

An electric current can influence the magnetic state of a ferromagnet by exerting a *spin transfer torque*(STT) on the magnetization.[43–46] This effect occurs whenever currents travel through non-collinear magnetic systems and is therefore promising for magnetoelectronic applications. Indeed, STT’s have already been exploited in a number of technological devices.[47–49] Partly for this reason and partly because the quantitative description of order parameter manipulation by out-of-equilibrium quasiparticles poses great theoretical challenges, the study of the STT effect has developed into a major research subfield of spintronics.

Spin transfer torques are important in both magnetic multilayers, where the magnetization changes abruptly,[14, 50] and in magnetic nanowires, where the magnetization changes smoothly.[23, 51, 52] Theories of the STT in systems with smooth magnetic textures identify two different types of spin transfer. On one hand, the adiabatic or Slonczewski[46] torque results when quasiparticle spins follow the underlying magnetic landscape adiabatically. It can be mathematically expressed as $(\mathbf{v}_s \cdot \nabla)\mathbf{s}_0$, where \mathbf{s}_0 stands for the magnetization and \mathbf{v}_s is the “spin velocity”, which is proportional to the charge drift velocity, and

²The contents of this chapter are based on the article: Ion Garate, K. Gilmore, M.D. Stiles and A.H. MacDonald, *Non-Adiabatic Spin Transfer Torque in Real Materials*, Phys. Rev. B **79**, 104416 (2009).

hence to the current and the applied electric field. The microscopic physics of the Slonczewski spin-torque is thought to be well understood[23, 50–56], at least[57] in systems with weak spin-orbit coupling. A simple angular momentum conservation argument argues that in the absence of spin-orbit coupling $\mathbf{v}_s = \sigma_s \mathbf{E} / e s_0$, where s_0 is the magnetization, σ_s is the spin conductivity and \mathbf{E} is the electric field. However, spin-orbit coupling plays an essential role in real magnetic materials and hence the validity of this simple expression for v_s needs to be tested by more rigorous calculations.

The second spin transfer torque in continuous media, $\beta \mathbf{s}_0 \times (\mathbf{v}_s \cdot \nabla) \mathbf{s}_0$, acts in the perpendicular direction and is frequently referred to as the non-adiabatic torque.[58] Unfortunately, the name is a misnomer in the present context. There are two contributions that have the preceding form. The first is truly non-adiabatic and occurs in systems in which the magnetization varies too rapidly in space for the spins of the transport electrons to follow the local magnetization direction as they traverse the magnetization texture. For wide domain walls, these effects are expected to be small.[59] The contribution of interest in this paper is a dissipative contribution that occurs in the adiabatic limit. The adiabatic torque discussed above is the reactive contribution in this limit. As we discuss below, processes that contribute to magnetic damping, whether they derive from spin-orbit coupling or spin-dependent scattering, also give a spin-transfer torque parameterized by β as above. In this paper, we follow the common convention and refer to this torque as non-adiabatic. However, it should be understood that it is a dissipative spin transfer torque

that is present in the adiabatic limit.

The non-adiabatic torque plays a key role in current-driven domain wall dynamics, where the ratio between β and the Gilbert parameter α can determine the velocity of domain walls under the influence of a transport current. There is no consensus on the magnitude of the parameter β . [23, 60] Although there have a few theoretical studies [19, 21, 22] of the STT in toy models, the relationship between toy model STT's and STT's in either transition metal ferromagnets or ferromagnetic semiconductors is far from clear. As we will discuss the toy models most often studied neglect spin-orbit interactions in the band-structure of the perfect crystal, namely *intrinsic* spin-orbit interactions, which can alter STT physics qualitatively.

The main objectives of this chapter are (i) to shed new light on the physical meaning of the non-adiabatic STT by relating it to the change in magnetization damping due to a transport current, (ii) to derive a concise formula that can be used to evaluate β in real materials from first principles and (iii) to demonstrate that α and β have the same qualitative dependence on disorder (or temperature), even though their ratio depends on the details of the band structure. As a byproduct of our theoretical study, we find that the expression for v_s in terms of the spin conductivity may not always be accurate in materials with strong spin-orbit coupling.

We begin in Sec. II by reviewing and expanding on microscopic theories of α , β and v_s . In short, our microscopic approach quantifies how the micromagnetic energy of an inhomogeneous ferromagnet is altered in response

to external rf fields and dc transport currents which drive the magnetization direction away from local equilibrium. These effects are captured by the spin transfer torques, damping torques, and effective magnetic fields that appear in the LLS equation. By relating magnetization dynamics to effective magnetic fields, we derive explicit expressions for α, β and v_s in terms of microscopic parameters. Important contributions to these materials parameters can be understood in clear physical terms using the breathing Fermi surface model.[61] Readers mainly interested in a qualitative explanation for our findings may skip directly to Sec. VIII where we discuss of our main results in that framework. Regardless of the approach, the non-adiabatic STT can be understood as the change in the Gilbert damping contribution to magnetization dynamics when the Fermi sea quasiparticle distribution function is altered by the transport electric field. The outcome of this insight is a concise analytical formula for β which is simple enough that it can be conveniently combined with first-principles electronic structure calculations to predict β -values in particular materials.³

In Secs. III-V we apply our expression for β to model ferromagnets. In Sec. III we perform a necessary reality check by applying our theory of β to the parabolic band Stoner ferromagnet, the only model for which more rigorous fully microscopic calculations[22, 52] of β have been completed. Sec. IV is devoted to the study of a two-dimensional electron-gas ferromagnet with Rashba spin-orbit interactions. Studies of this model provide a qualitative indication

³K. Gilmore, I. Garate, P.M. Haney, A.H. MacDonald and M.D. Stiles, in preparation

of the influence of intrinsic spin-orbit interactions on the non-adiabatic STT. We find that, as in the microscopic theory[34, 36] for α , spin-orbit interactions induce intra-band contributions to β which are proportional to the quasiparticle lifetimes. These considerations carry over to the more sophisticated 4-band spherical model that we analyze in Sec. V; there our calculation is tailored to (Ga,Mn)As. We show that intra-band (conductivity like) contributions are prominent in the 4-band model for experimentally relevant scattering rates.

Sec. VI discusses the phenomenologically important α/β ratio for real materials. Using our analytical results derived in Sec. II (or Sec. VIII) we are able to reproduce and extrapolate trends expected from toy models which indicate that α/β should vary across materials in approximately the same way as the ratio between the itinerant spin density and the total spin density. We also suggest that α and β may have the opposite signs in systems with both hole-like and electron-like carriers. We present concrete results for (Ga,Mn)As, where we obtain $\alpha/\beta \simeq 0.1$. This is reasonable in view of the weak spin polarization and the strong spin-orbit coupling of valence band holes in this material.

Sec. VII describes the generalization of the *torque-correlation* formula employed in *ab-initio* calculations of the Gilbert damping to the case of the non-adiabatic spin-transfer torque. The torque correlation formula incorporates scattering of quasiparticles simply by introducing a phenomenological lifetime for the Bloch states and assumes that the most important electronic transitions occur between states near the Fermi surface in the same band.

Our ability to make quantitative predictions based on this formula is limited mainly by an incomplete understanding of Bloch state scattering processes in real ferromagnetic materials. These simplifications give rise to ambiguities and inaccuracies that we dissect in Sec. VII. Our assessment indicates that the torque correlation formula for β is most accurate at low disorder and relatively weak spin-orbit interactions.

Sec. VIII restates and complements the effective field calculation explained in Sec. II. Within the adiabatic approximation, the instantaneous energy of a ferromagnet may be written in terms of the instantaneous occupation factors of quasiparticle states. We determine the effect of the external perturbations on the occupation factors by combining the relaxation time approximation and the master equation. In this way we recover the results of Sec. II and are able to interpret the intra-band contributions to β in terms of a generalized breathing Fermi surface picture.

Sec. IX contains a brief summary which concludes this chapter.

4.2 Microscopic Theory of α , β and v_s

The Gilbert damping parameter α , the non-adiabatic spin transfer torque coefficient β and the “spin velocity” \mathbf{v}_s appear in the generalized Landau-Lifshitz-Gilbert expression for collective magnetization dynamics of a ferromagnet under the influence of an electric current:

$$(\partial_t + \mathbf{v}_s \cdot \nabla) \hat{\Omega} - \hat{\Omega} \times \mathcal{H}_{\text{eff}} = -\alpha \hat{\Omega} \times \partial_t \hat{\Omega} - \beta \hat{\Omega} \times (\mathbf{v}_s \cdot \nabla) \hat{\Omega}. \quad (4.1)$$

In Eq. (4.1) \mathcal{H}_{eff} is an effective magnetic field which we elaborate on below and $\hat{\Omega} = \mathbf{s}_0/s_0 \simeq (\Omega_x, \Omega_y, 1 - (\Omega_x^2 + \Omega_y^2)/2)$ is the direction of the magnetization. Eq. (4.1) describes the slow dynamics of smooth magnetization textures in the presence of a weak electric field which induces transport currents. It explicitly neglects the dynamics of the magnetization magnitude which is implicitly assumed to be negligible. For small deviations from the easy direction (which we take to be the \hat{z} -direction), it reads

$$\begin{aligned}\mathcal{H}_{\text{eff},x} &= (\partial_t + \mathbf{v}_s \cdot \nabla) \Omega_y + (\alpha \partial_t + \beta \mathbf{v}_s \cdot \nabla) \Omega_x \\ \mathcal{H}_{\text{eff},y} &= -(\partial_t + \mathbf{v}_s \cdot \nabla) \Omega_x + (\alpha \partial_t + \beta \mathbf{v}_s \cdot \nabla) \Omega_y\end{aligned}\quad (4.2)$$

The gyromagnetic ratio has been absorbed into the units of the field \mathcal{H}_{eff} so that this quantity has inverse time units. We set $\hbar = 1$ throughout.

In this section we relate the α , β and \mathbf{v}_s parameters to microscopic features of the ferromagnet by considering the transverse total spin response function. For a technically more accessible (yet less rigorous) theory of α and β we refer to Sec. VIII. The transverse spin response function studied here describes the change in the micromagnetic energy due to the departure of the magnetization away from its equilibrium direction, where equilibrium is characterized by the absence of currents and external rf fields. This change in energy defines an effective magnetic field which may then be identified with Eq. (4.2), thereby allowing us to microscopically determine α, β and v_s . To first order in frequency ω , wave vector \mathbf{q} and electric field, the transverse spin

response function is given by

$$S_0 \hat{\Omega}_a = \sum_b \chi_{a,b} \mathcal{H}_{\text{ext},b} \simeq \sum_b \left[\chi_{a,b}^{(0)} + \omega \chi_{a,b}^{(1)} + (\mathbf{v}_s \cdot \mathbf{q}) \chi_{a,b}^{(2)} \right] \mathcal{H}_{\text{ext},b} \quad (4.3)$$

where $a, b \in \{x, y\}$, \mathcal{H}_{ext} is the external magnetic field with frequency ω and wave vector \mathbf{q} , $S_0 = s_0 V$ is the total spin of the ferromagnet (V is the sample volume), and χ is the transverse spin-spin response function in the presence of a uniform time-independent electric field:

$$\chi_{a,b}(\mathbf{q}, \omega; \mathbf{v}_s) = i \int_0^\infty dt \int d\mathbf{r} \exp(i\omega t - i\mathbf{q} \cdot \mathbf{r}) \langle [S^a(\mathbf{r}, t), S^b(\mathbf{0}, 0)] \rangle. \quad (4.4)$$

In Eq. (4.3), $\chi^{(0)} = \chi(\mathbf{q} = \mathbf{0}, \omega = 0; \mathbf{E} = \mathbf{0})$ describes the spin response to a constant, uniform external magnetic field in absence of a current, $\chi^{(1)} = \lim_{\omega \rightarrow 0} \chi(\mathbf{q} = \mathbf{0}, \omega; \mathbf{E} = \mathbf{0})/\omega$ characterizes the spin response to a time-dependent, uniform external magnetic field in absence of a current, and $\chi^{(2)} = \lim_{q, v_s \rightarrow 0} \chi(\mathbf{q}, \omega = 0; \mathbf{E})/\mathbf{q} \cdot \mathbf{v}_s$ represents the spin response to a constant, non-uniform external magnetic field combined with a constant, uniform electric field \mathbf{E} . Note that first order terms in \mathbf{q} are allowed by symmetry in presence of an electric field. In addition, $\langle \rangle$ is a thermal and quantum mechanical average over states that describe a uniformly magnetized, current carrying ferromagnet.

The approach underlying Eq. (4.3) comprises a linear response theory with respect to an inhomogeneous magnetic field *followed by* a linear response theory with respect to an electric field. Alternatively, one may treat the electric and magnetic perturbations on an equal footing without predetermined ordering; for further considerations on this matter we refer to Appendix A.

In the following we emulate and appropriately generalize a procedure outlined elsewhere.[36] First, we recognize that in the static limit and in absence of a current the transverse magnetization responds to the external magnetic field by adjusting its orientation to minimize the total energy including the internal energy E_{int} and the energy due to coupling with the external magnetic field, $E_{ext} = -S_0\hat{\Omega}\cdot\mathcal{H}_{ext}$. It follows that $\chi_{a,b}^{(0)} = S_0^2[\partial^2 E_{int}/\partial\hat{\Omega}_a\partial\hat{\Omega}_b]^{-1}$ and thus $\mathcal{H}_{int,a} = -(1/S_0)\partial E_{int}/\partial\hat{\Omega}_a = -S_0[\chi^{(0)}]_{a,b}^{-1}\hat{\Omega}_b$, where \mathcal{H}_{int} is the internal energy contribution to the effective magnetic field. Multiplying Eq. (4.3) on the left by $[\chi^{(0)}]^{-1}$ and using $\mathcal{H}_{eff} = \mathcal{H}_{int} + \mathcal{H}_{ext}$ we obtain a formal equation for \mathcal{H}_{eff} :

$$\mathcal{H}_{eff,a} = \sum_b \left[\mathcal{L}_{a,b}^{(1)}\partial_t + \mathcal{L}_{a,b}^{(2)}(\mathbf{v}_s \cdot \nabla) \right] \hat{\Omega}_b, \quad (4.5)$$

where

$$\begin{aligned} \mathcal{L}^{(1)} &= -iS_0[\chi^{(0)}]^{-1}\chi^{(1)}[\chi^{(0)}]^{-1} \\ \mathcal{L}^{(2)} &= iS_0[\chi^{(0)}]^{-1}\chi^{(2)}[\chi^{(0)}]^{-1}. \end{aligned} \quad (4.6)$$

Identifying Eqs. (4.5) and (4.2) results in concise microscopic expressions for α and β and \mathbf{v}_s :

$$\begin{aligned} \alpha &= \mathcal{L}_{x,x}^{(1)} = \mathcal{L}_{y,y}^{(1)} \\ \beta &= \mathcal{L}_{x,x}^{(2)} = \mathcal{L}_{y,y}^{(2)} \\ 1 &= \mathcal{L}_{x,y}^{(2)} \implies \mathbf{v}_s \cdot \mathbf{q} = iS_0 [(\chi^{(0)})^{-1}\chi(\chi^{(0)})^{-1}]_{x,y}. \end{aligned} \quad (4.7)$$

In the third line of Eq. (4.7) we have combined the second line of Eq. (4.6) with $\chi^{(2)} = \chi/(\mathbf{v}_s \cdot \mathbf{q})$.

When applying Eq. (4.7) to realistic conducting ferromagnets, one must invariably adopt a self-consistent mean-field (Stoner) theory description of the magnetic state derived within a spin-density-functional theory (SDFT) framework.[28, 29] In SDFT the transverse spin response function is expressed in terms of Kohn-Sham quasiparticle response to both external and induced magnetic fields; this allows us to transform[36] Eq. (4.7) into

$$\begin{aligned}
\alpha &= \frac{1}{S_0} \lim_{\omega \rightarrow 0} \frac{\text{Im}[\tilde{\chi}_{+,-}^{\text{QP}}(\mathbf{q} = 0, \omega, \mathbf{E} = 0)]}{\omega} \\
\beta &= -\frac{1}{S_0} \lim_{\mathbf{v}_s, \mathbf{q} \rightarrow 0} \frac{\text{Im}[\tilde{\chi}_{+,-}^{\text{QP}}(\mathbf{q}, \omega = 0, \mathbf{E})]}{\mathbf{q} \cdot \mathbf{v}_s} \\
\mathbf{v}_s \cdot \mathbf{q} &= -\frac{1}{S_0} \text{Re}[\tilde{\chi}_{+,-}^{\text{QP}}(\mathbf{q}, \omega = 0, \mathbf{E})], \tag{4.8}
\end{aligned}$$

where we have used⁴ $\chi_{a,b}^{(0)} = \delta_{a,b} S_0 / \bar{\Delta}$ and

$$\begin{aligned}
\tilde{\chi}_{+,-}^{\text{QP}}(\mathbf{q}, \omega; \mathbf{E}) &= \frac{1}{2} \sum_{i,j} \frac{f_j - f_i}{\epsilon_i - \epsilon_j - \omega - i\eta} \\
&\quad \langle j | S^+ \Delta_0(\mathbf{r}) e^{i\mathbf{q}\cdot\mathbf{r}} | i \rangle \langle i | S^- \Delta_0(\mathbf{r}) e^{-i\mathbf{q}\cdot\mathbf{r}} | j \rangle
\end{aligned} \tag{4.9}$$

is the quasiparticle response to changes in the direction of the exchange-correlation effective magnetic field.⁵ To estimate β this response function should be evaluated in the presence of an electric current. In the derivation of Eq. (4.8) we have made use of $S^\pm = S_x \pm iS_y$. Physically, “Im” and “Re”

⁴We assume that magnetic anisotropy and the external magnetic fields are weak compared to the exchange-correlation splitting of the ferromagnet. $\bar{\Delta}$ is the spin-density weighted average of $\Delta(\mathbf{r})$ (see Ref.[36]).

⁵For convenience in Eq. (4.8) we use $\langle S^+ S^- \rangle$ response functions instead of $\langle S^x S^x \rangle$ and $\langle S^y S^y \rangle$. They are related via $S^x = (S^+ + S^-)/2$ and $S^y = (S^+ - S^-)/2i$.

indicate that the Gilbert damping and the non-adiabatic STT are dissipative while the adiabatic STT is reactive. Furthermore, in the third line it is implicit that we expand $\text{Re}[\tilde{\chi}^{\text{QP}}]$ to first order in q and E .

In Eq. (4.9), S^\pm is the spin-rising/lowering operator, $|i\rangle$, ϵ_i and f_i are the Kohn-Sham eigenstates, eigenenergies and Fermi factors in presence of spin-dependent disorder, and $\Delta_0(\mathbf{r})$ is the difference in the magnetic ground state between the majority spin and minority spin exchange-correlation potential - the spin-splitting potential. This quantity is always spatially inhomogeneous at the atomic scale and is typically larger in atomic regions than in interstitial regions. Although the spatial dependence of $\Delta_0(\mathbf{r})$ plays a crucial role in realistic ferromagnets, we replace it by a phenomenological *constant* Δ_0 in the toy models we discuss below.

Our expression of v_s in terms of the transverse spin response function may be unfamiliar to readers familiar with the argument given in the introduction of this paper in which v_s is determined by the divergence in spin current. This argument is based on the assumption that the (transverse) angular momentum lost by spin polarized electrons traversing an inhomogeneous ferromagnet is transferred to the magnetization. However, this assumption fails when spin angular momentum is not conserved as it is not in the presence of spin-orbit coupling. In general, part of the transverse spin polarization lost by the current carrying quasiparticles is transferred to the lattice rather than to collective magnetic degrees of freedom[57] when spin-orbit interactions are present. It is often stated that the physics of spin non-conservation is captured

by the non-adiabatic STT; however, the non-adiabatic STT *per se* is limited to dissipative processes and cannot describe the changes in the reactive spin torque due to spin-flip events. Our expression in terms of the transverse spin response function does not rely on spin conservation, and while it agrees with the conventional picture[62] in simplest cases (see below), it departs from it when *e.g.* intrinsic spin-orbit interactions are strong.

In this paper we incorporate the influence of an electric field by simply shifting the Kohn-Sham orbital occupation factors to account for the energy deviation of the distribution function in a drifting Fermi sea:

$$f_i \simeq f^{(0)}(\epsilon_i + V_i) \simeq f^{(0)}(\epsilon_i) + V_i \partial f^{(0)} / \partial \epsilon_i \quad (4.10)$$

where V_i is the effective energy shift for the i -th eigenenergy due to acceleration between scattering events by an electric field and $f^{(0)}$ is the equilibrium Fermi factor. This approximation to the steady-state induced by an external electric field is known to be reasonably accurate in many circumstances, for example in theories of electrical transport properties, and it can be used[62] to provide a microscopic derivation of the adiabatic spin-transfer torque. As we discuss below, this *ansatz* provides a result for β which is sufficiently simple that it can be combined with realistic *ab initio* electronic structure calculations to estimate β values in particular magnetic metals. We support this *ansatz* by demonstrating that it agrees with full non-linear response calculations in the case of toy models for which results are available.

Using the Cauchy identity, $1/(x - i\eta) = 1/x + i\pi\delta(x)$, and $\partial f^{(0)} / \partial \epsilon \simeq$

$-\delta(\epsilon)$ we obtain

$$\begin{aligned}\text{Im}[\tilde{\chi}_{+,-}^{\text{QP}}] &\simeq \frac{\pi}{2} \sum_{i,j} [\omega - V_{j,i}] |\langle j|S^+ \Delta_0(\mathbf{r}) e^{i\mathbf{q}\cdot\mathbf{r}}|i\rangle|^2 \delta(\epsilon_i - \epsilon_{\text{F}}) \delta(\epsilon_j - \epsilon_{\text{F}}) \\ \text{Re}[\tilde{\chi}_{+,-}^{\text{QP}}] &\simeq -\frac{1}{2} \sum_{i,j} |\langle j|S^+ \Delta_0(\mathbf{r}) e^{i\mathbf{q}\cdot\mathbf{r}}|i\rangle|^2 \frac{V_j \delta(\epsilon_j - \epsilon_{\text{F}}) - V_i \delta(\epsilon_i - \epsilon_{\text{F}})}{\epsilon_i - \epsilon_j}\end{aligned}\quad (4.11)$$

where we have defined the difference in transport deviation energies by

$$V_{j,i} \equiv V_j - V_i. \quad (4.12)$$

In the first line of Eq. (4.11), the two terms within the square brackets correspond to the energy of particle-hole excitations induced by radio frequency magnetic and static electric fields, respectively. The imaginary part selects scattering processes that relax the spin of the particle-hole pairs mediated either by phonons or by magnetic impurities.[9] Substituting Eq. (4.11) into Eq. (4.8) we can readily extract α , β and \mathbf{v}_s :

$$\begin{aligned}\alpha &= \frac{\pi}{2S_0} \sum_{i,j} |\langle j|S^+ \Delta_0(\mathbf{r})|i\rangle|^2 \delta(\epsilon_i - \epsilon_{\text{F}}) \delta(\epsilon_j - \epsilon_{\text{F}}) \\ \beta &= \lim_{q, v_s \rightarrow 0} \frac{\pi}{2S_0 \mathbf{q} \cdot \mathbf{v}_s} \sum_{i,j} |\langle j|S^+ \Delta_0(\mathbf{r}) e^{i\mathbf{q}\cdot\mathbf{r}}|i\rangle|^2 V_{j,i} \delta(\epsilon_i - \epsilon_{\text{F}}) \delta(\epsilon_j - \epsilon_{\text{F}}) \\ \mathbf{v}_s \cdot \mathbf{q} &= \frac{1}{2S_0} \sum_{i,j} |\langle j|S^+ \Delta_0(\mathbf{r}) e^{i\mathbf{q}\cdot\mathbf{r}}|i\rangle|^2 \frac{V_j \delta(\epsilon_j - \epsilon_{\text{F}}) - V_i \delta(\epsilon_i - \epsilon_{\text{F}})}{\epsilon_i - \epsilon_j}\end{aligned}\quad (4.13)$$

where we have assumed a uniform precession mode for the Gilbert damping.

Eq. (4.13) and Eq. (4.11) identify the non-adiabatic STT as a *correction* to the Gilbert damping in the presence of an electric current; in other words, the magnetization damping at finite current is given by the sum of the Gilbert damping and the non-adiabatic STT. We feel that this simple interpretation

of the non-adiabatic spin-transfer torque has not received sufficient emphasis in the literature.

Strictly speaking the influence of a transport current on magnetization dynamics should be calculated by considering non-linear response of transverse spin to both effective magnetic fields and the external electric field which drives the transport current. Our approach, in which we simply alter the occupation probabilities which appear in the transverse spin response function is admittedly somewhat heuristic. We demonstrate below that it gives approximately the same result as the complete calculation for the case of the very simplistic model for which that complete calculation has been carried out.

In Eq. (4.13), the eigenstates indexed by i are not Bloch states of a periodic potential but instead the eigenstates of the Hamiltonian that includes all of the static disorder. Although Eq. (4.13) provides compact expressions valid for arbitrary metallic ferromagnets, its practicality is hampered by the fact that the characterization of disorder is normally not precise enough to permit a reliable solution of the Kohn-Sham equations with arbitrary impurities. An approximate yet more tractable treatment of disorder consists of the following steps: (i) replace the actual eigenstates of the disordered system by Bloch eigenstates corresponding to a pure crystal, *e.g.* $|i\rangle \rightarrow |\mathbf{k}, a\rangle$, where \mathbf{k} is the crystal momentum and a is the band index of the perfect crystal; (ii) switch V_i to $V_a = \tau_{\mathbf{k},a} \mathbf{v}_{\mathbf{k},a} \cdot e\mathbf{E}$, where τ is the Bloch state lifetime and $\mathbf{v}_{\mathbf{k},a} = \partial\epsilon_{\mathbf{k},a}/\partial\mathbf{k}$ is the quasiparticle group velocity, (iii) substitute the $\delta(\epsilon_{\mathbf{k},a} - \epsilon_F)$ spectral function of a Bloch state by a broadened spectral function evaluated at the Fermi

energy: $\delta(\epsilon_{\mathbf{k},a} - \epsilon_F) \rightarrow A_a(\epsilon_F, \mathbf{k})/(2\pi)$, where

$$A_a(\epsilon_F, \mathbf{k}) = \frac{\Gamma_{\mathbf{k},a}}{(\epsilon_F - \epsilon_{\mathbf{k},a})^2 + \frac{\Gamma_{\mathbf{k},a}^2}{4}} \quad (4.14)$$

and $\Gamma_{a,\mathbf{k}} = 1/\tau_{a,\mathbf{k}}$ is the inverse of the quasiparticle lifetime. This minimal prescription can be augmented by introducing impurity vertex corrections in one of the spin-flip operators, which restores an exact treatment of disorder in the limit of dilute impurities. This task is for the most part beyond the scope of this paper (see next section, however). The expression for α in Eq. (4.13) has already been discussed in a previous paper;^[36] hence from here on we shall concentrate on the expression for β which now reads

$$\begin{aligned} \beta^{(0)} = & \lim_{q, v_s \rightarrow 0} \frac{1}{8\pi s_0} \sum_{a,b} \int_{\mathbf{k}} |\langle \mathbf{k} + \mathbf{q}, b | S^+ \Delta_0(\mathbf{r}) | \mathbf{k}, a \rangle|^2 A_a(\epsilon_F, \mathbf{k}) A_b(\epsilon_F, \mathbf{k} + \mathbf{q}) \\ & \times \frac{(\mathbf{v}_{\mathbf{k}+\mathbf{q},b} \tau_{\mathbf{k}+\mathbf{q},b} - \mathbf{v}_{\mathbf{k},a} \tau_{\mathbf{k},a}) \cdot e\mathbf{E}}{\mathbf{q} \cdot \mathbf{v}_s} \end{aligned} \quad (4.15)$$

where we have used $\sum_{\mathbf{k}} \rightarrow V \int d^D k / (2\pi)^D \equiv V \int_{\mathbf{k}}$ with D as the dimensionality, V as the volume and

$$\mathbf{q} \cdot \mathbf{v}_s = \frac{1}{2s_0} \sum_{a,b} \int_{\mathbf{k}} |\langle \mathbf{k} + \mathbf{q}, b | S^+ \Delta_0(\mathbf{r}) | \mathbf{k}, a \rangle|^2 \frac{e\mathbf{v}_{\mathbf{k}+\mathbf{q},b} \tau_{\mathbf{k}+\mathbf{q},b} \delta(\epsilon_F - \epsilon_{\mathbf{k}+\mathbf{q},b}) - e\mathbf{v}_{\mathbf{k},a} \tau_{\mathbf{k},a} \delta(\epsilon_F - \epsilon_{\mathbf{k},a})}{\epsilon_{\mathbf{k},a} - \epsilon_{\mathbf{k}+\mathbf{q},b}}. \quad (4.16)$$

In Eq. (4.15) the superscript “0” is to remind of the absence of impurity vertex corrections; . In addition, we recall that $s_0 = S_0/V$ is the magnetization of the ferromagnet and $|a\mathbf{k}\rangle$ is a band eigenstate of the ferromagnet *without* disorder. It is straightforward to show that Eq. (4.16) reduces to the usual expression $v_s = \sigma_s E / (e s_0)$ for vanishing intrinsic spin-orbit coupling. However, we find

that in presence of spin-orbit interaction Eq. (4.16) is no longer connected to the spin conductivity. Determining the precise way in which Eq. (4.16) departs from the conventional formula in real materials is an open problem that may have fundamental and practical repercussions. Expanding the integrand in Eq. (4.15) to first order in q and rearranging the result we arrive at

$$\begin{aligned}
\beta^{(0)} = & -\frac{1}{8\pi s_0 \mathbf{q} \cdot \mathbf{v}_s} \sum_{a,b} \int_{\mathbf{k}} [|\langle a, \mathbf{k} | S^+ \Delta_0(\mathbf{r}) | b, \mathbf{k} \rangle|^2 + |\langle a, \mathbf{k} | S^- \Delta_0(\mathbf{r}) | b, \mathbf{k} \rangle|^2] \\
& \times A_a(\epsilon_F, \mathbf{k}) A'_b(\epsilon_F, \mathbf{k}) (\mathbf{v}_{\mathbf{k},a} \cdot e\mathbf{E}) (\mathbf{v}_{\mathbf{k},b} \cdot \mathbf{q}) \tau_a \\
& -\frac{1}{4\pi s_0 \mathbf{q} \cdot \mathbf{v}_s} \sum_{a,b} \int_{\mathbf{k}} \text{Re} [\langle b, \mathbf{k} | S^- \Delta_0(\mathbf{r}) | a, \mathbf{k} \rangle \langle a, \mathbf{k} | S^+ \Delta_0(\mathbf{r}) \mathbf{q} \cdot \partial_{\mathbf{k}} | b, \mathbf{k} \rangle \\
& + (S^+ \leftrightarrow S^-)] A_a(\epsilon_F, \mathbf{k}) A_b(\epsilon_F, \mathbf{k}) (\mathbf{v}_{\mathbf{k},a} \cdot e\mathbf{E}) \tau_a
\end{aligned} \tag{4.17}$$

where $A'(\epsilon_F, \mathbf{k}) \equiv 2(\epsilon_F - \epsilon_{\mathbf{k},a})\Gamma_a / [(\epsilon_F - \epsilon_{\mathbf{k},a})^2 + \Gamma_a^2/4]^2$ stands for the derivative of the spectral function and we have neglected $\partial\Gamma/\partial\mathbf{k}$. Eq. (4.17) (or Eq. (4.15)) is the central result of this work and it provides a gateway to evaluate the non-adiabatic STT in materials with complex band structures;[?] for a diagrammatic interpretation see Fig. (4.1). An alternative formula with a similar aspiration has been proposed recently,[63] yet that formula ignores intrinsic spin-orbit interactions and relies on a detailed knowledge of the disorder scattering mechanisms. In the following three sections we apply Eq. (4.17) to three different simplified models of ferromagnets. For a simpler-to-implement approximate version of Eq. (4.15) or Eq. (4.17) we refer to Sec. VI.

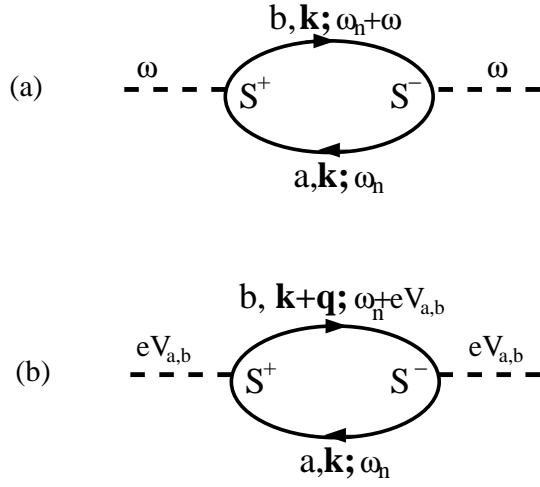


Figure 4.1: Feynman diagrams for (a) α and (b) $\beta(\mathbf{q} \cdot \mathbf{v}_s)$, the latter with a heuristic consideration of the electric field (for a more rigorous treatment see Appendix A). Solid lines correspond to Green's functions of the band quasiparticles in the Born approximation, dashed lines stand for the magnon of frequency ω and wavevector \mathbf{q} , ω_n is the Matsubara frequency and $eV_{a,b}$ is the difference in the transport deviation energies.

4.3 Non-Adiabatic STT for the Parabolic Two-Band Ferromagnet

The model described in this section bears little resemblance to any real ferromagnet. Yet, it is the only model in which rigorous microscopic results for β are presently available, thus providing a valuable test bed for Eq. (4.17). The mean-field Hamiltonian for itinerant carriers in a two-band Stoner model with parabolic bands is simply

$$H^{(k)} = \frac{k^2}{2m} - \Delta_0 S^z \quad (4.18)$$

where Δ_0 is the exchange field and $S_{a,b}^z = \delta_{a,b} \text{sgn}(a)$. In this model the eigenstates have no momentum dependence and hence Eq. (4.17) simplifies to

$$\begin{aligned} (\mathbf{v}_s \cdot \mathbf{q})\beta^{(0)} &= -\frac{\Delta_0^2}{2\pi s_0} \sum_a \int_{\mathbf{k}} A_a(\epsilon_F, \mathbf{k}) A'_{-a}(\epsilon_F, \mathbf{k}) \\ &\quad \frac{\mathbf{k} \cdot \mathbf{q}}{m} \frac{\mathbf{k} \cdot e\mathbf{E}}{m} \tau_{\mathbf{k},a}, \end{aligned} \quad (4.19)$$

where $a = +(-)$ for majority (minority) spins, $\mathbf{v}_{\mathbf{k},\pm} = \mathbf{k}/m$, and $S^\pm = S^x \pm iS^y$ with $S_{a,b}^x = \delta_{a,b}$. Also, from here on repeated indexes will imply a sum. Taking $\Delta_0 \leq E_F$ and $\Delta_0 \gg 1/\tau$, the momentum integral in Eq. (4.19) is performed in the complex energy plane using a keyhole contour around the branch cut that stems from the 3D density of states:

$$\begin{aligned} (\mathbf{v}_s \cdot \mathbf{q})\beta^{(0)} &= -\frac{\Delta_0^2}{2\pi s_0} \frac{2e\mathbf{E} \cdot \mathbf{q}}{3m} \int_0^\infty \nu(\epsilon) A_a(\epsilon_{F,a} - \epsilon) A'_{-a}(\epsilon_{F,-a} - \epsilon) \epsilon \tau_{\mathbf{k},a} \\ &\simeq \frac{e\mathbf{E} \cdot \mathbf{q}}{6m\Delta_0 s_0} \text{sgn}(a) \nu_a \epsilon_{F,a} \tau_a \Gamma_{-a} \\ &= \frac{e\mathbf{E} \cdot \mathbf{q}}{2m\Delta_0 s_0} (n_\uparrow \tau_\uparrow \gamma_\downarrow - n_\downarrow \tau_\downarrow \gamma_\uparrow) \end{aligned} \quad (4.20)$$

where $\epsilon_{F,a} = \epsilon_F + \text{sgn}(a)\Delta_0$, ν_a is the spin-dependent density of states at the Fermi surface, $n_a = 2\nu_a\epsilon_{F,a}/3$ is the corresponding number density, and $\gamma_a \equiv \Gamma_a/2$. The factor $1/3$ on the first line of Eq. (4.20) comes from the angular integration. In the second line of Eq. (4.20) we have neglected a term that is smaller than the one retained by a factor of $\Delta_0^2/(12\epsilon_F^2)$; such extra term (which would have been absent in a two-dimensional version of the model) appears to be missing in previous work.[21, 22]

The simplicity of this model enables a partial incorporation of impurity vertex corrections. By adding to $\beta^{(0)}$ the contribution from the leading order vertex correction ($\beta^{(1)}$), we shall recover the results obtained previously for this model by a full calculation of the transverse spin response function. As it turns out, $\beta^{(1)}$ is qualitatively important because it ensures that only spin-dependent impurities contribute to the non-adiabatic STT in the absence of an intrinsic spin-orbit interaction. In Appendix B we derive the following result:

$$(\mathbf{v}_s \cdot \mathbf{q})\beta^{(1)} = \frac{e\Delta_0^2}{4\pi s_0} \int_{\mathbf{k}, \mathbf{k}'} u^i \text{Re} [S_{a,b}^+ S_{b,b'}^i S_{b',a'}^- S_{a',a}^i] \frac{A_a(\epsilon_F, \mathbf{k})}{(\epsilon_F - \epsilon_{k',a'})} \times \left[\frac{A_b(\epsilon_F, \mathbf{k} + \mathbf{q})}{(\epsilon_F - \epsilon_{\mathbf{k}'+\mathbf{q},b'})} V_{b,a} + \frac{A_{b'}(\epsilon_F, \mathbf{k}' + \mathbf{q})}{(\epsilon_F - \epsilon_{\mathbf{k}+\mathbf{q},b})} V_{b',a} \right], \quad (4.21)$$

where $u^i \equiv n_i \overline{w_i^2}$ ($i = 0, x, y, z$), n_i is the density of scatterers, w_i is the Fourier transform of the scattering potential and the overline denotes an average over different disorder configurations.[21] Also, $V_{a,b} = (\tau_b v_{\mathbf{k}+\mathbf{q},b} - \tau_a v_{\mathbf{k},a}) \cdot e\mathbf{E}$. Expanding Eq. (4.21) to first order in q , we arrive at

$$(\mathbf{v}_s \cdot \mathbf{q})\beta^{(1)} = -\frac{\Delta_0^2}{2\pi s_0} (u^0 - u^z) \int_{\mathbf{k}, \mathbf{k}'} \frac{A_a(\epsilon_F, \mathbf{k})}{\epsilon_F - \epsilon_{\mathbf{k}',a}} \left[\frac{A'_{-a}(\epsilon_F, \mathbf{k})}{\epsilon_F - \epsilon_{\mathbf{k}',-a}} + \frac{A_{-a}(\epsilon_F, \mathbf{k}')}{(\epsilon_F - \epsilon_{\mathbf{k},-a})^2} \right] \frac{\mathbf{k} \cdot \mathbf{q}}{m} \frac{\mathbf{k} \cdot e\mathbf{E}}{m} \tau_{\mathbf{k},a} \quad (4.22)$$

In the derivation of Eq. (4.22) we have used $S^\pm = S^x \pm iS^y$ and assumed that $u^x = u^y \equiv u^{x,y}$, so that $u^i \text{Re} [S_{a,b}^x S_{b,b'}^i S_{b',a'}^x S_{a',a}^i] = (u^0 - u^z) \delta_{a,a'} \delta_{b,b'} \delta_{a,-b}$. In addition, we have used $\int_{\mathbf{k},\mathbf{k}'} F(|\mathbf{k}|, |\mathbf{k}'|) k_i k'_j = 0$. The first term inside the square brackets of Eq. (4.22) can be ignored in the weak disorder regime because its contribution is linear in the scattering rate, as opposed to the second term, which contributes at zeroth order. Then,

$$\begin{aligned}
(\mathbf{v}_s \cdot \mathbf{q})\beta^{(1)} &= -\frac{\Delta_0^2}{\pi s_0} (u^0 - u^z) \int_{\mathbf{k},\mathbf{k}'} \frac{A_a(\epsilon_F, \mathbf{k}) A_{-a}(\epsilon_F, \mathbf{k}')}{(\epsilon_F - \epsilon_{\mathbf{k}',a})(\epsilon_F - \epsilon_{\mathbf{k},-a})^2} \frac{\mathbf{k} \cdot \mathbf{q} \mathbf{k} \cdot e\mathbf{E}}{m} \tau_{\mathbf{k},a} \\
&\simeq -\frac{\Delta_0^2}{\pi s_0} (u^0 - u^z) \frac{2e\mathbf{E} \cdot \mathbf{q}}{3m} \int_{-\infty}^{\infty} d\epsilon d\epsilon' \nu(\epsilon) \nu(\epsilon') \frac{A_a(\epsilon_F, a - \epsilon) A_{-a}(\epsilon_F, -a - \epsilon')}{(\epsilon_F - \epsilon'_a)(\epsilon_F - \epsilon_{-a})^2} \epsilon \tau_a \\
&\simeq -\pi (u^0 - u^z) \frac{e\mathbf{E} \cdot \mathbf{q}}{2m\Delta_0 s_0} \text{sign}(a) n_a \tau_a \nu_{-a}
\end{aligned} \tag{4.23}$$

Combining this with Eq. (4.20), we get

$$\begin{aligned}
(\mathbf{v}_s \cdot \mathbf{q})\beta &\simeq (\mathbf{v}_s \cdot \mathbf{q})\beta^{(0)} + (\mathbf{v}_s \cdot \mathbf{q})\beta^{(1)} \\
&= \frac{e\mathbf{E} \cdot \mathbf{q}}{2ms_0\Delta_0} [n_\uparrow \tau_\uparrow \gamma_\downarrow - n_\downarrow \tau_\downarrow \gamma_\uparrow - \pi(u^0 - u^z)(n_\uparrow \tau_\uparrow \nu_\downarrow - n_\downarrow \tau_\downarrow \nu_\uparrow)] \\
&= \pi \frac{e\mathbf{E} \cdot \mathbf{q}}{ms_0\Delta_0} [n_\uparrow \tau_\uparrow (u^z \nu_\downarrow + u^{x,y} \nu_\uparrow) - n_\downarrow \tau_\downarrow (u^z \nu_\uparrow + u^{x,y} \nu_\downarrow)] \tag{4.24}
\end{aligned}$$

where we have used $\gamma_a = \pi [(u^0 + u^z)\nu_a + 2u^{x,y}\nu_{-a}]$. In this model it is simple to solve Eq. (4.16) for \mathbf{v}_s analytically, whereupon Eq. (4.24) agrees with the results published by other authors in Refs.[21, 22] from full non-linear response function calculations. However, we reiterate that in order to reach such agreement we had to neglect a term of order Δ_0^2/ϵ_F^2 in Eq. (4.20). This extra term is insignificant in all but nearly half metallic ferromagnets.

4.4 Non-Adiabatic STT for a Magnetized Two-Dimensional Electron Gas

The model studied in the previous section misses the intrinsic spin-orbit interaction that is inevitably present in the band structure of actual ferromagnets. Furthermore, since intrinsic spin-orbit interaction is instrumental for the Gilbert damping at low temperatures, a similarly prominent role may be expected in regards to the non-adiabatic spin transfer torque. Hence, the present section is devoted to investigate the relatively unexplored[63, 64] effect of intrinsic spin-orbit interaction on β . The minimal model for this enterprise is the two-dimensional electron-gas ferromagnet with Rashba spin-orbit interaction, represented by

$$H^{(k)} = \frac{k^2}{2m} - \mathbf{b} \cdot \mathbf{S}, \quad (4.25)$$

where $\mathbf{b} = (\lambda k_y, -\lambda k_x, \Delta_0)$, λ is the Rashba spin-orbit coupling strength and Δ_0 is the exchange field.

The eigenspinors of this model are $|+, \mathbf{k}\rangle = (\cos(\theta/2), -i \exp(i\phi) \sin(\theta/2))$ and $|-, \mathbf{k}\rangle = (\sin(\theta/2), i \exp(i\phi) \cos(\theta/2))$, where the spinor angles are defined through $\cos \theta = \Delta_0 / \sqrt{\lambda^2 k^2 + \Delta_0^2}$ and $\tan \phi = k_y / k_x$. The corresponding eigenenergies are $E_{\mathbf{k}\pm} = k^2 / (2m) \mp \sqrt{\Delta_0^2 + \lambda^2 k^2}$. Therefore, the band velocities are given by $\mathbf{v}_{\mathbf{k}\pm} = \mathbf{k} \left(1/m \mp \lambda^2 / \sqrt{\lambda^2 k^2 + \Delta_0^2} \right) = \mathbf{k} / m_{\pm}$. Disregarding the vertex corrections, the non-adiabatic spin-torque of this model may be evaluated analytically starting from Eq. (4.17). We find that (see Appendix

C):

$$\begin{aligned}
(\mathbf{v}_s \cdot \mathbf{q})\beta^{(0)} &\simeq \frac{\Delta_0^2 e \mathbf{E} \cdot \mathbf{q}}{8\pi s_0} \left[\frac{m^2}{4m_+m_-} \left(1 + \frac{\Delta_0^2}{b^2} \right) \frac{1}{b^2} + \frac{1}{4} \frac{\lambda^2 k_F^2 \Delta_0^2}{b^6} \right] \\
&+ \frac{\Delta_0^2 e \mathbf{E} \cdot \mathbf{q}}{8\pi s_0} \left[\frac{1}{2} \frac{m^2}{m_+^2} \frac{\lambda^2 k_F^2}{b^2} \left(1 - \frac{\delta m_+}{m} \frac{\Delta_0^2}{b^2} \right) \tau^2 \right. \\
&\left. + \frac{1}{2} \frac{m^2}{m_-^2} \frac{\lambda^2 k_F^2}{b^2} \left(1 - \frac{\delta m_-}{m} \frac{\Delta_0^2}{b^2} \right) \tau^2 \right] \quad (4.26)
\end{aligned}$$

where $b = \sqrt{\lambda^2 k_F^2 + \Delta_0^2}$ ($k_F = \sqrt{2m\epsilon_F}$), and $\delta m_{\pm} = m - m_{\pm}$. As we explain in Appendix C, Eq. (4.26) applies for $\lambda k_F, \Delta_0, 1/\tau \ll \epsilon_F$; for a more general analysis, Eq. (4.17) must be solved numerically (e.g. see Fig. (4.2)). Eq. (4.26) reveals that intrinsic spin-orbit interaction enables *intra-band* contributions to β , whose signature is the $O(\tau^2)$ dependence on the second line. In contrast, the *inter-band* contributions appear as $O(\tau^0)$. Since \mathbf{v}_s itself is linear in the scattering time, it follows that β is proportional to the electrical conductivity in the clean regime and the resistivity in the disordered regime, much like the Gilbert damping α . We expect this qualitative feature to be model-independent and applicable to real ferromagnets.

4.5 Non-Adiabatic STT for (Ga,Mn)As

In this section we shall apply Eq. (4.17) to a more sophisticated model which provides a reasonable description of (III,Mn)V magnetic semiconductors.[37,38] Since the orbitals at the Fermi energy are very similar to the states near the top of the valence band of the host (III,V) semiconductor, the electronic structure of (III,Mn)V ferromagnets is remarkably simple. Using a

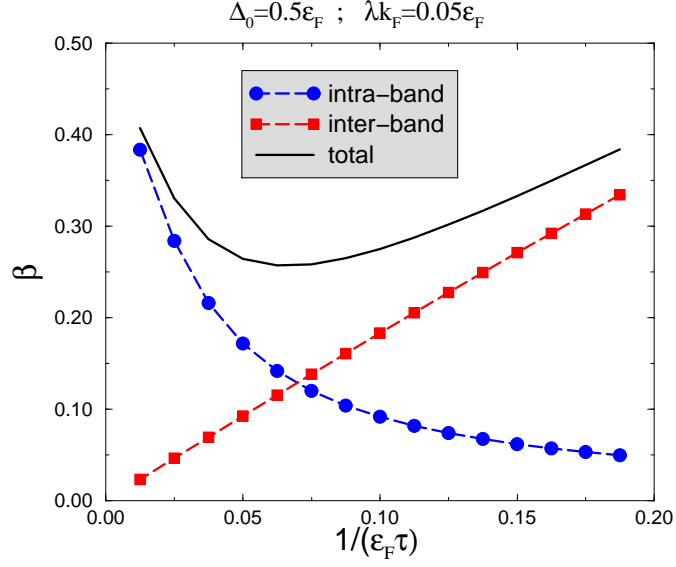


Figure 4.2: **M2DEG**: inter-band contribution, intra-band contribution and the total non-adiabatic STT for a magnetized two-dimensional electron gas (M2DEG). In this figure the exchange field dominates over the spin-orbit splitting. At higher disorder the inter-band part (proportional to resistivity) dominates, while at low disorder the inter-band part (proportional to conductivity) overtakes. For simplicity, the scattering time τ is taken to be the same for all sub-bands.

p-d mean field theory model for the ferromagnetic ground state and a four-band spherical model for the host semiconductor band structure, $\text{Ga}_{1-x}\text{Mn}_x\text{As}$ may be described by

$$H^{(k)} = \frac{1}{2m} \left[\left(\gamma_1 + \frac{5}{2}\gamma_2 \right) k^2 - 2\gamma_3(\mathbf{k} \cdot \mathbf{S})^2 \right] + \Delta_0 S_z, \quad (4.27)$$

where \mathbf{S} is the spin operator projected onto the $J=3/2$ total angular momentum subspace at the top of the valence band and $\{\gamma_1 = 6.98, \gamma_2 = \gamma_3 = 2.5\}$ are the Luttinger parameters for the spherical approximation to the valence bands of GaAs. In addition, $\Delta_0 = J_{\text{pd}}sN_{\text{Mn}} = J_{\text{pd}}s_0$ is the exchange field, $J_{\text{pd}} = 55 \text{ meVnm}^3$ is the p-d exchange coupling, $s = 5/2$ is the spin of Mn ions, $N_{\text{Mn}} = 4x/a^3$ is the density of Mn ions and $a = 0.565 \text{ nm}$ is the lattice constant of GaAs. We solve Eq. (4.27) numerically and input the outcome in Eqs. (4.16), (4.17).

The results are summarized in Fig. (4.3). We find that the intra-band contribution dominates as a consequence of the strong intrinsic spin-orbit interaction, much like for the Gilbert damping;[34]. Incidentally, β barely changes regardless of whether the applied electric field is along the easy axis of the magnetization or perpendicular to it.

4.6 α/β in real materials

The preceding three sections have been focused on testing and analyzing Eq. (4.17) for specific models of ferromagnets. In this section we return to more general considerations and survey the phenomenologically important

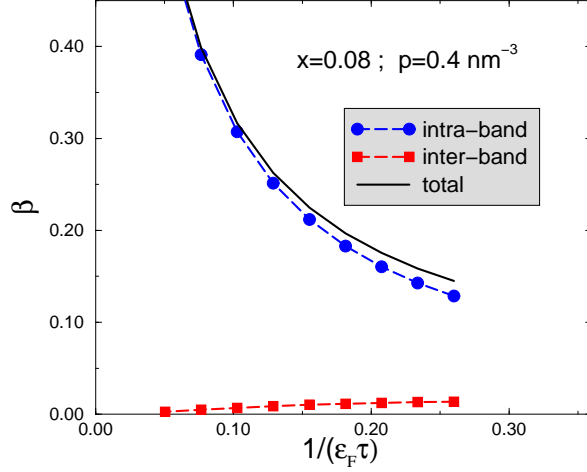


Figure 4.3: **GaMnAs**: $\beta^{(0)}$ for \mathbf{E} perpendicular to the easy axis of magnetization (\hat{z}). x and p are the Mn fraction and the hole density, respectively. The intra-band contribution is considerably larger than the inter-band contribution, due to the strong intrinsic spin-orbit interaction. Since the 4-band model typically overestimates the influence of intrinsic spin-orbit interaction, it is likely that the dominion of intra-band contributions be reduced in the more accurate 6-band model. By evaluating β for $\mathbf{E} \parallel \hat{z}$ (not shown) we infer that it does not depend significantly on the relative direction between the magnetic easy axis and the electric field.

quantitative relationship between α and β in realistic ferromagnets, which always have intrinsic spin-orbit interactions. We begin by recollecting the expression for the Gilbert damping coefficient derived elsewhere:[36]

$$\alpha = \frac{1}{8\pi s_0} \sum_{a,b} \int_{\mathbf{k}} |\langle b, \mathbf{k} | S^+ \Delta_0 | a, \mathbf{k} \rangle|^2 A_a(\epsilon_F, \mathbf{k}) A_b(\epsilon_F, \mathbf{k}) \quad (4.28)$$

where we have ignored disorder vertex corrections. This expression is to be compared with Eq. (4.15); for pedagogical purposes we discuss intra-band and inter-band contributions separately.

Starting from Eq. (4.15) and expanding the integrand to first order in \mathbf{q} we obtain

$$\beta_{intra} = \frac{1}{8\pi s_0} \int_{\mathbf{k}} |\langle a, \mathbf{k} | S^+ \Delta_0 | a, \mathbf{k} \rangle|^2 A_a(\epsilon_F, \mathbf{k})^2 \frac{e\tau_a q^i \partial_{k_i} v_{\mathbf{k},a}^j E^j}{\mathbf{q} \cdot \mathbf{v}_s} \quad (4.29)$$

where we have neglected the momentum dependence of the scattering lifetime and a sum over repeated indices is implied. Remarkably, only matrix elements that are diagonal in momentum space contribute to β_{intra} ; the implications of this will be highlighted in the next section. Recognizing that $\partial_{k_j} v_{\mathbf{k},a}^i = (\mathbf{1}/\mathbf{m})_a^{i,j}$, where $(1/\mathbf{m})_a$ is the inverse effective mass tensor corresponding to band a , Eq. (4.29) can be rewritten as

$$\beta_{intra} = \frac{1}{8\pi s_0} \int_{\mathbf{k}} |\langle a, \mathbf{k} | S^+ \Delta_0 | a, \mathbf{k} \rangle|^2 A_a(\epsilon_F, \mathbf{k})^2 \frac{\mathbf{q} \cdot \mathbf{v}_{d,a}}{\mathbf{q} \cdot \mathbf{v}_s}, \quad (4.30)$$

where

$$\mathbf{v}_{d,a}^i = e\tau_a (\mathbf{m}^{-1})_a^{i,j} \mathbf{E}^j \quad (4.31)$$

is the “drift velocity” corresponding to the quasiparticles in band a . For Galilean invariant systems[65] $v_{d,a} = v_s$ for any (\mathbf{k}, a) and consequently $\beta_{\text{intra}} = \alpha_{\text{intra}}$. At first glance, it might appear that v_s , which (at least in absence of spin-orbit interaction) is determined by the spin current, must be different than $v_{d,a}$. However, recall that v_s is determined by the ratio of the spin current to the magnetization. If the same electrons contribute to the transport as to the magnetization, $v_s = v_{d,a}$ provided the scattering rates and the masses are the same for all states. These conditions are the conditions for an electron system to be Galilean invariant. The interband contribution can be simplified by noting that

$$\tau_b v_{\mathbf{k}+\mathbf{q},b}^i - \tau_a v_{\mathbf{k},a}^i = (\tau_b v_{\mathbf{k}+\mathbf{q},b}^i - \tau_a v_{\mathbf{k}+\mathbf{q},a}^i) + (\tau_a v_{\mathbf{k}+\mathbf{q},a}^i - \tau_a v_{\mathbf{k},a}^i). \quad (4.32)$$

The second term on the right hand side of Eq.(4.32) can then be manipulated exactly as in the intra-band case to arrive at

$$\beta_{\text{inter}} = \frac{1}{8\pi s_0} \sum_{a,b(a \neq b)} \int_{\mathbf{k}} |\langle b, \mathbf{k} | S^+ \Delta_0 | a, \mathbf{k} \rangle|^2 A_a(\epsilon_F, \mathbf{k}) A_b(\epsilon_F, \mathbf{k}) \frac{\mathbf{q} \cdot \mathbf{v}_{d,a}}{\mathbf{q} \cdot \mathbf{v}_s} + \delta\beta_{\text{inter}} \quad (4.33)$$

where

$$\delta\beta_{\text{inter}} = \frac{1}{8\pi s_0} \sum_{a,b(a \neq b)} \int_{\mathbf{k}} |\langle a, \mathbf{k}-\mathbf{q} | S^+ \Delta_0 | b, \mathbf{k} \rangle|^2 A_a(\epsilon_F, \mathbf{k}-\mathbf{q}) A_b(\epsilon_F, \mathbf{k}) \frac{(\tau_b \mathbf{v}_{\mathbf{k},b} - \tau_a \mathbf{v}_{\mathbf{k},a}) \cdot \mathbf{E}}{\mathbf{q} \cdot \mathbf{v}_s}. \quad (4.34)$$

When Galilean invariance is preserved the quasiparticle velocity and scattering times are the same for all bands, which implies that $\delta\beta = 0$ and hence that $\beta_{\text{inter}} = \alpha_{\text{inter}}$. Although realistic materials are not Galilean invariant, $\delta\beta$ is

nevertheless probably not significant because the term between parenthesis in Eq. (4.34) has an oscillatory behavior prone to cancellation. The degree of such cancellation must ultimately be determined by realistic calculations for particular materials.

With this proviso, we estimate that

$$\beta \simeq \frac{1}{8\pi s_0} \int_{\mathbf{k}} |\langle b, \mathbf{k} | S^+ \Delta_0 | a, \mathbf{k} \rangle|^2 A_a(\epsilon_F, \mathbf{k}) A_b(\epsilon_F, \mathbf{k}) \frac{\mathbf{q} \cdot \mathbf{v}_{d,a}}{\mathbf{q} \cdot \mathbf{v}_s}. \quad (4.35)$$

As long as $\delta\beta \simeq 0$ is justified, the simplicity of Eq. (4.35) in comparison to Eq. (4.15) or (4.17) makes of the former the preferred starting point for electronic structure calculations. Even when $\delta\beta \neq 0$ Eq. (4.35) may be an adequate platform for *ab-initio* studies on weakly disordered transition metal ferromagnets and strongly spin-orbit coupled ferromagnetic semiconductors,⁶ where β is largely determined by the intra-band contribution. Furthermore, a direct comparison between Eq. (4.28) and Eq. (4.35) leads to the following observations. First, for nearly parabolic bands with nearly identical curvature, where the “drift velocity” is weakly dependent on momentum or the band index, we obtain $\beta \simeq (v_d/v_s)\alpha$ and thus β/α is roughly proportional to the ratio of the total spin density to the itinerant spin density, in concordance with predictions from toy models.[19] Second, if $\alpha/\beta > 0$ for a system with purely

⁶For actual *ab-initio* calculations it may be more convenient to substitute $|\langle a, \mathbf{k} | \Delta_0 S^+ | b, \mathbf{k} \rangle|^2$ in Eq. (4.35) by $|\langle a, \mathbf{k} | K | b, \mathbf{k} \rangle|^2$, where K is the spin-torque operator discussed in Section VII. In either case we are disregarding impurity vertex corrections, which may become significant in disordered and/or strongly spin-orbit coupled systems.

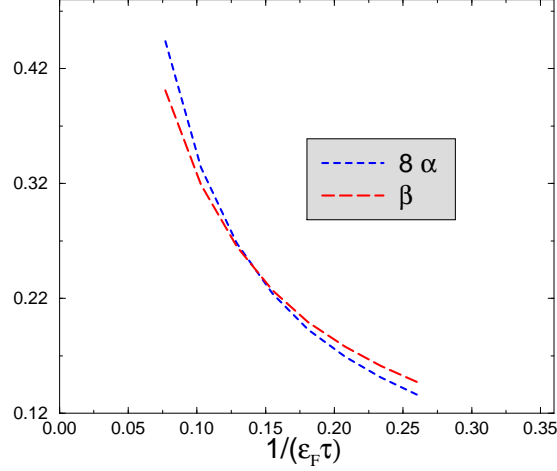


Figure 4.4: Comparison of α and β in (Ga,Mn)As for $x = 0.08$ and $p = 0.4nm^{-3}$. It follows that $\beta/\alpha \simeq 8$, with a weak dependence on the scattering rate off impurities. If we use the torque correlation formula (Section VII), we obtain $\beta/\alpha \simeq 10$.

electron-like carriers, then $\alpha/\beta > 0$ for the same system with purely hole-like carriers because for a fixed carrier polarization v_d^a and v_s reverse their signs under $m \rightarrow -m$. However, if both hole-like and electron-like carriers coexist at the Fermi energy, then the integrand in Eq. (4.35) is positive for some values of a and negative for others. In such situation it is conceivable that α/β be either positive or negative. A negative value of β implies a *decrease* in magnetization damping due to an applied current.

As an illustration of the foregoing discussion, in Fig. (4.4) we evaluate α/β for (Ga,Mn)As. We find β to be about an order of magnitude larger than α , which is reasonable because (i) the local moment magnetization is larger than the valence band hole magnetization, and (ii) the spin-orbit coupling in

the valence band decreases the transport spin polarization. Accordingly β is of the order of unity, in qualitative agreement with recent theoretical work[66].

4.7 Torque-Correlation Formula for the Non-Adiabatic STT

Thus far we have evaluated non-adiabatic STT using the bare vertex $\langle a, \mathbf{k} | S^+ | b, \mathbf{k} + \mathbf{q} \rangle$. In this section, we shall analyze an alternative matrix element denoted $\langle a, \mathbf{k} | K | b, \mathbf{k} + \mathbf{q} \rangle$ (see below for an explicit expression), which may be better suited to realistic electronic structure calculations.[26, 27] We begin by making the approximation that the exchange splitting can be written as a constant spin-dependent shift $H_{\text{ex}} = \Delta_0 S^z$. Then, the mean-field quasi-particle Hamiltonian $H^{(k)} = H_{\text{kin}}^{(k)} + H_{\text{so}}^{(k)} + H_{\text{ex}}$ can be written as the sum of a spin-independent part $H_{\text{kin}}^{(k)}$, the exchange term, and the spin-orbit coupling $H_{\text{so}}^{(k)}$. With this approximation, we have the identity:

$$\begin{aligned} & \langle a, \mathbf{k} | S^+ | b, \mathbf{k} + \mathbf{q} \rangle \\ &= \frac{1}{\Delta_0} \langle a, \mathbf{k} | [H^{(k)}, S^+] | b, \mathbf{k} + \mathbf{q} \rangle \\ &- \frac{1}{\Delta_0} \langle a, \mathbf{k} | [H_{\text{so}}^{(k)}, S^+] | b, \mathbf{k} + \mathbf{q} \rangle. \end{aligned} \quad (4.36)$$

The last term in the right hand side of Eq. (4.36) is the generalization of the torque matrix element used in *ab-initio* calculations of the Gilbert damping:

$$\langle a, \mathbf{k} | K | b, \mathbf{k} + \mathbf{q} \rangle \equiv \frac{1}{\Delta_0} \langle a, \mathbf{k} | [H_{\text{so}}^{(k)}, S^+] | b, \mathbf{k} + \mathbf{q} \rangle \quad (4.37)$$

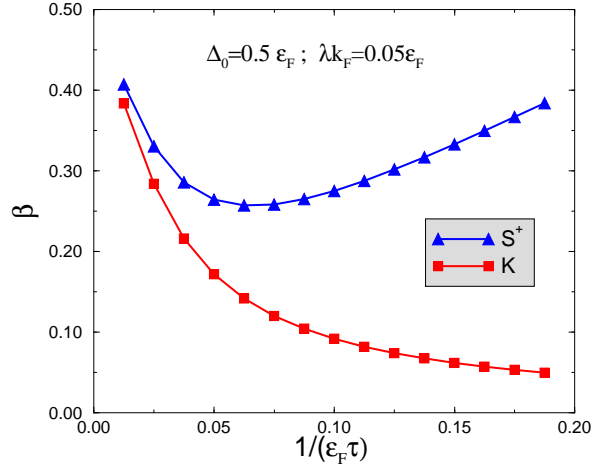


Figure 4.5: **M2DEG**: comparing S and K matrix element expressions for the non-adiabatic STT formula in the weakly spin-orbit coupled regime. Both formulations agree in the clean limit, where the intra-band contribution is dominant. In more disordered samples inter-band contributions become more visible and S and K begin to differ; the latter is known to be more accurate in the weakly spin-orbit coupled regime.

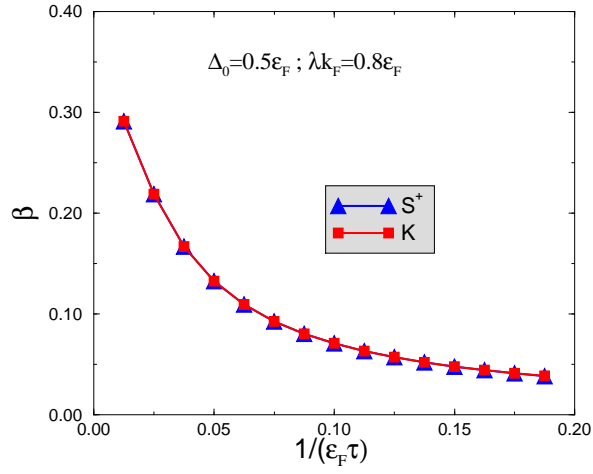


Figure 4.6: **M2DEG**: In the strongly spin-orbit coupled limit the intra-band contribution reigns over the inter-band contribution and accordingly S and K matrix element expressions display a good (excellent in this figure) agreement. Nevertheless, this agreement does not guarantee quantitative reliability, because for strong spin-orbit interactions impurity vertex corrections may play an important role.

Eq. (4.36) implies that at $\mathbf{q} = \mathbf{0}$ $\langle b, \mathbf{k} | S^+ | a, \mathbf{k} \rangle \simeq \langle b, \mathbf{k} | K | a, \mathbf{k} \rangle$ provided that $(E_{\mathbf{k},a} - E_{\mathbf{k},b}) \ll \Delta_0$, which is trivially satisfied for intra-band transitions but less so for inter-band transitions.[34] For $\mathbf{q} \neq \mathbf{0}$ the agreement between intra-band matrix elements is no longer obvious and is affected by the momentum dependence of the band eigenstates. At any rate, Eq. (4.29) demonstrates that only $\mathbf{q} = \mathbf{0}$ matrix elements contribute to β_{intra} ; therefore β_{intra} has the same value for S and K matrix elements. The disparity between the two formulations is restricted to β_{inter} , and may be significant if the most prominent inter-band matrix elements connect states that are *not* close in energy. When they disagree, it is generally unclear⁷ whether S or K matrix elements will yield a better estimate of β_{inter} . The weak spin-orbit limit is a possible exception, in which the use of K appears to offer a practical advantage over S . In this regime S generates a spurious inter-band contribution in the absence of magnetic impurities (recall Section III) and it is only after the inclusion of the leading order vertex correction that such deficiency gets remedied. In contrast, K vanishes identically in absence of spin-orbit interactions, thus bypassing the pertinent problem without having to introduce vertex corrections.

Figs. (4.5)- (4.7) display a quantitative comparison between the non-adiabatic STT obtained from K and S , both for the M2DEG and (Ga,Mn)As. Fig. (4.5) reflects the aforementioned overestimation of S in the inter-band dominated regime of weakly spin-orbit coupled ferromagnets. In the strong

⁷In order to gauge the accuracy of either matrix element, one must obtain an exact evaluation of the non-adiabatic STT, which entails a ladder-sum renormalization[34] of S^\pm . This is beyond the scope of the present work.

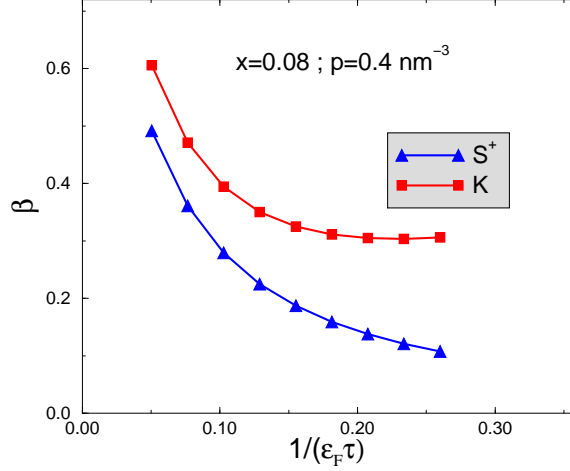


Figure 4.7: **GaMnAs**: comparison between S and K matrix element expressions for $\mathbf{E} \perp \hat{z}$. The disagreement between both formulations stems from inter-band transitions, which are less important as τ increases. Little changes when $\mathbf{E} \parallel \hat{z}$.

spin-orbit limit, where intra-band contributions dominate in the disorder range of interest, K and S agree fairly well (Figs. (4.6) and (4.7)). Summing up, insofar as impurity vertex corrections play a minor role and the dominant contribution to β stems from intra-band transitions the torque-correlation formula will provide a reliable estimate of β .

4.8 Connection to the Effective Field Model

As explained in Section II we view the non-adiabatic STT as the change in magnetization damping due to a transport current. The present section is designed to complement that understanding from a different perspective based on an effective field formulation, which provides a simple physical interpreta-

tion for both intra-band and inter-band contributions to β .

An effective field \mathcal{H}^{eff} may be expressed as the variation of the system energy with respect to the magnetization direction $\mathcal{H}_i^{\text{eff}} = -(1/s_0)\partial E/\partial\Omega_i$. Here we approximate the energy with the Kohn-Sham eigenvalue sum

$$E = \sum_{\mathbf{k},a} n_{\mathbf{k},a} \epsilon_{\mathbf{k},a}. \quad (4.38)$$

The variation of this energy with respect to the magnetization direction yields

$$\mathcal{H}_i^{\text{eff}} = -\frac{1}{s_0} \sum_{\mathbf{k},a} \left[n_{\mathbf{k},a} \frac{\partial \epsilon_{\mathbf{k},a}}{\partial \Omega_i} + \frac{\partial n_{\mathbf{k},a}}{\partial \Omega_i} \epsilon_{\mathbf{k},a} \right]. \quad (4.39)$$

It has previously been shown that, in the absence of current, the first term in the sum leads to intra-band Gilbert damping[24, 25, 61] while the second term produces inter-band damping.[67] In the following, we generalize these results by allowing the flow of an electrical current. α and β may be extracted by identifying the the dissipative part of the effective field with $-\alpha\partial\hat{\Omega}/\partial t - \beta\mathbf{v}_s \cdot \nabla\hat{\Omega}$ that appears in the LLS equation.

Intra-band terms: We begin by recognizing that as the direction of magnetization changes in time, so does the shape of the Fermi surface, provided that there is an intrinsic spin-orbit interaction. Consequently, empty (full) states appear below (above) the Fermi energy, giving rise to an out-of-equilibrium quasiparticle distribution. This configuration tends to relax back to equilibrium, but repopulation requires a time τ . Due to the time delay, the quasiparticle distribution lags behind the dynamical configuration of the

Fermi surface, effectively creating a friction (damping) force on the magnetization. From a quantitative standpoint, the preceding discussion means that the quasiparticle energies $\epsilon_{\mathbf{k},a}$ follow the magnetization adiabatically, whereas the occupation numbers $n_{\mathbf{k},a}$ deviate from the instantaneous equilibrium distribution $f_{\mathbf{k},a}$ via

$$n_{\mathbf{k},a} = f_{\mathbf{k},a} - \tau_{\mathbf{k},a} \left(\frac{\partial f_{\mathbf{k},a}}{\partial t} + \dot{\mathbf{r}}_a \cdot \frac{\partial f_{\mathbf{k},a}}{\partial \mathbf{r}} + \dot{\mathbf{k}} \cdot \frac{\partial f_{\mathbf{k},a}}{\partial \mathbf{k}} \right), \quad (4.40)$$

where we have used the relaxation time approximation. As we explain below, the last two terms in Eq. (4.40) do not contribute to damping in the absence of an electric field and have thus been ignored by prior applications of the breathing Fermi surface model, which concentrate on Gilbert damping. It is customary to associate intra-band magnetization damping with the torque exerted by the part of the effective field

$$\mathcal{H}_{\text{intra}}^{\text{eff}} = -\frac{1}{s_0} \sum_{\mathbf{k},a} n_{\mathbf{k},a} \frac{\partial \epsilon_{\mathbf{k},a}}{\partial \hat{\Omega}} \quad (4.41)$$

that is lagging behind the instantaneous magnetization. Plugging Eq. (4.40) in Eq. (4.41) we obtain

$$\begin{aligned} \mathcal{H}_{\text{intra},i}^{\text{eff}} = & \frac{1}{s_0} \sum_{\mathbf{k},a} \left[-f_{\mathbf{k},a} \frac{\partial \epsilon_{\mathbf{k},a}}{\partial \Omega_i} + \tau_a \frac{\partial f_{\mathbf{k},a}}{\partial \epsilon_{\mathbf{k},a}} \frac{\partial \epsilon_{\mathbf{k},a}}{\partial \Omega_i} \frac{\partial \epsilon_{\mathbf{k},a}}{\partial \Omega_j} \frac{\partial \Omega_j}{\partial t} + \tau_a \dot{r}_a^i \frac{\partial f_{\mathbf{k},a}}{\partial \epsilon_{\mathbf{k},a}} \frac{\partial \epsilon_{\mathbf{k},a}}{\partial \Omega_i} \frac{\partial \epsilon_{\mathbf{k},a}}{\partial \Omega_j} \frac{\partial \Omega_j}{\partial r_l} \right. \\ & \left. + \tau_a \dot{k}^j \frac{\partial f_{\mathbf{k},a}}{\partial \epsilon_{\mathbf{k},a}} \frac{\partial \epsilon_{\mathbf{k},a}}{\partial k_j} \frac{\partial \epsilon_{\mathbf{k},a}}{\partial \Omega_i} \right] \end{aligned} \quad (4.42)$$

where a sum is implied over repeated Latin indices. The first term in Eq. (4.42) is a contribution to the anisotropy field; it evolves in synchrony with the

dynamical Fermi surface and is thus the reactive component of the effective field. The remaining terms, which describe the time lag of the effective field due to a nonzero relaxation time, are responsible for intra-band damping. The last term vanishes in crystals with inversion symmetry because $\dot{k} = eE$ and $\partial\epsilon/\partial\mathbf{k}$ is an odd function of momentum. Similarly, if we take $\dot{\mathbf{r}} = \partial\epsilon(\mathbf{k})/\partial\mathbf{k}$ the second to last term ought to vanish as well. This leaves us with the first two terms in Eq. (4.42), which capture the intra-band Gilbert damping but not the non-adiabatic STT. This is not surprising as the latter involves the *coupled* response to spatial variations of magnetization and a weak electric field, rendering linear order in perturbation theory insufficient (see Appendix A). In order to account for the relevant non-linearity we use $\dot{\mathbf{r}} = \partial\epsilon(\mathbf{k} - e\mathbf{v} \cdot \mathbf{E}\tau)/\partial\mathbf{k}$ in Eq.(4.42), where $\mathbf{v} = \partial\epsilon(\mathbf{k})/\partial\mathbf{k}$. The dissipative part of $\mathcal{H}_{\text{intra}}^{\text{eff}}$ then reads

$$\mathcal{H}_{\text{intra},i}^{\text{eff,damp}} = \frac{1}{s_0} \sum_{\mathbf{k},a} \tau_{\mathbf{k},a} \frac{\partial f_{\epsilon_{\mathbf{k},a}}}{\partial \epsilon_{\mathbf{k},a}} \frac{\partial \epsilon_{\mathbf{k},a}}{\partial \Omega_i} \frac{\partial \epsilon_{\mathbf{k},a}}{\partial \Omega_j} \left[\frac{\partial \Omega_j}{\partial t} + \mathbf{v}_{d,a}^l \frac{\partial \Omega_j}{\partial r^l} \right], \quad (4.43)$$

where $\mathbf{v}_{d,a}^i = e\tau_a(m^{-1})_a^{i,j} \mathbf{E}^j$ is the ‘‘drift velocity’’ corresponding to band a . Eq. (4.43) may now be identified with $-\alpha_{\text{intra}} \partial \hat{\Omega} / \partial t - \beta_{\text{intra}} \mathbf{v}_s \cdot \nabla \hat{\Omega}$ that appears in the LLS equation. For an isotropic system this results in

$$\begin{aligned} \alpha_{\text{intra}} &= -\frac{1}{s_0} \sum_{\mathbf{k},a,i} \tau_{\mathbf{k},a} \frac{\partial f_{\mathbf{k},a}}{\partial \epsilon_{\mathbf{k},a}} \left(\frac{\partial \epsilon_{\mathbf{k},a}}{\partial \Omega_i} \right)^2 \\ \beta_{\text{intra}} &= -\frac{1}{s_0} \sum_{\mathbf{k},a,i} \tau_{\mathbf{k},a} \frac{\partial f_{\mathbf{k},a}}{\partial \epsilon_{\mathbf{k},a}} \left(\frac{\partial \epsilon_{\mathbf{k},a}}{\partial \Omega_i} \right)^2 \frac{\mathbf{q} \cdot \mathbf{v}_{d,a}}{\mathbf{q} \cdot \mathbf{v}_s}. \end{aligned} \quad (4.44)$$

Since $\langle [S^x, H_{so}] \rangle = \partial_\phi \langle \exp(iS^x \phi) H_{so} \exp(-iS^x \phi) \rangle = \partial\epsilon/\partial\phi$ for an infinitesimal angle of rotation ϕ around the instantaneous magnetization, β in Eq. (4.44)

may be rewritten as

$$\beta_{\text{intra}} = \frac{\Delta_0^2}{2s_0} \sum_{\mathbf{k}, a} \tau_{\mathbf{k}, a} \frac{\partial f_{\mathbf{k}, a}}{\partial \epsilon_{\mathbf{k}, a}} |\langle \mathbf{k}, a | K | \mathbf{k}, a \rangle|^2 \frac{\mathbf{q} \cdot \mathbf{v}_{d, a}}{\mathbf{q} \cdot \mathbf{v}_s} \quad (4.45)$$

where $K = [S^+, H_{so}]/\Delta_0$ is the spin-torque operator introduced in Eq. (4.37) and we have claimed spin rotational invariance via $|\langle [S^x, H_{so}] \rangle|^2 = |\langle [S^y, H_{so}] \rangle|^2$. Using $\partial f/\partial \epsilon \simeq -\delta(\epsilon - \epsilon_F)$ and recalling from Section VII that $K_{a, a} = S_{a, a}^+$, Eq. (4.45) is equivalent to Eq. (4.30); note that the product of spectral functions in the latter yields a factor of $4\pi\tau$ upon momentum integration. These observations prove that β_{intra} describes the contribution from a transport current to the “breathing Fermi surface” type of damping. Furthermore, Eq. (4.44) highlights the importance of the ratio between the two characteristic velocities of a current carrying ferromagnet, namely v_s and v_d . As explained in Section VI these two velocities coincide in models with Galilean invariance. Only in these artificial models, which never apply to real materials, does $\alpha = \beta$ hold.

Inter-band terms: The Kohn-Sham orbitals are effective eigenstates of a mean-field Hamiltonian where the spins are aligned in the equilibrium direction. As spins precess in response to external rf fields and dc transport currents, the time-dependent part of the mean-field Hamiltonian drives transitions between the ground-state Kohn-Sham orbitals. These processes lead to the second term in the effective field and produce the inter-band contribution to damping.

We thus concentrate on the second term in Eq. (4.39),

$$\mathcal{H}_{\text{inter}}^{\text{eff}} = -\frac{1}{s_0} \sum_{\mathbf{k},a} \frac{\partial n_{\mathbf{k},a}}{\partial \hat{\Omega}} \epsilon_{\mathbf{k},a}. \quad (4.46)$$

Multiplying Eq. (4.46) with $\partial_t \hat{\Omega}$ we get

$$\begin{aligned} \mathcal{H}_{\text{inter}}^{\text{eff,damp}} \cdot \partial_t \hat{\Omega} &= -\frac{1}{s_0} \sum_{\mathbf{k},a} \epsilon_{\mathbf{k},a} \left[\partial n_{a,\mathbf{k}} / \partial \hat{\Omega} \cdot \partial \hat{\Omega} / \partial t \right] \\ &= -\frac{1}{s_0} \sum_{\mathbf{k},a} \epsilon_{\mathbf{k},a} \partial n_{a,\mathbf{k}} / \partial t. \end{aligned} \quad (4.47)$$

The rate of change of the populations of the Kohn-Sham states can be approximated by the following master equation:

$$\frac{\partial n_{a,\mathbf{k}}}{\partial t} = - \sum_{b,\mathbf{k}'} W_{a,b} (n_{\mathbf{k},a} - n_{\mathbf{k}',b}), \quad (4.48)$$

where

$$W_{a,b} = 2\pi |\langle b, \mathbf{k}' | \Delta_0 S^x | a, \mathbf{k} \rangle|^2 \delta_{\mathbf{k}', \mathbf{k}+\mathbf{q}} \delta(\epsilon_{b,\mathbf{k}'} - \epsilon_{a,\mathbf{k}} - \omega) \quad (4.49)$$

is the spin-flip inter-band transition probability as dictated by Fermi's golden rule. Eqs. (4.48) and (4.49) rely on the principle of microscopic reversibility⁸ and are rather *ad hoc* because they circumvent a rigorous analysis of the quasiparticle-magnon scattering, which would for instance require keeping track of magnon occupation numbers. Furthermore, quasiparticle-phonon

⁸This principle states that $W_{a,b} = W_{b,a} \exp((\epsilon_a - \epsilon_b)/T)$. Since the magnon energy is much smaller than the uncertainty in the quasiparticle energies, we approximate $W_{a,b} \simeq W_{b,a}$.

and quasiparticle-impurity scattering are allowed for simply by broadening the Kohn-Sham eigenenergies (see below). The right hand side of Eq. (4.48) is now closely related to inter-band magnetization damping because it agrees[1] with the *net* decay rate of magnons into particle-hole excitations, where the particle and hole are in different bands. Combining Eq. (4.47) and (4.48) and rearranging terms we arrive at

$$\mathcal{H}_{\text{inter}}^{\text{eff}} \cdot \partial_t \hat{\Omega} = \frac{1}{2s_0} \sum_{\mathbf{k}, \mathbf{k}', a, b} W_{a,b}(n_{\mathbf{k},a} - n_{\mathbf{k}',b})(\epsilon_{\mathbf{k},a} - \epsilon_{\mathbf{k}',b}). \quad (4.50)$$

For the derivation of α_{inter} it is sufficient to approximate $n_{\mathbf{k},a}$ as a Fermi distribution in Eq. (4.50); here we account for a transport current by shifting the Fermi seas as $n_{\mathbf{k},a} \rightarrow n_{\mathbf{k},a} - e\mathbf{v}_{\mathbf{k},a} \cdot \mathbf{E}\tau_{\mathbf{k},a} \partial n_{\mathbf{k},a} / \partial \epsilon_{\mathbf{k},a}$, which to leading order yields

$$\begin{aligned} \mathcal{H}_{\text{inter}}^{\text{eff}} \cdot \partial_t \hat{\Omega} &= -\frac{\pi\omega}{2s_0} \sum_{\mathbf{k}, a, b} |\langle b, \mathbf{k} + \mathbf{q} | \Delta_0 S^+ | a, \mathbf{k} \rangle|^2 \delta(\epsilon_{b, \mathbf{k} + \mathbf{q}} - \epsilon_{a, \mathbf{k}} - \omega) \frac{\partial n_{\mathbf{k},a}}{\partial \epsilon_{\mathbf{k},a}} (-\omega + eV_{b,a}) \\ &= \frac{\omega}{8\pi s_0} \sum_{\mathbf{k}, a, b} |\langle b, \mathbf{k} + \mathbf{q} | \Delta_0 S^+ | a, \mathbf{k} \rangle|^2 A_a(\mathbf{k}, \epsilon_F) A_b(\mathbf{k} + \mathbf{q}, \epsilon_F) (-\omega + eV_{b,a}) \end{aligned} \quad (4.51)$$

where we have used $S^x = (S^+ + S^-)/2$ and defined $V_{b,a} = e\mathbf{v}_{\mathbf{k} + \mathbf{q}, b} \cdot \mathbf{E}\tau_{\mathbf{k} + \mathbf{q}, b} - e\mathbf{v}_{\mathbf{k}, a} \cdot \mathbf{E}\tau_{\mathbf{k}, a}$. In the second line of Eq.(4.51) we have assumed low temperatures, and have introduced a finite quasiparticle lifetime by broadening the spectral functions of the Bloch states into Lorentzians with the convention outlined in Eq. (4.14): $\delta(x) \rightarrow A(x)/(2\pi)$. Identifying Eq.(4.51) with

$(-\alpha_{\text{inter}}\partial_t\hat{\Omega} - \beta_{\text{inter}}(\mathbf{v}_s \cdot \nabla)\hat{\Omega}) \cdot \partial_t\hat{\Omega} = -\alpha_{\text{inter}}\omega^2 + \beta_{\text{inter}}\omega(\mathbf{q} \cdot \mathbf{v}_s)$ we arrive at

$$\alpha_{\text{inter}} = \frac{1}{8\pi s_0} \sum_{a,b \neq a} \sum_{\mathbf{k}, a, b} |\langle b, \mathbf{k} + \mathbf{q} | \Delta_0 S^+ | a, \mathbf{k} \rangle|^2 A_a(\mathbf{k}, \epsilon_F) A_b(\mathbf{k} + \mathbf{q}, \epsilon_F)$$

$$\beta_{\text{inter}} = \frac{1}{8\pi s_0 \mathbf{q} \cdot \mathbf{v}_s} \sum_{a,b \neq a} \sum_{\mathbf{k}, a, b} |\langle b, \mathbf{k} + \mathbf{q} | \Delta_0 S^+ | a, \mathbf{k} \rangle|^2 A_a(\mathbf{k}, \epsilon_F) A_b(\mathbf{k} + \mathbf{q}, \epsilon_F) V_{b,a}$$

in agreement with our results of Section II.

4.9 Summary and Conclusions

Starting from the Gilbert damping α and including the influence of an electric field in the transport orbitals semiclassically, we have proposed a concise formula for the non-adiabatic spin transfer torque coefficient β that can be applied to real materials with arbitrary band structures. Our formula for β reproduces results obtained by more rigorous non-linear response theory calculations when applied to simple toy models. By applying this expression to a two-dimensional electron-gas ferromagnet with Rashba spin-orbit interaction, we have found that it implies a conductivity-like contribution to β , related to the corresponding contribution to the Gilbert damping α , which is proportional to scattering time rather than scattering rate and arises from intra-band transitions. Our subsequent calculations using a four-band model have shown that intra-band contributions dominate in ferromagnetic semiconductors such as (Ga,Mn)As. We have then discussed the α/β ratio in realistic materials and have confirmed trends expected from toy models, in addition to suggesting that α and β can have the opposite sign in systems where both hole-like and electron-like bands coexist at the Fermi surface. Afterwards, we

have analyzed the spin-torque formalism suitable to *ab-initio* calculations, and have concluded that it may provide a reliable estimate of the intra-band contribution to β ; for the inter-band contribution the spin-torque formula offers a physically sensible result in the weak spin-orbit limit but its quantitative reliability is questionable unless the prominent inter-band transitions connect states that are close in energy. Finally, we have extended the breathing Fermi surface model for the Gilbert damping to current carrying ferromagnets and have accordingly found a complementary physical interpretation for the intra-band contribution to β ; similarly, we have applied the master equation in order to offer an alternative interpretation for the inter-band contribution to β . Possible avenues for future research consist of carefully analyzing the importance of higher order vertex corrections in β , better understanding the disparities between the different approaches to v_s , and finding real materials where α/β is negative.

Chapter 5

Influence of a Transport Current on Magnetic Anisotropy in Gyrotropic Ferromagnets

Current-induced torques are commonly used to manipulate non-collinear magnetization configurations. In this chapter we discuss current-induced torques present in a certain class of collinear magnetic systems, relating them to current-induced changes in magnetic anisotropy energy. We present a quantitative estimate of their characteristics in uniform strained ferromagnetic (Ga,Mn)As.

5.1 Introduction

The interplay between transport currents and magnetization dynamics continues to be a major research topic in ferromagnetic metal spintronics.[14, 23, 51] The current understanding of this class of phenomena has been derived mainly from numerous studies of spin-transfer torques (STTs), which arise when spin polarized currents traverse *non-collinear* magnetic systems. STTs can be exploited to achieve current-induced magnetization reversal and current-induced domain-wall motion, both of which have potentially important technological applications.

There have been comparatively few studies of the influence of transport currents on magnetization in *uniform* ferromagnets, presumably because spin transfer torques vanish in these systems. Yet, as pointed out independently by several researchers,[68–71] current-induced reorientation of magnetization does occur in some uniform ferromagnets. The first experimental fingerprint of this phenomenon was uncovered by Chernyshov *et al.*[70] who demonstrated that an electric current alters magnetization reversal characteristics in strained (Ga,Mn)As films with a single magnetic domain.

STTs can be considered to be one member of a family of current-induced torque (CIT) effects by which transport currents influence magnetization in ferromagnetic or antiferromagnetic[72, 73] systems. The aim of this chapter is to contribute to the theoretical analysis of current-induced torques in uniformly magnetized ferromagnets.

In Sec. II we study the effect responsible for this type of torque, which we refer to as the ferromagnetic inverse spin-galvanic effect.[74–80] In non-magnetic conductors the inverse spin-galvanic effect (ISGE) refers to current-induced spin density. Since a non-zero spin-density already appears in the equilibrium state of a ferromagnet, the ferromagnetic inverse spin-galvanic effect has a distinct experimental signature. Specifically, we find that in gyrotropic ferromagnets the magnetization direction is altered by a steady-state transport current. At a conceptual level, we associate this reorientation with a change in magnetic anisotropy in the presence of a transport current. An important implication of this connection is that the magnetic anisotropy en-

ergy in the transport steady state of a ferromagnet which exhibits the ISGE is *not* invariant under magnetization reversal, essentially because the applied current breaks time reversal invariance. At a practical level, we provide a concise analytical expression for the current-induced change in the magnetic anisotropy. This expression is suitable for evaluation from first principles because it requires the knowledge of only the band structure of the ferromagnet and the lifetime of the Bloch states. At a technical level, our theory allows for the spatial inhomogeneities that inevitably occur in the *magnitude* of the ferromagnet's exchange field at atomic lengthscales.

In Sec. III we carry out quantitative calculations for the ISGE of strained (Ga,Mn)As using a 4-band Kohn-Luttinger model. This calculation directly addresses the experiment by Chernyshov *et al.*[70] and corroborates their interpretation of the data. By computing the anisotropy field both in absence and in presence of an electric current, we find that in (Ga,Mn)As magnetization reversal may in principle be achieved solely by electric means: the required critical current densities are in the order of $10^6 - 10^7$ A/cm² and depend on the strain, Mn concentration and hole density. Sec. IV contains a brief summary and presents our conclusions.

The main conclusions of our work coincide with those reached by Manchon and Zhang in their independent and previously published work described in Refs.[68, 69]. Yet, our analysis highlights aspects that have not been emphasized previously. First, we assert that in ferromagnets with inversion symmetry, the current-induced spin-density vanishes *to all orders* in the strength of

the spin-orbit interaction. Second, when evaluating the current-induced spin polarization we include a contribution from interband coherence which can become quantitatively important in disordered ferromagnets such as (Ga,Mn)As. Third, we identify the current-induced transverse spin-density associated with the ISGE in ferromagnets as a consequence of a change in magnetic anisotropy in the presence of an electric current. We thus promote transport currents to the same status as temperature,[81] gate voltages,[82–84] strain[85, 86] and chemical processes,[87] all of which are well-established control parameters for the tuning of magnetic anisotropy.

5.2 Theory of the Ferromagnetic Inverse Spin-Galvanic Effect

In non-magnetic metals or semiconductors that are gyrotropic, *i.e.* non-centrosymmetric *and* chiral,¹ a DC charge current is generically accompanied by a non-zero spin polarization.[74–80] This phenomenon is sometimes referred to as the inverse spin galvanic effect (ISGE).[80] Because of the advent of spintronics and subsequent attempts to control spin polarization by electric means, even in paramagnetic materials, the ISGE has received widespread experimental[88–92] and theoretical[93–96] attention. The ISGE is purely a consequence of symmetry since i) current, which is odd under time reversal, is the dissipative response of a conductor to a DC electric-field, ii) spin is also odd

¹All gyrotropic crystals are non-centrosymmetric, but not all non-centrosymmetric crystals are gyrotropic.

under time reversal and therefore allowed as part of the dissipative response, and iii) axial vectors (like spin) and polar vectors (like current) are coupled in gyrotropic materials.² The direction of the carriers' spin is determined by the direction of the electric field as well as by the axis along which inversion symmetry is broken.³

The ISGE is sometimes viewed as a possible route toward the development of spintronics effects in paramagnetic materials that are as robust as effects like giant magnetoresistance that occur only in ferromagnetic materials. Partly because spin-orbit interactions tend to be fairly weak, it appears to be difficult to make spin-galvanic effects in normal metals useful. In this section we turn the tables on this strategy by concentrating on the inverse spin-galvanic effect in *magnetic* conductors.

In uniformly magnetized ferromagnets with inversion symmetry, the transport current is spin polarized because the conductivities of majority and

²By definition, axial vectors and polar vectors transform in identical manner under operations belonging to gyrotropic point groups. Consequently, gyrotropic crystals (which are invariant under transformations from gyrotropic point groups) enable the coupling between axial and polar vectors. As a simple example, consider a two dimensional electron gas (2DEG) with Rashba spin-orbit coupling. Under a 90° rotation around the \hat{z} axis (perpendicular to the 2DEG), the current $\mathbf{j} = (j_x, j_y)$ changes to $\mathbf{j}' = (j_y, -j_x)$ and the spin operator $\mathbf{S} = (S_x, S_y)$ changes in the same manner, namely to $\mathbf{S}' = (S_y, -S_x)$. Since the 90° rotation around \hat{z} is a symmetry of the Rashba Hamiltonian, a nonzero current-induced spin polarization is allowed under such operation.

³For paramagnetic metals it is straightforward to deduce the relative orientation between the applied electric field and the induced spin polarization from symmetry arguments. For instance, the Hamiltonian for a 2DEG with Rashba spin-orbit interaction is invariant under a 90° rotation around the \hat{z} as well as under a reflection with respect to the plane perpendicular to \hat{y} . According to Neumann's principle, the tensor relating the electric field and the spin polarization must be invariant under the above mentioned symmetry operations. From this requirement it follows that the spin polarization must be perpendicular to the current.

minority spin channels are different. This familiar fact is unrelated to the ISGE. Since spin-polarization is already present in the thermodynamic equilibrium state of a ferromagnet, the ferromagnetic ISGE is manifested not by the presence of a non-zero spin-density but instead by a change in magnetization direction in the non-equilibrium steady-state which is dependent on the magnitude and direction of the electric field. In this paper we formulate a theory of the ISGE in ferromagnets by evaluating the torque which acts on the collective magnetization of a magnetic conductor due to spin-orbit interactions in the presence of a transport current. When the current is set to zero, the torque we evaluate vanishes along easy (and hard) magnetization directions and is normally viewed[97] as a precessional torque due to magnetocrystalline anisotropy fields. These torques are in turn associated with the magnetization-direction dependence of the magnetocrystalline anisotropy energy. At zero current, the anisotropy torques must change sign when the magnetization direction is reversed because time reversal symmetry requires that the anisotropy energy be invariant under reversal. The ferromagnetic ISGE in gyrotropic crystals may be viewed as a change in anisotropy torque due to a transport current. Significantly, the ISGE torques are *not* odd under magnetization reversal.

The ferromagnetic ISGE is reminiscent of the magnetoelectric phenomena that have been extensively studied in multiferroic materials,[98, 99] *i.e.* materials in which magnetism coexists with ferroelectricity. A common characteristic of multiferroic perovskites is the presence of canted magnetism that

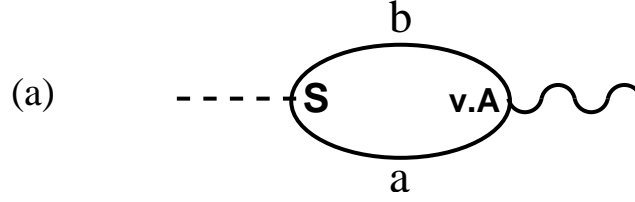


Figure 5.1: Feynman diagram that encodes the transverse spin density induced by a current (ferromagnetic ISGE effect) which results in a change in the steady-state magnetization direction. a and b are band labels for the quasiparticle and the quasihole.

stems from the Dzyaloshinskii-Moriya interaction. Since the direction of canting is determined by the symmetry of the crystal, one can envisage [100] scenarios in which an electric-field-mediated reversal of the ferroelectric polarization causes a simultaneous reversal of the canting angle or of the magnetization. Another interesting property of multiferroic materials is the coupling between ferroelectricity and antiferromagnetism. [101] This coupling makes it possible to switch the magnetization of an exchange-biased ferromagnet by the application of an electric field. In spite of the contextual similarities, there are fundamental differences between the aforementioned phenomena and the ferromagnetic ISGE. For one thing, ferroelectricity occurs only in insulators while the ISGE occurs only in conductors.

We evaluate the ferromagnetic ISGE microscopically within the framework of linear response theory (Fig. (5.1a)):

$$\delta s^i = \chi_{S,E}^{i,j} E^j, \quad (5.1)$$

where δs^i is the current-induced spin density ($i \in \{x, y, z\}$), \mathbf{E} is the applied

electric field, and χ the dissipative spin-current response function:

$$\chi_{S,E}^{i,j} = \frac{1}{2\pi} \text{Re} \sum_{\mathbf{k},a,b} s_{a,b}^i(\mathbf{k}) v_{b,a}^j(\mathbf{k}) (G_{\mathbf{k},a}^R G_{\mathbf{k},b}^A - G_{\mathbf{k},a}^R G_{\mathbf{k},b}^R). \quad (5.2)$$

This linear response theory expression applies for time-independent uniform applied electric fields, and may be derived in the standard way[39] by analytically continuing the imaginary ⁴ part of $\lim_{\omega \rightarrow 0} \tilde{\chi}_{S,E}^{i,j}/\omega$, where

$$\tilde{\chi}_{S,E}^{i,j} = -T \sum_{i\omega_n \mathbf{k}, a, b} s_{a,b}^i(\mathbf{k}) v_{b,a}^j(\mathbf{k}) G_{\mathbf{k},a}(i\omega_n) G_{\mathbf{k},b}(i\omega_n + i\omega), \quad (5.3)$$

$\omega_n = (2n + 1)\pi T$ is the Matsubara frequency at temperature T and ω is the frequency of the external field. In Eq.(5.2) $s_{a,b}^i(\mathbf{k})$ and $v_{b,a}^j(\mathbf{k})$ are the \mathbf{k} -dependent matrix-elements of the spin and velocity operators ($O_{a,b}(\mathbf{k}) \equiv \langle a, \mathbf{k} | O | b, \mathbf{k} \rangle$) between Bloch states ($|a, \mathbf{k}\rangle$) in bands a and b . Note that the Bloch states are in general spinors in which orbital and spin degrees of freedom are entangled. $G_{\mathbf{k},a}^{R(A)} = 1/(\epsilon_F - \epsilon_{\mathbf{k},a} + (-)i/2\tau_{\mathbf{k},a})$ is the retarded (advanced) Green's function evaluated at the Fermi energy ϵ_F , and $\tau_{\mathbf{k},a}$ is the quasiparticle lifetime. For simplicity we have ignored disorder vertex corrections to both velocity and spin operators. In the numerical calculations discussed in Sec. III we will in addition take the quasiparticle lifetime to be a phenomenological parameter which is independent of momentum and band labels.

As we discuss below, the transverse components of the spin-density are directly related to the anisotropy field, which exerts a torque on the macrospin.

⁴In the zero frequency limit the real part of $\tilde{\chi}/\omega$ is cancelled out by the diamagnetic response. This reflects the fact that in non-superconducting metals the current induced spin density is dissipative.

On the same footing, the current-induced contribution to the transverse spin density is directly related to the current-induced contribution to the anisotropy field.

For a ferromagnet with inversion symmetry $\chi_{S,E} = 0$ irrespective of spin-orbit interaction strength, for essentially the same reasons as the ISGE vanishes in normal conductors with inversion symmetry.[102] This property can be verified by recognizing that in presence of inversion symmetry the Hamiltonian of the ferromagnet is invariant under $\mathbf{k} \rightarrow -\mathbf{k}$, which implies that $G_{\mathbf{k}} = G_{-\mathbf{k}}$, $s_{a,b}(\mathbf{k}) = s_{a,b}(-\mathbf{k})$ and $v_{a,b}(\mathbf{k}) = -v_{a,b}(-\mathbf{k})$. Consequently, the right hand side of Eq. (5.2) vanishes after summing over all \mathbf{k} . From a crystal symmetry classification standpoint there are 21 non-centrosymmetric crystal classes, among which three (T_d , C_{3h} and D_{3h}) are not gyrotropic. The occurrence of the ISGE is therefore restricted to 18 crystal classes.[80]

The main objective of this section is to relate the ferromagnetic ISGE to a current-induced change in the magnetic anisotropy field, yet before we do so it is beneficial to pave the way by reviewing the nuances of magnetic anisotropy in electric equilibrium. In the absence of currents, magnetic anisotropy describes the dependence of the free energy of a ferromagnet on the direction of its magnetization.[103] Magnetic anisotropy originates from[104–106] magnetic dipolar interactions and spin-orbit interactions. The former lead to shape anisotropy in non-spherical samples while the latter produce magnetocrystalline anisotropy by communicating the lack of rotational symmetry in the crystalline lattice to the spin degrees of freedom. In practice,

magnetic anisotropy reveals itself in dynamical processes such as ferromagnetic resonance through an anisotropy field that forces the magnetization to precess unless it is along an easy or hard axis, *i.e.* along a direction in which the anisotropy energy is minimized or maximized. This precessional magnetization dynamics is properly characterized by the Landau-Lifshitz equation, $\partial_t \hat{\Omega} = \hat{\Omega} \times H_{\text{eff}}$, where $\hat{\Omega}$ is the direction of the ferromagnet's collective dynamical variable (which may be chosen to be either the magnetization or the ferromagnetic exchange field) and H_{eff} is an effective magnetic field, taken here to include reactive as well as dissipative processes.[25, 36] The anisotropy field may then be defined as the contribution to the non-dissipative part of the effective magnetic field which survives in the absence of true magnetic fields:

$$\mathbf{H}_{\text{an}} = -\frac{1}{S_0} \frac{\partial E_{\text{GS}}}{\partial \hat{\Omega}}, \quad (5.4)$$

where E_{GS} is the ground state energy of the ferromagnet in equilibrium (we take zero temperature throughout) and S_0 is the total spin (magnetization \times volume) of the ferromagnet.

When we discuss (Ga,Mn)As in the following section, we will use spherical coordinates (Fig. 5.2) in which the anisotropy field may be written as

$$\mathbf{H}_{\text{an}} = H_\phi \hat{\phi} + H_\theta \hat{\theta}, \quad (5.5)$$

where $\hat{\phi}$ and $\hat{\theta}$ are the azimuthal and the polar unit vectors, respectively. The longitudinal component of the anisotropy field is irrelevant because $\hat{\Omega} \times \hat{\Omega} = 0$.

In order to elaborate on the microscopic theory of the anisotropy field in a concrete way we work within the spin-density-functional theory of a magnetic

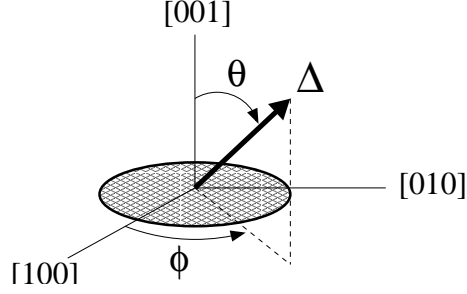


Figure 5.2: Cartoon of a magnetic thin film (shaded area). The exchange field Δ is an effective magnetic field which is parallel to the magnetization only when it points along easy or hard crystalline directions. The orientation of Δ can be specified by the polar and azimuthal angles θ and ϕ . The relationship between the direction of Δ and the direction of magnetization is altered by an electric current in gyrotropic ferromagnets.

material, in which the effective Hamiltonian that describes the theory's Kohn-Sham quasiparticles can be expressed as

$$\mathcal{H} = \mathcal{H}_{\text{kin}} + \mathcal{H}_{\text{so}} - \Delta \cdot \mathbf{s}. \quad (5.6)$$

In Eq. (5.6) $\Delta = \Delta_0(\mathbf{r})\hat{\Omega}$ is the exchange effective-magnetic-field of the ferromagnet, $\hat{\Omega}$ is the direction of the exchange field, \mathbf{s} is the quasiparticle spin operator, \mathcal{H}_{so} captures spin-orbit interactions, and \mathcal{H}_{kin} collects all spin-independent terms in the Kohn-Sham Hamiltonian. In this work we characterize the macrostate of a ferromagnet by specifying the direction of the exchange field. $\hat{\Omega}$ is assumed to be uniform in space but the magnitude $\Delta_0(\mathbf{r})$ of the exchange field is allowed to have spatial dependence at the atomic length-scale.[36] We neglect dipolar interactions since they are not directly influenced by currents and can normally be cleanly separated from magnetocrystalline

anisotropy.

It follows that the zero-temperature anisotropy field is given by

$$\mathbf{H}_{\text{an}} = -\frac{1}{S_0} \sum_{\mathbf{k},a} \frac{\partial \epsilon_{\mathbf{k},a}}{\partial \hat{\Omega}} f_{\mathbf{k},a}. \quad (5.7)$$

In Eq. (5.7) we have used ⁵ $E_{\text{GS}} = \sum_{\mathbf{k},a} \epsilon_{\mathbf{k},a} f_{\mathbf{k},a}$, where $\epsilon_{\mathbf{k},a}$ is the energy of the Bloch state quasiparticles and $f_{\mathbf{k},a} = \Theta(\epsilon_F - \epsilon_{\mathbf{k},a})$ is the equilibrium occupation factor at zero temperature. Furthermore we have exploited the fact that

$$\sum_{\mathbf{k},a} \epsilon_{\mathbf{k},a} \frac{\partial f_{\mathbf{k},a}}{\partial \hat{\Omega}} \simeq \epsilon_F \sum_{\mathbf{k},a} \frac{\partial f_{\mathbf{k},a}}{\partial \hat{\Omega}} = 0, \quad (5.8)$$

since the number of electrons in the ferromagnet is invariant under rotations of the magnetization. This implies a $\hat{\Omega}$ -dependence of the Fermi energy,[109, 111] which is taken into account in the calculations of Sec. III.

Eq. (5.7) may be rewritten in a more informative manner using the Feynman-Hellmann theorem, which implies that

$$\frac{\partial \epsilon_{\mathbf{k},a}}{\partial \Omega_i} = \langle a, \mathbf{k} | \frac{\partial \mathcal{H}}{\partial \Omega_i} | a, \mathbf{k} \rangle = -\langle a, \mathbf{k} | \Delta_0(\mathbf{r}) s_i | a, \mathbf{k} \rangle. \quad (5.9)$$

Then,

$$\mathbf{H}_{\text{an}} = \frac{1}{S_0} \sum_{\mathbf{k},a} \langle a, \mathbf{k} | \Delta_0(\mathbf{r}) \mathbf{s} | a, \mathbf{k} \rangle f_{\mathbf{k},a}, \quad (5.10)$$

⁵The sum of the single-particle Kohn-Sham eigenvalues does not account for the actual ground state energy of the ferromagnet because it neglects the double-counted Hartree and exchange-correlation contributions. However, we invoke the *force theorem* which states that the extra terms will cancel when one takes the difference in total energies between two macrostates with non-collinear exchange fields. See for instance Refs.[107], [108] and [109]; see also the chapter by A.R. Mackintosh and O.K. Andersen in Ref. [110].

where $\langle a, \mathbf{k} | \Delta_0(\mathbf{r}) \mathbf{s} | a, \mathbf{k} \rangle \equiv \int d\mathbf{r} \Delta_0(\mathbf{r}) \langle a, \mathbf{k} | \mathbf{r} \rangle \mathbf{s}(\mathbf{r}) \langle \mathbf{r} | a, \mathbf{k} \rangle$.

For the envelope-function model we use in the next section, the magnitude of the exchange field is a spatially constant Δ_0 and the torque exerted by the anisotropy field is simply equal to the Δ_0 times the transverse spin-density divided by the total spin of the ferromagnet. In *ab initio* calculations, the magnitude of the exchange field always varies substantially on an atomic scale and, as we have emphasized previously,[36] this variation must be accounted for. In this case the anisotropy field is evaluated by integrating the product of the exchange field magnitude and transverse spin density over space.

Eq. (5.10) may be separated into azimuthal and polar components:

$$\begin{aligned} H_\phi &= \frac{1}{S_0} \sum_{\mathbf{k}, a} \langle a, \mathbf{k} | \hat{z} \cdot (\mathbf{\Delta} \times \mathbf{s}) | a, \mathbf{k} \rangle \\ H_\theta &= \frac{1}{S_0} \sum_{\mathbf{k}, a} \langle a, \mathbf{k} | \hat{\phi} \cdot (\mathbf{\Delta} \times \mathbf{s}) | a, \mathbf{k} \rangle \end{aligned} \quad (5.11)$$

If we neglect spatial variations of $\Delta_0(\mathbf{r})$, Eqs. (5.10) and (5.11) indicate that the torque created by the anisotropy field will vanish when the (spin) magnetization $\sum \langle \mathbf{s} \rangle f$ is parallel to the exchange field. Conversely, whenever the direction of magnetization is misaligned with $\mathbf{\Delta}$, the anisotropy field will be nonzero and will produce a torque on the magnetization. In transition metals spin-orbit interactions produce a misalignment between the exchange field and the magnetization, unless $\hat{\Omega}$ is pointing along some special crystalline direction that corresponds (by definition) to an easy or hard axis. A similar picture applies to local-moment ferromagnets as well, where due to spin-orbit coupling

the direction of the local moments is generally misaligned with the direction of the itinerant spin density.

One of the targets of this section is to present formulae that are useful for researchers working on both model systems as well as *ab-initio* electronic structure calculations. Therefore, we digress to explain that Eq. (5.10) is equivalent to the alternative expressions found in *ab-initio* studies. In first principles magnetic anisotropy theory[109, 112] Eq. (5.9) has been approached from a different perspective. In such approach it is customary to choose the spin quantization axis along the direction of magnetization, so that $\mathbf{\Delta} \cdot \mathbf{s} \equiv \Delta_0 s_z$ is independent of $\hat{\Omega}$. When this choice is made, the spin-orbit term in the Hamiltonian becomes explicitly $\hat{\Omega}$ -dependent. Consequently,

$$\frac{\partial \epsilon_{\mathbf{k},a}}{\partial \hat{\Omega}} = \langle a, \mathbf{k} | \frac{\partial \mathcal{H}_{\text{so}}}{\partial \hat{\Omega}} | a, \mathbf{k} \rangle. \quad (5.12)$$

The anisotropy field is then evaluated combining Eq. (5.12) with the force theorem and a full-potential electronic-structure calculation.[112] Of course, the final result is invariant with respect to the choice of the spin quantization axis. In order to prove the equivalence of Eqs. (5.9) and (5.12) it is convenient to rewrite[26] Eq. (5.12) as $\partial \epsilon / \partial \phi = \langle \partial_\phi [\exp(i\mathbf{s} \cdot \hat{z}\phi) \mathcal{H}_{\text{so}} \exp(-i\mathbf{s} \cdot \hat{z}\phi)] \rangle_0$ and $\partial \epsilon / \partial \theta = \langle \partial_\theta [\exp(i\mathbf{s} \cdot \hat{\phi}\theta) \mathcal{H}_{\text{so}} \exp(-i\mathbf{s} \cdot \hat{\phi}\theta)] \rangle_0$. To see that these expressions agree with Eq. (5.11) note that $[\mathcal{H}_{\text{so}}, \mathbf{s}] = [\mathcal{H} - \mathcal{H}_{\text{kin}} + \mathbf{\Delta} \cdot \mathbf{s}, \mathbf{s}]$, that $[\mathcal{H}_{\text{kin}}, \mathbf{s}] \equiv 0$, and that $\langle a, \mathbf{k} | [\mathcal{H}, \mathbf{s}] | a, \mathbf{k} \rangle = (\epsilon_{\mathbf{k},a} - \epsilon_{\mathbf{k},a}) \langle a, \mathbf{k} | \mathbf{s} | a, \mathbf{k} \rangle = 0$. In this way the derivative of energy with respect to magnetization direction can be related to the exchange term in the Kohn-Sham equation rather than to the spin-orbit

coupling term. Eqs. (5.10) and (5.11) are recovered after using $[s_i, s_j] = i\epsilon_{ijk}s_k$ to simplify $\langle[\Delta \cdot \mathbf{s}, \mathbf{s}]\rangle$.

We now show that the Green's function expression we use to evaluate the ferromagnetic ISGE (Eq.(5.3)) corresponds to the current-induced change in Eq. (5.10). We begin by mentioning that the application of an electric current can alter the magnetic anisotropy field, which leads to a current-induced torque on the magnetization. For an arbitrary orientation of the exchange field, the change is given by

$$\delta\mathbf{H}_{\text{an}} = \frac{1}{S_0} \sum_{\mathbf{k},a} \delta(\langle a, \mathbf{k} | \Delta_0(\mathbf{r}) \mathbf{s} | a, \mathbf{k} \rangle) f_{\mathbf{k},a} + \frac{1}{S_0} \sum_{\mathbf{k},a} \langle a, \mathbf{k} | \Delta_0(\mathbf{r}) \mathbf{s} | a, \mathbf{k} \rangle \delta f_{\mathbf{k},a}. \quad (5.13)$$

Adopting the relaxation-time approximation, δf reads

$$\delta f_{\mathbf{k},a} = \mathbf{E} \cdot \mathbf{v}_{a,a} \frac{\partial f_{\mathbf{k},a}}{\partial \epsilon_{\mathbf{k},a}} \tau_{\mathbf{k},a}, \quad (5.14)$$

and for the change in the matrix elements we use

$$\delta(\langle a, \mathbf{k} | \Delta_0 \mathbf{s} | a, \mathbf{k} \rangle) = \langle a, \mathbf{k} | \Delta_0 \mathbf{s} \delta(|a, \mathbf{k} \rangle) + \text{c.c} \quad (5.15)$$

with

$$\delta(|a, \mathbf{k} \rangle) = \frac{e^{i\omega t}}{i\omega} \sum_{b \neq a} |b, \mathbf{k} \rangle \frac{\langle b, \mathbf{k} | \mathbf{v} \cdot \mathbf{E} | a, \mathbf{k} \rangle}{\epsilon_{\mathbf{k},a} - \epsilon_{\mathbf{k},b} + \omega} + (\omega \rightarrow -\omega). \quad (5.16)$$

In Eq. (5.16) we have once again appealed to linear response theory and have used the fact that the electric field is uniform.

Eqs. (5.14) and (5.16) highlight the two ways in which a current alters the magnetic anisotropy field. Eq. (5.14) captures the shift in the effective

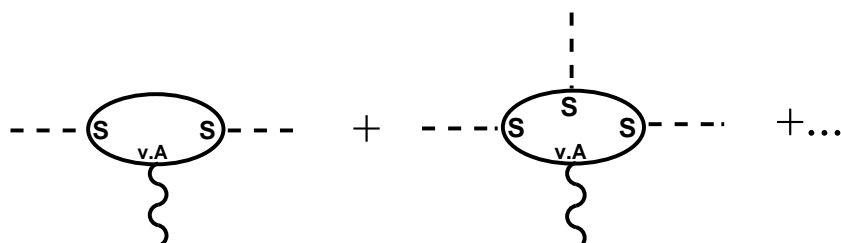


Figure 5.3: Spin response to a transverse magnetic field \mathbf{B}_\perp in the presence of a current: perturbation theory to all orders in \mathbf{B}_\perp . The quasiparticles (quasiholes) in these diagrams diagonalize a Hamiltonian whose exchange field is pointing along an easy direction and \mathbf{B}_\perp is by definition perpendicular to this easy direction. Provided that in Eq. (5.10) we take the exact eigenstates of the mean field Hamiltonian (within which the exchange field need not be pointing along an easy direction), all the diagrams of this figure are implicit in the diagram of Fig. (5.1). In particular, the ferromagnetic ISGE captures the influence of currents on ferromagnetic resonance.

quasiparticle energies due to acceleration by an electric field, while Eq. (5.15) describes the modification of the quasiparticle wavefunctions. As will become clear below the former is associated with intraband contributions to the anisotropy field whereas the latter may be traced to the interband contributions. Interband contributions are often neglected [69, 102] because they are parametrically smaller by a factor of scattering rate τ^{-1} in good conductors. However, as we show in the next section they may become quantitatively significant in disordered magnets like the (III,Mn)V materials.[37, 38] Admittedly, other corrections with the same parametric dependence on disorder strength could also be present - but the description of these would require a detailed characterization of the disorder potential and a more sophisticated transport theory. The effect we retain is analogous to the intrinsic contribution to the anomalous Hall effect.[113] Substituting Eqs. (5.14), (5.15) and (5.16) in Eq. (5.13) we obtain

$$\delta\mathbf{H}_{\text{an}} = \delta\mathbf{H}_{\text{an}}^{\text{intra}} + \delta\mathbf{H}_{\text{an}}^{\text{inter}}$$

where

$$\begin{aligned} \delta\mathbf{H}_{\text{an}}^{\text{intra}} &= \frac{1}{S_0} \sum_{\mathbf{k},a} [\Delta_0(\mathbf{r})\mathbf{s}]_{a,a} \mathbf{v}_{a,a} \cdot \mathbf{E} \frac{\partial f_{\mathbf{k},a}}{\partial \epsilon_{\mathbf{k},a}} \tau_{\mathbf{k},a} \\ \delta\mathbf{H}_{\text{an}}^{\text{inter}} &= \frac{1}{i\omega} \frac{1}{S_0} \sum_{\mathbf{k},a \neq b} [\Delta_0(\mathbf{r})\mathbf{s}]_{a,b} \mathbf{v}_{b,a} \cdot \mathbf{E} \\ &\quad \times \frac{f_{\mathbf{k},a} - f_{\mathbf{k},b}}{\epsilon_{\mathbf{k},b} - \epsilon_{\mathbf{k},a} + \omega + i\eta} \end{aligned} \quad (5.17)$$

In the expression for $\delta\mathbf{H}_{\text{an}}^{\text{inter}}$ we have selected the coefficient of $\exp(i\omega t)$ in the perturbation expansion, have neglected disorder scattering and have allowed

for a small positive imaginary part in the frequency.

Several remarks are pertinent in regards to our derivation of the interband component. First, it should be noted that in the zero frequency limit the imaginary part of $\delta\mathbf{H}_{\text{an}}^{\text{inter}}$ gets cancelled by the diamagnetic contribution, in such a way that the anisotropy field induced by a DC current is finite and real. Second, it is instructive to elaborate on the real part of $\delta\mathbf{H}_{\text{an}}^{\text{inter}}$:

$$\begin{aligned} \delta\mathbf{H}_{\text{an}}^{\text{inter}} &= \\ &= \frac{-\pi}{S_0\omega} \sum_{\mathbf{k}, a \neq b} \text{Re} [(\Delta_0\mathbf{s})_{a,b}\mathbf{v}_{b,a}] \cdot \mathbf{E}(f_{\mathbf{k},a} - f_{\mathbf{k},b})\delta(\omega_{b,a} + \omega) \\ &+ \frac{1}{S_0\omega} \sum_{\mathbf{k}, a \neq b} \text{Im} [(\Delta_0\mathbf{s})_{a,b}\mathbf{v}_{b,a}] \cdot \mathbf{E}f_{\mathbf{k},a} \frac{2\omega}{\omega^2 - \omega_{b,a}^2}, \end{aligned} \quad (5.18)$$

where $\omega_{b,a} \equiv \epsilon_{\mathbf{k},b} - \epsilon_{\mathbf{k},a}$. From Eq. (5.18) it is clear that $\delta\mathbf{H}_{\text{an}}^{\text{inter}}$ remains finite as $\omega \rightarrow 0$. When disorder is included in the above expressions, the contribution from the second line in Eq. (5.18) scales as τ^{-1} and thus is unimportant when the broadening of the energy bands due to impurity scattering is small compared to the energy difference between states connected by interband transitions. In contrast, the third line scales as τ^0 , and therefore it supplies the bulk of the interband contribution in weakly disordered ferromagnets.

Recognizing the fact that the integration of equal-band Green's functions gives rise to a factor of τ , $\delta\mathbf{H}_{\text{an}}^{\text{intra}}$ yields the intraband piece of Eq. (5.2) modulo a factor of Δ_0/S_0 . Similarly, $\delta\mathbf{H}_{\text{an}}^{\text{inter}}$ brings in the interband part of

Eq. (5.2) modulo a factor of Δ_0/S_0 ; in order to verify this we recall ⁶ that

$$\sum_{\mathbf{k}} \frac{f_{\mathbf{k},a} - f_{\mathbf{k},b}}{\epsilon_{\mathbf{k},b} - \epsilon_{\mathbf{k},a} + i\omega} = -T \sum_{\omega_n, \mathbf{k}} G_a(i\omega_n, \mathbf{k}) G_b(i\omega_n + i\omega, \mathbf{k}). \quad (5.19)$$

In sum, we find

$$\frac{\partial \delta H_{\text{an}}^i}{\partial E^j} = \frac{1}{2\pi S_0} \text{Re} \sum_{\mathbf{k}, a, b} \langle a, \mathbf{k} | \Delta_0(\mathbf{r}) s^i | b, \mathbf{k} \rangle \langle b, \mathbf{k} | v^j | a, \mathbf{k} \rangle (G_{\mathbf{k},a}^R G_{\mathbf{k},b}^A - G_{\mathbf{k},a}^R G_{\mathbf{k},b}^R), \quad (5.20)$$

which agrees with the ISGE expression for the current-induced spin density (Eq. (5.2)) except for an overall normalization factor ($1/S_0$) and the fact that the spin-operator is weighted by an spatially inhomogeneous magnitude of the exchange field. With the aim of making Eq. (5.20) more manageable for first principles calculations, we will ignore the interband contribution as well as the $G^R G^R$ term; both omissions are justified in most metallic ferromagnets. ⁷ In this case Eq. (5.20) simplifies into

$$\frac{\partial \delta H_{\text{an}}^i}{\partial E^j} \simeq \frac{1}{S_0} \sum_{\mathbf{k}, a} \langle a, \mathbf{k} | \frac{\partial \mathcal{H}_{\text{so}}}{\partial \Omega_i} | a, \mathbf{k} \rangle \langle a, \mathbf{k} | v^j | a, \mathbf{k} \rangle \frac{\partial f_{\mathbf{k},a}(\hat{\Omega})}{\partial \epsilon_{\mathbf{k},a}} \tau_{\mathbf{k},a}, \quad (5.21)$$

where we have re-inserted $\langle a | \Delta_0(\mathbf{r}) \mathbf{s} | a \rangle = \langle a | \partial \mathcal{H}_{\text{so}} / \partial \hat{\Omega} | a \rangle$. While approximate, Eq. (5.21) may provide a valid platform to explore current induced magnetization reversal in real gyrotropic ferromagnets with a single magnetic domain. In the next section we will describe in detail how a large δH_{an} can produce a large reorientation of the magnetization.

⁶Strictly speaking Eqs. (5.16) and (5.19) are accurate only in absence of disorder. Nevertheless, the connection between them remains intact in presence of impurities.

⁷The leading $O(\tau^0)$ correction due to interband transitions would be captured by the second line of Eq. (5.18).

If the spatial dependence of $\Delta_0(\mathbf{r})$ is negligible (as it will be in the model studied in the next section), Eq. (5.20) may be rewritten in a more compact way:

$$\chi_{S,E}^{i,j} = \frac{S_0}{\Delta_0} \frac{\partial \delta H_{\text{an}}^i}{\partial E^j}. \quad (5.22)$$

where $\chi_{S,E}$ is the spin-current susceptibility introduced in Eq. (5.2). Eq. (5.22) proves that the ferromagnetic ISGE describes the change in the magnetic anisotropy field due to a current. In other words, ferromagnetic ISGE determines how an electric current changes the location of the extrema in the micromagnetic energy functional. This is the central idea of this section.

As a final sidenote, we point out that this section has concentrated on evaluating the change in magnetic anisotropy under a perturbation represented by $\mathbf{v} \cdot \mathbf{A}$, where \mathbf{A} is the electromagnetic vector potential. The anisotropy is evaluated by calculating the change in the expectation value of $\Delta_0 s$, thus leading to a rather standard linear response function calculation. We could in the same way calculate the change in the transverse spin-spin response function due to an electric field as indicated in Fig.(5.3), in order to determine how small amplitude magnetic fluctuations are altered. If, however, we are interested only in uniform magnetization dynamics no additional information is obtained by doing this calculation. The key point is that the response to a transverse field \mathbf{B}_\perp is already built in our expression for the equilibrium anisotropy field (Eq. (5.10)), to *all* orders in \mathbf{B}_\perp . In other words, the reference (unperturbed) macrostate to which we apply a current contains a magnetization that is “arbitrarily” misaligned with the exchange field. Hence, Eq. (5.22)

along with Eq. (5.10) offers a complete account of the nonequilibrium magnetic anisotropy of uniform magnetic states in the presence of a transport current.

5.3 Current-Driven Magnetization Reversal in Monodomain (Ga,Mn)As

Magnetoelectric phenomena in dilute magnetic semiconductors[37, 38] such as (Ga,Mn)As have attracted special attention because these materials are more compatible with current microelectronics technology than metals. In addition, electric field control of magnetism has turned out to be more feasible in (Ga,Mn)As than in conventional dense-moment metallic ferromagnets because of their small magnetization, high carrier spin polarization, strong spin-orbit interactions, and carrier-mediated ferromagnetism.[82, 114, 115] In particular, the recent experiment[70] by Chernyshov *et al.* on (Ga,Mn)As wafers under compressive strain has demonstrated the ability of transport currents to reversibly *assist* the reorientation of magnetization in *single-domain* ferromagnets. As we demonstrate here this effect is dependent on having both spin-orbit interactions and broken inversion symmetry. In this section we compute the change in the magnetic anisotropy due to an electric current for a realistic model of (Ga,Mn)As. Our calculation is directly relevant to the experiment of Chernyshov *et al.*. Our results corroborate their interpretation of the data and predict the possibility of all-electric magnetization switching in (Ga,Mn)As. Our analysis is limited to zero temperature and neglects the shape anisotropy, which for typical Mn doping concentrations is 10-100 times

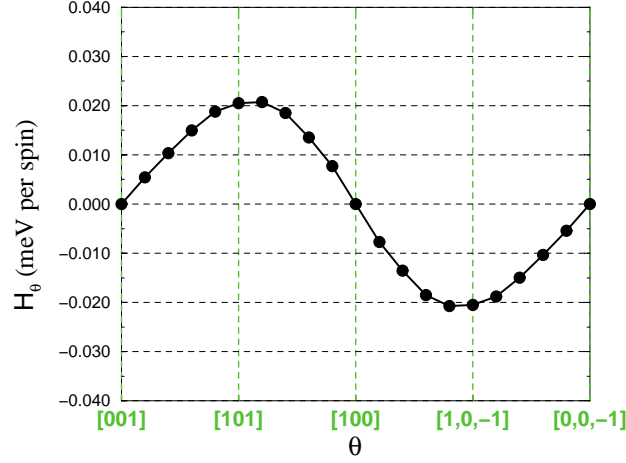


Figure 5.4: Equilibrium anisotropy field (meV per spin) in (Ga,Mn)As for $\phi = 0$, and $\theta \in (0, \pi)$. The parameters used for this calculation were: Mn fraction $x = 0.08$, hole concentration $p \simeq 0.15\text{nm}^{-3}$, $\epsilon_F\tau = 3$, and axial strain $\epsilon_{\text{ax}} = -0.5\%$. These anisotropy field results were evaluated using the model explained in the text.

weaker than in conventional ferromagnets.

The dependence of the magnetic anisotropy of (Ga,Mn)As on doping, external electric fields, temperature and strain has been successfully explained[116–118] by combining (i) a mean-field theory of the exchange coupling between localized Mn moments and valence band carriers with (ii) a phenomenological four or six band envelope function model in which the valence band holes are characterized by Luttinger, spin-orbit splitting and strain-energy parameters. The results presented below predict the rate at which these fields change with external electric field.

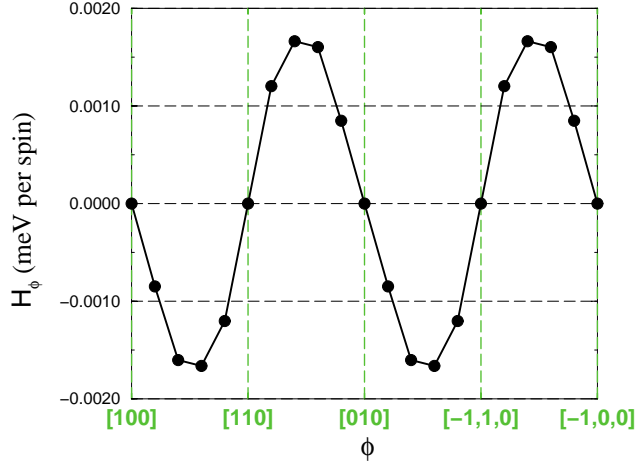


Figure 5.5: Equilibrium anisotropy field (meV per spin) in (Ga,Mn)As for $\theta = \pi/2$ and $\phi \in (0, \pi)$. The parameters are: Mn fraction $x = 0.08$, hole concentration $p \simeq 0.15\text{nm}^{-3}$, $\epsilon_F\tau = 3$, and axial strain $\epsilon_{\text{ax}} = -0.5\%$. These results were evaluated using the model explained in the text. Due to strain, the in-plane anisotropy is notably weaker than the out-of-plane anisotropy represented in the previous figure.

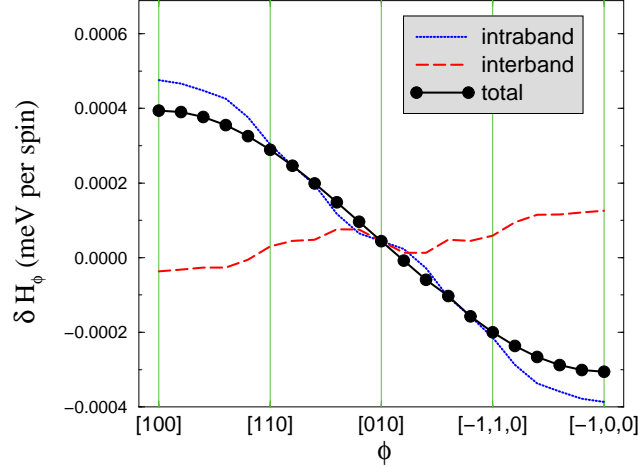


Figure 5.6: Change in the magnetic anisotropy field of (Ga,Mn)As (in meV per spin) due to the inverse spin-galvanic effect, for an electric field of 1mV/nm along [010]. The parameters are: Mn fraction $x = 0.08$, hole concentration $\simeq 0.25\text{nm}^{-3}$, $\epsilon_F\tau = 2$, and axial strain $\epsilon_{ax} = -1\%$. We compare between interband and intraband contributions: in contrast to the case of good metals, the interband contributions are not negligible in (Ga,Mn)As. For the present case, had we neglected the interband contribution the minimum electric field needed to reorient the magnetization by 90° would be off by approximately 20%. The sum of interband and intraband pieces gives rise to a smooth curve that reflects the Dresselhaus symmetry of the axial strain. Reversing the sign of the axial strain (i.e. making it tensile) leads to a sign reversal of δH_ϕ .

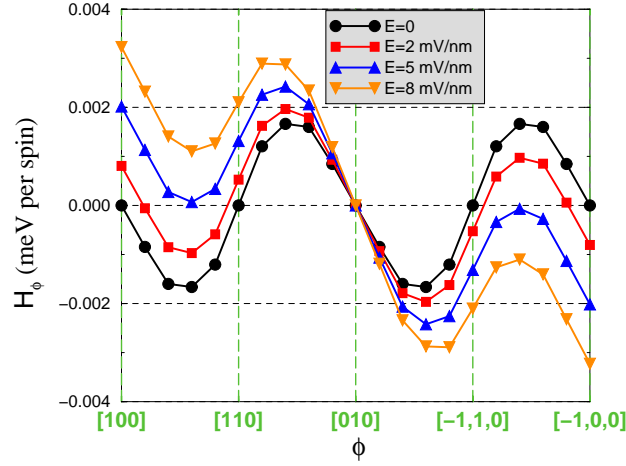


Figure 5.7: Reorientation of the magnetization due to an electric current. An initial magnetization along $[100]$ can be rotated (assisted by damping) into $[010]$ by applying a sufficiently strong electric field with a nonzero projection along the $[010]$ direction (a current along $[100]$ would not destabilize the $[100]$ easy axis). For the parameters of this figure ($x = 0.08$, $p \simeq 0.15 \text{nm}^{-3}$, $\epsilon_F \tau = 3$, $\epsilon_{\text{ax}} = -0.5\%$) the critical electric field is $\simeq 5 \text{mV/nm}$, which corresponds roughly to a critical current density of $5 \times 10^7 \text{A/cm}^2$.

In line with this we adopt the following Hamiltonian for $\text{Ga}_{1-x}\text{Mn}_x\text{As}$:

$$\mathcal{H} = \mathcal{H}_{\text{KL}} + \mathcal{H}_{\text{strain}} + \mathbf{S} \cdot \mathbf{\Delta}. \quad (5.23)$$

\mathcal{H}_{KL} is the 4-band Kohn-Luttinger Hamiltonian[42] with Luttinger parameters $\gamma_1 = 6.98$, $\gamma_2 = 2.1$ and $\gamma_3 = 2.9$. \mathbf{S} is the spin operator projected onto the $J=3/2$ total angular momentum subspace at the top of the valence band. $\mathbf{\Delta} = \Delta_0 \hat{\Omega} = J_{\text{pd}} S N_{\text{Mn}} \hat{\Omega}$ is the exchange field, $\hat{\Omega}$ denotes the orientation of the local moments, $J_{\text{pd}} = 55 \text{ meV nm}$ is the p-d exchange coupling parameter, $S = 5/2$ is the spin of the Mn ions, and $N_{\text{Mn}} = 4x/a^3$ is the Mn concentration ($a = 0.565 \text{ nm}$ is the lattice constant of GaAs). This four-band model is expected to be adequate for small and intermediate Mn doping strengths. $\mathcal{H}_{\text{strain}}$ is the strain Hamiltonian[70, 119, 120] given by

$$\begin{aligned} \mathcal{H}_{\text{strain}} = & -b \left[\left(J_x^2 - \frac{\mathbf{J}^2}{3} \right) \epsilon_{xx} + c.p. \right] \\ & + C_4 [J_x (\epsilon_{yy} - \epsilon_{zz}) k_x + c.p.], \end{aligned} \quad (5.24)$$

where \mathbf{J} is the total angular momentum ($\mathbf{J} = 3\mathbf{S}$ by the Wigner-Eckart theorem), $\epsilon_{i,i}$ are diagonal elements of the stress tensor, $b = -1.7 \text{ eV}$ is the axial deformation potential and the parameter $C_4 = 5 \text{ eV \AA}$ captures the strain-induced linear in k spin-splitting of the valence bands in paramagnetic GaAs. In Eq. (5.24) the notation *c.p.* stands for cyclic permutations and $\epsilon_{x,x} = \epsilon_{y,y} \neq \epsilon_{z,z}$ for [001] growth lattice-matching strains. The term proportional to C_4 is crucial for the occurrence of the ferromagnetic ISGE because it breaks inversion symmetry (we are neglecting the intrinsic lack of inversion

symmetry of the zinc-blende structure, which is relatively inconsequential), and it introduces chirality. (A bulk, unstrained zinc-blende crystal is not gyrotropic because it corresponds to the T_d symmetry point group.) Eq. (5.24) may be simplified to

$$\mathcal{H}_{\text{strain}} = -b\epsilon_{\text{ax}} \left(J_z^2 - \frac{\mathbf{J}^2}{3} \right) + C_4\epsilon_{\text{ax}} (J_y k_y - J_x k_x), \quad (5.25)$$

where $\epsilon_{\text{ax}} = \epsilon_{zz} - \epsilon_{xx}$ is the purely axial strain component. In this paper we take $\epsilon_{\text{ax}} < 0$ (compressive strain), which applies when (Ga,Mn)As is grown on top of a GaAs substrate.

Using Eqs. (5.10), (5.22) and (5.23) we evaluate the magnetic anisotropy field both with and without electric current; the results are highlighted in Figs. (5.4)- (5.8). Figs. (5.4) and (5.5) correspond to electrical equilibrium and illustrate $H_\theta = -1/S_0 \sum_{\mathbf{k},a} (\partial \epsilon_{\mathbf{k},a} / \partial \theta) f_{\mathbf{k},a}$ for $\phi = 0$ and $H_\phi = -1/S_0 \sum_{\mathbf{k},a} (\partial \epsilon_{\mathbf{k},a} / \partial \phi) f_{\mathbf{k},a}$ for $\theta = \pi/2$, respectively. The extrema of the micro-magnetic energy functional are characterized by $H_\phi = H_\theta = 0$ and by inspection we locate them at $\theta = 0$ and $(\theta, \phi) = (\pi/2, n\pi/4)$ where $n = 0, 1, 2, \dots$. For our parameters (see figure captions) the energy minima that define metastable magnetic configurations are found at $(\theta, \phi) = (\pi/2, n\pi/2)$. That is to say, the easy directions correspond to $[100]$, $[010]$, $[\bar{1}00]$ and $[0\bar{1}0]$, which are contained in the plane of the (Ga,Mn)As wafer. For later reference, we consider an initial condition in which the magnetization is pointing along $[100]$. If a small static perturbation tilts it towards $[110]$, the negative anisotropy field ($H_\phi < 0$ for

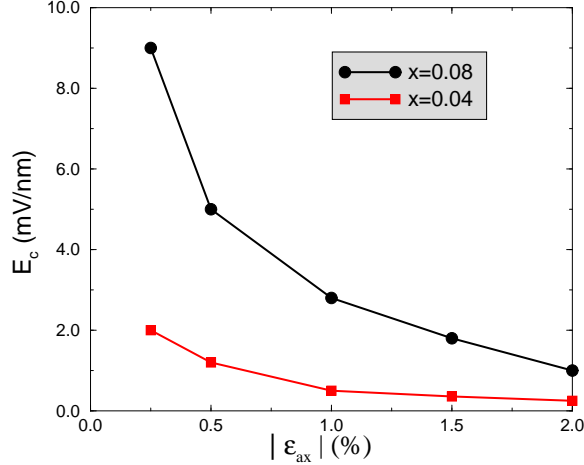


Figure 5.8: Dependence of the critical electric field (at which the magnetization gets reoriented by 90°) on (compressive) axial strain. The critical current is (roughly) inversely proportional to ϵ_{ax} . The reason behind this relationship is that the equilibrium, *azimuthal* anisotropy is largely indifferent to ϵ_{ax} . For $x = 0.04$ and $\epsilon_{ax} = -2\%$ we find $E_c \simeq 0.25\text{mV/nm}$, which corresponds to a critical current on the order of 10^6A/cm^2 . These results are for a (Ga,Mn)As model with carrier density $p \simeq 0.15\text{nm}^{-3}$ and $\epsilon_F\tau = 3$.

$\phi > 0$) creates a torque that will, in conjunction with damping,⁸ turn the magnetization back to [100].

Fig. (5.6) illustrates how an electric current along [010] alters the azimuthal anisotropy field⁹ for fixed $\theta = \pi/2$. The cosine-like shape is consistent with the Dresselhaus symmetry of the C_4 term in the strain Hamiltonian. If the

⁸In absence of damping the magnetization would keep precessing indefinitely. The combined action of the anisotropy field and damping is what ultimately drives the system to the minimum energy state.

⁹Our discussion concentrates on H_ϕ . Although H_θ too generally changes in presence of a current, it is not pertinent to the [100]→[010] or [100]→[$\bar{1}$ 00] magnetization reorientations that we are interested in.

system had a perfect Dresselhaus symmetry the change in the micromagnetic energy functional under an electric current \mathbf{j} would read

$$\delta E_{GS} \propto C_4 \epsilon_{\text{ax}} (\Omega_y j_y - \Omega_x j_x), \quad (5.26)$$

which means that a current along $[010]$ ($[100]$) would tilt the steady-state magnetization direction along $[010]$ ($[\bar{1}00]$). Using $\Omega_x = \sin \theta \cos \phi$ and $\Omega_y = \sin \theta \sin \phi$ it follows that $\delta H_\phi \propto j_y \cos \phi + j_x \sin \phi$, and hence a cosine-like dependence in ϕ is indeed expected for a current along $[010]$. We have verified that a current along \mathbf{x} gives rise to a sine-like dependence with the appropriate sign. Nevertheless, Eq. (5.26) is not exact because the magnetization vector introduces another preferred direction; for instance, we find that an electric field pointing along \hat{z} (i.e. $[001]$) can also alter the steady-state spin orientation. This effect, which vanishes in the paramagnetic limit, highlights one instance in which the ferromagnetic and paramagnetic ISGEs differ. Another attribute of Fig. (5.6) is that it determines the quantitative importance of interband contributions to the current-induced spin density in (Ga,Mn)As. Although normally neglected, interband transitions become quantitatively significant in strongly disordered ferromagnets. In particular, interband and intraband contributions are largely indistinguishable in ferromagnets with $\Delta_0 \tau < 1$. We note parenthetically that neither intraband nor interband contributions display the smooth sinusoidal shape portrayed by their sum. In addition, we remark that reversing the sign of the axial strain (i.e. making it tensile) leads to a sign

reversal of δH_ϕ without substantial changes in its magnitude.¹⁰

Fig. (5.7) demonstrates that a sufficiently strong current is able to rotate the magnetization by 90° or 180° . We explain this property by considering the case in which the equilibrium magnetization is pointing along $[100]$. If a small current is applied along $[010]$, then $[100]$ is no longer an extremum of the micromagnetic energy functional (because $H_\phi(\phi = 0) \propto E_y \neq 0$). The modified *easy* direction remains in the neighborhood of $[100]$ since the restoring torque ($H_\phi < 0$) again crosses zero at $\phi > 0$. Once the applied electric field exceeds a critical value ($E_c \simeq 5.5\text{mV/nm}$ in the present figure) the $H_\phi < 0$ region near $[100]$ disappears completely and hence assisted by damping the magnetization eventually points along $[010]$. In other words, at (and above) the critical switching field the energy minimum that is nearest to $[100]$ is located at $[010]$ (note that this direction remains stable when the current flows along $[010]$). Once the magnetization is aligned with $[010]$, an equally strong electric current in the $[100]$ direction will rotate it towards $[\bar{1}00]$. In this fashion it is possible to switch the direction of magnetization by 180° solely by application of transport currents.

The procedure sketched above accomplishes magnetization switching by application of two perpendicular current pulses, each of which forces a 90° rotation. Yet, it is also possible to achieve the $[100] \rightarrow [\bar{1}00]$ switching with

¹⁰It is known that in GaAs quantum wells the strain-induced \mathbf{k} -linear terms have negligible impact if the strain is compressive, yet they matter if the strain is tensile (see *e.g.* [119]). This observation does not apply to bulk (Ga,Mn)As.

a single *unidirectional* pulse, provided the electric field along [100] is ramped up sufficiently ($E_{c,2} \simeq 20\text{mV/nm}$ for the parameters of the present figure). In order to understand this, recall that $\mathbf{j}||\hat{\mathbf{x}} \rightarrow \delta\mathbf{H}_{\text{an}}||-\hat{\mathbf{x}}$. Consequently, for a strong electric current $[\bar{1}00]$ is the only easy direction ($[100]$ becomes a hard direction). The inequivalence between $[100]$ and $[\bar{1}00]$ does not violate any symmetry principles; [121] in effect, an electric current breaks time reversal symmetry and can thus connect time-reversed magnetic states.

Using $\rho = 10^{-3}\Omega\text{cm}$ as the typical resistivity for (Ga,Mn)As samples we deduce that $E = 1\text{mV/nm}$ corresponds approximately to a current density of 10^7A/cm^2 , hence the critical switching current is on the order of $10^6 - 10^7\text{A/cm}^2$. It is plausible that a detailed exploration of the parameter space comprised by the Mn concentration x , the hole density p and the axial strain ϵ_{ax} will enable lower critical currents, thereby diminishing the importance of the Joule heating. As a word of caution, we note that the 4-band model employed here typically overestimates the effect of spin-orbit interactions, thus potentially leading to an underestimate of these critical currents. There is in addition some uncertainty associated with the use of a life-time approximation for Bloch state quasiparticles in these strongly disordered metallic conducting ferromagnets.

Overall, the magnitude of the critical switching current depends on (a) the size of the equilibrium anisotropy barrier, (b) the extent to which inversion symmetry is broken and (c) the strength of spin-orbit interaction. In (Ga,Mn)As the first two factors are tunable. On one hand, (a) may be

optimized by choosing appropriate doping concentrations: in general lower Mn density is beneficial (Fig. (5.8)), as it reduces the equilibrium anisotropy without significantly affecting the magnitude of ISGE. However, for very low Mn concentrations a metal-insulator transition is impending, which hampers ISGE. On the other hand, (b) may be modified via strain engineering: as shown in Fig. (5.8), the critical current is (roughly) inversely proportional to the strength of the uniaxial strain that breaks inversion symmetry. The inverse proportionality may be understood on the basis of Eq. (5.26) combined with the fact that the equilibrium anisotropy does not change to *first* order in ϵ_{ax} (because \mathbf{k} -linear terms vanish after summing over all momenta).

5.4 Summary and Conclusions

In this work we have presented a theory of the current-induced spin torques in uniform ferromagnets. The torques can be viewed as due to a difference between the magnetic anisotropy energy of a ferromagnet which carries no current and the magnetic anisotropy of a ferromagnet in the transport steady state, which give rise to a corresponding change in anisotropy effective magnetic fields. When the transport steady state is described using a relaxation time approximation, the current-induced contribution to the anisotropy field of a strongly metallic ferromagnet is given in energy units by

$$\delta\mathbf{H}_{\text{an}} = \frac{1}{S_0} \sum_{\mathbf{k},a} [\Delta_0(\mathbf{r})\mathbf{s}]_{a,a} \mathbf{v}_{a,a} \cdot \mathbf{E} \frac{\partial f_{\mathbf{k},a}}{\partial \epsilon_{\mathbf{k},a}} \tau_{\mathbf{k},a}. \quad (5.27)$$

where $[\Delta_0(\mathbf{r})\mathbf{s}]_{a,a}$ is the spin-density weighted average of the exchange splitting of a particular state. We refer to the existence of this current-induced anisotropy field as the ferromagnetic inverse spin-galvanic effect.

In bulk materials this current induced field is non-zero only in gyrotropic ferromagnets, *i.e.* only in ferromagnets that have broken inversion symmetry and are chiral. Although uniform ferromagnetism may appear to be incompatible with broken inversion symmetry because of the the Dzyaloshinskii-Moriya interaction, the equilibrium magnetic anisotropy is often strong enough (or at least can be engineered so that it is strong enough) to prevent the formation of spiral magnetic states.

As an illustration of our theory, we have estimated current induced torques in uniform (Ga,Mn)As, which is not gyrotropic when it has pseudocubic symmetry but becomes gyrotropic when strained. Since substrate-dependent strains are present in all (Ga,Mn)As thin films, the strength of the ferromagnetic ISGE is expected to be strongly sample-dependent. We have concluded that it should *a priori* be feasible to design (Ga,Mn)As samples in which it is possible to switch the magnetization purely by electrical means. For typical sample parameters the necessary switching currents are on the order of $10^6 - 10^7 \text{A/cm}^2$, but the value may be tuned by adjusting the doping concentration and the axial strain. At these critical currents the Joule heating is not negligible; however, it is possible that further studies exploring the entire parameter space of Mn concentration, hole density, and the axial strain will identify circumstances under which the critical currents are smaller.

Another possible avenue for further research consists of evaluating the anisotropy fields which can be generated by electrical currents in strain engineered samples of appropriate technologically useful ferromagnets. Since we are not aware of room-temperature transition metal ferromagnets that are gyrotropic,[122] we propose arranging a room-temperature, non-gyrotropic ferromagnet (e.g. permalloy) in contact with a non-magnetic, gyrotropic material (e.g. strained GaAs). In these artificial heterostructures room-temperature magnetism and gyrotropic symmetry would coexist by virtue of the proximity effect.

Finally, effects similar to those studied in this work would allow transport currents to change spiral states, and possibly to induce or remove them.

Chapter 6

Landau-Lifshitz-Slonczewski Equation Approach to Nonequilibrium Superconductivity

This chapter represents a study of nonequilibrium superconductivity from the viewpoint of nonequilibrium magnetism, and stands out from previous chapters in both form and content. For one thing, the present chapter contains a substantial amount of introductory material because nonequilibrium superconductivity may be unfamiliar to the readers of this thesis. Moreover, the new calculations and ideas developed in this chapter are unpublished and preliminary.

Sections I and II present a somewhat lengthy albeit inevitably cursory introduction to the conventional theory of nonequilibrium superconductivity. At first glance, these sections bear no relation to magnetism. Such perception is abolished in Section III, where we bridge nonequilibrium superconductivity and nonequilibrium magnetism by mediation of the Landau-Lifshitz-Slonczewski equation. The motivation for this connection lies on the particle-hole transformation, which portrays a superconductor as a pseudospin ferromagnet. Sections IV, V, VI and VII explore the analogies of magnetic relaxation and spin torques in superconductors, and culminate with some

potentially new predictions that might be experimentally testable. Section VIII hints at an unconventional magnetogalvanic effect in spiral ferromagnets, which is inspired by its counterpart in superconductors.

This chapter constitutes work in progress and barely scratches the surface of what might be a new subfield emerging at the interface of two venerable disciplines.

6.1 Basics of Nonequilibrium Superconductivity

A superconductor can be regarded as a coupled system of three components: a condensate, quasiparticles, and phonons.¹ The condensate of Cooper pairs, which is characterized by a complex order parameter, is responsible for the Meissner effect as well as superfluidity. Quasiparticles are excitations above the condensate that appear at nonzero temperatures. The states occupied by quasiparticles are described by a distribution function, which as we shall see below plays a central role in nonequilibrium superconductivity. Quasiparticles can exchange both charge and energy with the condensate and only energy with phonons.

Any external perturbation that couples to either component can lead to nonequilibrium superconducting states. Supercurrents and pair-tunneling couple to the condensate, quasiparticle currents and tunneling affect the quasiparticle distribution, electromagnetic fields couple to both electronic compo-

¹The contents of this section are largely based on the chapter by A.M. Kadin and A.M. Goldman in Ref. [11].

nents, the phonon injection and external heating enter the superconductor via the phonon system.

For a simple BCS superconductor in equilibrium, the condensate consists of an assembly of time-reversed pairs of electron states with an occupation probability for electron \mathbf{k} -states given by

$$v_{\mathbf{k}}^2 = \frac{1}{2} \left(1 - \frac{\xi_{\mathbf{k}}}{E_{\mathbf{k}}} \right), \quad (6.1)$$

where $\xi_{\mathbf{k}} = k^2/(2m) - \mu_s$ is the kinetic energy of the electrons measured with respect to the condensate chemical potential ² μ_s , $E_{\mathbf{k}} = \sqrt{\xi_{\mathbf{k}}^2 + \Delta^2}$ is the energy of the quasiparticle excitations and Δ is the mean-field order parameter. The latter obeys the BCS gap equation:

$$1 = g \sum_{\mathbf{k}} \frac{1 - 2f_0(E_{\mathbf{k}})}{2E_{\mathbf{k}}} \simeq gN(0) \int_{|\xi| \leq \omega_D} d\xi \frac{1 - 2f_0(\xi)}{2\sqrt{\xi^2 + \Delta^2}}, \quad (6.2)$$

where g is the electron-phonon coupling constant, f_0 is the Fermi distribution function, $N(0)$ is the single-spin density of states at the Fermi energy (in the normal state) and ω_D is the cut-off (Debye) energy that removes logarithmic divergences.

In presence of an external perturbation the quasiparticle population is

²In equilibrium, μ_s coincides with the Fermi energy, which we take as the zero of energy. Out of equilibrium this need no longer be the case.

driven out of equilibrium and the modified gap equation ³ reads

$$1 = g \sum_{\mathbf{k}} \frac{1 - 2f(E_{\mathbf{k}})}{2E_{\mathbf{k}}}, \quad (6.3)$$

where $f(E_{\mathbf{k}}) = f_0(E_{\mathbf{k}}) + \delta f_{\mathbf{k}}$ is the nonequilibrium quasiparticle distribution. Eq. (6.3) indicates how $\delta f_{\mathbf{k}}$ alters the superconducting order parameter. Strictly speaking the distribution $f(E_{\mathbf{k}})$ has as many degrees of freedom as there are quasiparticles. However, only a small number of simple modes appear to be relevant in practice. These are classified into a “longitudinal” or “energy” mode δf_L and a “transverse” or “charge” mode δf_T , so that

$$\delta f = \delta f_L + \delta f_T. \quad (6.4)$$

By definition $\delta f_L(\xi_{\mathbf{k}}) = \delta f_L(-\xi_{\mathbf{k}})$ and $\delta f_T(\xi_{\mathbf{k}}) = -\delta f_T(-\xi_{\mathbf{k}})$. Physically, the energy mode is equivalent to introducing an effective temperature in the Fermi distribution, which differs from the actual temperature of the system. On the other hand, the charge mode is equivalent to having a *net* charge for quasiparticles, commonly known as *quasiparticle charge imbalance*. ⁴ As it turns out, the quasiparticle charge imbalance is one of the central quantities in nonequilibrium superconductivity. It is defined as

$$Q^* = 2 \sum_{\mathbf{k}} q_{\mathbf{k}} f_{\mathbf{k}}, \quad (6.5)$$

³Besides quasiparticle occupation numbers, the coherence factors (quasiparticle eigenstates) too change in presence of a perturbation. However, it can be shown that for slowly varying perturbations the equation for the energy gap in the nonequilibrium state has the same form as in equilibrium: see *e.g.* the chapter by A.G. Aronov *et al.* in Ref. [11].

⁴See *e.g.* chapter 11 of Ref. [5].

where $q_{\mathbf{k}} = e\xi_{\mathbf{k}}/E_{\mathbf{k}}$ is the effective quasiparticle charge. Much like in a normal metal, quasiparticles are electron-like ($q_{\mathbf{k}} \simeq e$) well above the Fermi energy ($\xi_{\mathbf{k}} \gg 0$) and hole-like ($q_{\mathbf{k}} \simeq -e$) deep inside the Fermi sea ($\xi_{\mathbf{k}} \ll 0$). The peculiarity of the superconducting state becomes manifest in the close neighborhood of the Fermi energy ($|\xi_{\mathbf{k}}| \leq \Delta$), where quasiparticle states are neither filled nor empty and instead constitute a quantum mechanical superposition of electrons and holes with a non-integer charge given by $q_{\mathbf{k}}$.

In equilibrium $f(\xi_{\mathbf{k}}) = f(-\xi_{\mathbf{k}})$ and thus the electron-like and hole-like branches of the quasiparticle spectrum are equally populated, yielding $Q^* = 0$.

⁵ This need not be the case for a nonequilibrium state. In any event, the total electronic charge given by

$$Q_{\text{tot}} = 2e \sum_{\mathbf{k}} v_{\mathbf{k}}^2 |_{\mu_s=0} \quad (6.6)$$

remains approximately constant even out-of-equilibrium because charge neutrality holds over far shorter times and distances than those relevant to superconductivity. The excess charge of the quasiparticles must thus be compensated by a change δQ_{cond} in the charge of the condensate, ⁶ with the concurrent

⁵Throughout this chapter we use $\sum_{\mathbf{k}} \simeq N(0) \int_{-\infty}^{\infty} d\xi$, because states that are near the Fermi energy matter the most for both equilibrium and nonequilibrium superconductivity. Note that the particle and hole branches do not have a symmetric energy dispersion far away from the Fermi energy.

⁶The change in the quasiparticle charge is associated with the deviation from equilibrium of the quasiparticle occupation factors, whereas the change in the condensate charge is related to the modification of the coherence factors. See *e.g.* C.J. Pethick and H. Smith in Ref. [10].

change in its chemical potential away from $\mu_s = 0$. In sum,

$$\begin{aligned}
Q^* &= -\delta Q_{\text{cond}} \\
&= 2e \sum_{\mathbf{k}} (v_{\mathbf{k}}^2|_{\mu_s=0} - v_{\mathbf{k}}^2|_{\mu_s \neq 0}) \\
&\simeq 2N(0)e \int d\xi (v^2|_{\mu_s=0} - v^2|_{\mu_s \neq 0}) \\
&\simeq -2N(0)e\mu_s,
\end{aligned} \tag{6.7}$$

where in the last line we have performed an expansion to first order in μ_s . Hence the quasiparticle charge imbalance is proportional to the deviation of the condensate chemical potential from the Fermi energy. Identifying Eq. (6.7) with Eq. (6.5), it follows that

$$-\mu_s = \int_{-\infty}^{\infty} d\xi f(\xi) q(\xi) / e, \tag{6.8}$$

where

$$q(\xi) \equiv e \frac{\xi - \mu_s}{\sqrt{(\xi - \mu_s)^2 + \Delta^2}} \tag{6.9}$$

is the effective charge of the quasiparticles. Remarkably, there is a charge imbalance only when the quasiparticle distribution function has a component that is *odd* around the chemical potential of the condensate. That is why transverse modes lead to charge imbalance whereas longitudinal modes do not. ⁷ This imbalance in the populations of electron and hole branches has been measured ⁸ in normal-metal/insulator/superconductor junctions.

⁷The parity of the perturbation with respect to ξ will play a very important role in the following sections.

⁸See *e.g.* the chapter by J. Clarke in Ref. [10].

For latter reference, it is convenient to subdivide longitudinal and transverse perturbations based on their parity on momentum: ⁹

(i) *Even in $\xi_{\mathbf{k}}$ and odd in \mathbf{k} .*

This longitudinal mode induces an electric current, but not a quasiparticle charge imbalance. For example,

$$\delta f_{\mathbf{k}} = q_{\mathbf{k}} \mathbf{v}_{\mathbf{k}} \cdot \mathbf{E} \frac{\partial f_{\mathbf{k}}}{\partial E_{\mathbf{k}}} \tau_{\mathbf{k}} \quad (6.10)$$

gives rise to a dissipative current. \mathbf{E} is the applied electric field, $\mathbf{v}_{\mathbf{k}} = \partial E_{\mathbf{k}} / \partial \mathbf{k}$ is the quasiparticle group velocity, $\tau_{\mathbf{k}}$ is the elastic scattering lifetime and $q_{\mathbf{k}} = e \xi_{\mathbf{k}} / E_{\mathbf{k}}$ is the effective quasiparticle charge. Another important example of the same class is

$$\delta f_{\mathbf{k}} = \mathbf{v}_F \cdot \mathbf{Q} \frac{\partial f_{\mathbf{k}}}{\partial E_{\mathbf{k}}}, \quad (6.11)$$

which produces a dissipationless current. \mathbf{v}_F is the Fermi velocity and \mathbf{Q} is the superfluid momentum proportional to the applied current.

(ii) *Even in $\xi_{\mathbf{k}}$ and even in \mathbf{k} .*

This longitudinal mode generates neither a current nor a charge imbalance, but instead alters the superconducting gap. A representative example is the heating of quasiparticles by a microwave field or sound waves, which remarkably leads to an enhancement of the superconducting gap. These perturbations relax through inelastic scattering, *e.g.* via phonons.

(iii) *Odd in $\xi_{\mathbf{k}}$ and even in \mathbf{k} .*

⁹See the chapter by A.G. Aronov *et al.* in Ref. [11].

This kind of transverse perturbation creates a charge imbalance, which relaxes through scattering off phonons, magnetic impurities, or (in presence of supercurrents or anisotropy of the gap) non-magnetic impurities.

(iv) *Odd in $\xi_{\mathbf{k}}$ and odd in \mathbf{k} .*

This class of transverse perturbation gives rise to thermoelectric phenomena, which we will analyze in latter sections. A typical case involves

$$\delta f_{\mathbf{k}} = \mathbf{v}_{\mathbf{k}} \cdot \nabla T \frac{E_{\mathbf{k}}}{T} \frac{\partial f_{\mathbf{k}}}{\partial E_{\mathbf{k}}} \tau_{\mathbf{k}}, \quad (6.12)$$

where T is the temperature of the system.

6.2 Theories of Nonequilibrium Superconductivity

In this section we provide a bird's-eye view of the principal theoretical methods that have been developed for the study of nonequilibrium processes in superconductors. In the next section we will introduce a new technique that may complement the ones that are currently in use.

6.2.1 Time-Dependent Ginzburg-Landau Theory

Solving the BCS equations out of equilibrium is a complicated task even in the limit of slow time and space variations of the field and the order parameter. However, it is possible to write a relatively simple model equation in the vicinity of the transition temperature T_c , which reflects the qualitative aspects of the order parameter dynamics. This equation is the simplest generalization of the equilibrium Ginzburg-Landau equations as it assumes that for

small deviations from equilibrium the time derivative of the order parameter is proportional to the variational derivative of the free energy $\partial F/\partial\Delta^*$.¹⁰ The free energy of the superconductor within the Ginzburg-Landau formalism is given by

$$F = \int d\mathbf{r} \left[\alpha|\Delta|^2 + \frac{\beta}{2}|\Delta|^4 + \gamma|(-i\nabla - \frac{2e}{c}\mathbf{A})\Delta|^2 + \frac{(\nabla \times \mathbf{A})^2}{8\pi} \right], \quad (6.13)$$

which produces the well-known equilibrium Ginzburg-Landau equations via $\delta F/\delta\Delta = 0$ and $\delta F/\delta\mathbf{A} = -\mathbf{j}_s$, where \mathbf{j}_s is the supercurrent. The generalization of these equations to time-dependent situations is realized as

$$\begin{aligned} \frac{\delta F}{\delta\Delta} &= -\Gamma(\partial_t + 2ieV)\Delta \\ \frac{\delta F}{\delta\mathbf{A}} &= -(\mathbf{j} - \mathbf{j}_N) = -(\mathbf{j} - \sigma_N\mathbf{E}), \end{aligned} \quad (6.14)$$

where Γ is a positive constant and V is the electrostatic potential that ensures the gauge-invariance of the time-derivative. The second line of Eq. (6.14) follows from the assumption that the total current \mathbf{j} can be written as the sum of a supercurrent and a quasiparticle current \mathbf{j}_N , where the latter is determined by the normal-state conductivity σ_N .¹¹ Often the TDGL equations are augmented with Langevin forces that model the thermodynamic fluctuations of the order parameter.

Eqs. (6.14) can be derived microscopically;¹² it follows that they are valid only in the vicinity of T_c , close to equilibrium and in the gapless regime.

¹⁰This is a relaxation-time approximation.

¹¹This assumption is justifiable close to the critical temperature.

¹²For a careful treatment see *e.g.* Ref. [123].

6.2.2 Kinetic Equation Approach

At the same time in which the TDGL equations were being conceived, the resemblance between quasiparticles in superconductors and electrons in normal metals ignited the search for a transport equation that could be applied to superconductors. Such an equation was indeed constructed¹³ and turned out to be closely related to the classical Boltzmann equation for normal conductors:

$$\frac{\partial f_{\mathbf{k}}}{\partial t} + \mathbf{v}_{\mathbf{k}} \cdot \nabla f_{\mathbf{k}} + \mathbf{F} \cdot \frac{\partial f_{\mathbf{k}}}{\partial \mathbf{k}} = I[f_{\mathbf{k}}], \quad (6.15)$$

where $f_{\mathbf{k}}$ is the nonequilibrium quasiparticle distribution function, $\mathbf{F} = -\partial E_{\mathbf{k}}/\partial \mathbf{r} + \mathbf{v}_F \times \mathbf{B}$ is the force acting on the quasiparticles (\mathbf{B} is the magnetic field) and I is the collision integral.

Despite formal similarities between Eq. (6.15) and the ordinary Boltzmann equation, the kinetic equation for superconductors is more convoluted. For instance, superconductors have a condensate of Cooper pairs whose dynamics can alter the occupation number of the quasiparticle states. In turn, the normal excitation distribution may influence the energy gap, as evidenced by Eq. (6.3). Consequently, Eq. (6.15) and Eq. (6.3) must be solved self-consistently. Another essential difference between the kinetic equation for normal metals and superconductors is that quantum effects are much more pronounced in the latter because the coherence length $\zeta = v_F/\Delta$ of the superconducting wavefunction is typically two or three orders of magnitude larger

¹³For an extensive review see *e.g.* A.G. Aronov *et al.* in Ref. [11].

than the Fermi wavelength.

The assets of the kinetic equation approach are twofold. First, it is an intuitive method because its results may be interpreted in terms of the excitation distribution function, which is a quantity with clear physical meaning. Second, this method can handle low temperatures and large deviations from equilibrium. On the other hand, the main drawback of the kinetic equation approach is that it is applicable to superconductors that are nearly clean and homogeneous.

6.2.3 Keldysh Green's Function Method

The Boltzmann kinetic equation fails unless the mean free path and the range in which the order parameter changes exceed the coherence length. A more general quasiclassical equation can be derived, which is based on the smallness of the electron wavelength compared to all other characteristic lengths. This equation is a generalization of the static Eilenberger equations.

14

The fundamental quantities of this formalism are the retarded, ad-

¹⁴For a detailed exposition of the quasiclassical Green's function method see *e.g.* Ref. [124]. The present discussion is based on the chapter by A.I. Larkin and Y.N. Ovchinnikov in Ref. [11].

vanced and Keldysh Green's functions, which can be expressed as

$$G^R(1, 2) = \Theta(t_1 - t_2) [G^>(1, 2) - G^<(2, 1)] \quad (6.16)$$

$$G^A(1, 2) = -\Theta(t_2 - t_1) [G^>(1, 2) - G^<(2, 1)] \quad (6.17)$$

$$G^K(1, 2) = G^>(1, 2) + G^<(1, 2), \quad (6.18)$$

where

$$\begin{aligned} G^>(1, 2) &\equiv -i \begin{pmatrix} \langle \psi_\uparrow(1) \psi_\uparrow^\dagger(2) \rangle & \langle \psi_\uparrow(1) \psi_\downarrow(2) \rangle \\ -\langle \psi_\downarrow^\dagger(1) \psi_\uparrow^\dagger(2) \rangle & -\langle \psi_\downarrow^\dagger(1) \psi_\downarrow(2) \rangle \end{pmatrix} \\ G^<(1, 2) &\equiv i \begin{pmatrix} \langle \psi_\uparrow^\dagger(2) \psi_\uparrow(1) \rangle & \langle \psi_\downarrow(2) \psi_\uparrow(1) \rangle \\ -\langle \psi_\uparrow^\dagger(2) \psi_\downarrow^\dagger(1) \rangle & -\langle \psi_\downarrow(2) \psi_\downarrow^\dagger(1) \rangle \end{pmatrix}, \end{aligned} \quad (6.19)$$

Θ is the step function and $\langle \rangle$ denotes the expectation value taken on the nonequilibrium state. The matrices in Eq. (6.19) are written in the particle-hole basis, which is also known as the Nambu-Gorkov representation. Superconducting correlations, which mix particles and holes, appear in the off-diagonal matrix elements. This representation forms the backbone of the rest of the chapter.

As shown by Keldysh, the dynamical Green's functions can in principle be evaluated by solving the following Dyson's equation:

$$(\check{G}_0^{-1} - \check{\Sigma})\check{G} = \check{1}, \quad (6.20)$$

where

$$\check{G} = \begin{pmatrix} G^R & G^K \\ 0 & G^A \end{pmatrix} \quad (6.21)$$

is the Green's function matrix that completely describes the nonequilibrium state of the system and

$$\check{\Sigma} = \begin{pmatrix} \Sigma^R & \Sigma^K \\ 0 & \Sigma^A \end{pmatrix} \quad (6.22)$$

is the self-energy matrix that encodes the departures from the equilibrium Green's function G_0 .¹⁵ $\check{1}$ stands for the 4×4 identity matrix. In addition, the product in Eq. (6.20) means multiplication of matrices and convolution with respect to the coordinates and time.

Solving Eq. (6.20) is as arduous a task as solving the full BCS equations. Fortunately, it contains more information than is needed and can be replaced with a simpler equation by virtue of the quasiclassical approximation. In this approximation the rapid oscillations in relative spatial coordinates of the Green's functions are integrated out because they are physically irrelevant on the important lengthscales for superconductivity, *e.g.* the coherence length.¹⁶ Therefore one can integrate out the relative spatial coordinates in Eq. (6.20) and arrive at an alternative Dyson equation for the quasiclassical Green's function

$$\check{g}(\mathbf{p}, \mathbf{r}) \equiv \frac{i}{\pi} \int d\xi \check{G}(\mathbf{p}, \mathbf{r}). \quad (6.23)$$

All observables of interest such as the current density and the superconducting gap can then be expressed in terms of g^K . While the quasiclassical equation is

¹⁵Note incidentally that the self-energy $\check{\Sigma}$ is in general a function of \check{G} .

¹⁶This statement is valid provided that the superconducting coherence length is much larger than the Fermi wavelength. This requirement is easily satisfied in all low-temperature superconductors, wherein $\Delta/E_F \ll 1$.

more general than either the TDGL or kinetic equations, its solution is more complicated and less transparent.

6.3 LLS Equation Approach to Superconductivity

The TDGL, kinetic and quasiclassical equations have been in place for three decades. In this section we introduce a new point of view to describe nonequilibrium superconductivity. Our approach is motivated by the mathematical mapping between magnetism and superconductivity first discussed by Anderson,[125] and is based on a formalism put forward by Gorkov[126] and Nambu.[127] We apply these ideas to posit a Landau-Lifshitz-Slonczewski equation for the dynamics of the superconducting order parameter.¹⁷ At first glance, this equation is somewhat phenomenological and appears to offer a limited leverage because it ignores the oft-important amplitude fluctuations¹⁸ of the order parameter. Nevertheless, it inspires a number of potentially interesting analogies between the seemingly unrelated fields of nonequilibrium magnetism and nonequilibrium superconductivity, some of which we shall explore in the remaining sections of this chapter.

For pedagogical reasons, we begin by considering a ferromagnet whose equilibrium magnetization is pointing along \hat{x} . The LLS equations that de-

¹⁷For illuminating applications in other systems of see *e.g.* Ref. [128].

¹⁸Amplitude fluctuations are believed to be important even at low temperatures in superconductors with reduced dimensionality. For a recent review see Ref. [129].

scribe small departures from equilibrium can be written as

$$\begin{aligned}
\dot{\Omega}_x &\simeq 0 \simeq \nabla \Omega_x \\
\dot{\Omega}_y + \mathbf{v} \cdot \nabla \Omega_y &= \Omega_z H_x - H_z + \alpha_{z,z} \dot{\Omega}_z + \beta_{z,z} \mathbf{v} \cdot \nabla \Omega_z \\
\dot{\Omega}_z + \mathbf{v} \cdot \nabla \Omega_z &= H_y - \Omega_y H_x - \alpha_{y,y} \dot{\Omega}_y + \beta_{y,y} \mathbf{v} \cdot \nabla \Omega_y.
\end{aligned} \tag{6.24}$$

Unlike in previous chapters, in Eq. (6.59) we allow anisotropies in the damping coefficient by raising α and β to matrix status;¹⁹ the motivation behind this will become clear below.

As mentioned previously, α and β originate from microscopic processes that break spin conservation, such as spin-orbit interactions and magnetic impurities. Let us assume that the spin-orbit interaction is zero and that there are spin-dependent impurities with their spins aligned along \hat{z} . The misalignment between the impurity spins and the equilibrium magnetization may seem unphysical, but once again its relevance will become clear below. An important observation for this setup is that $\alpha_{y,y} = 0$ because

$$\left. \frac{d\Omega_z}{dt} \right|_{\text{imp}} \propto [\mathcal{H}_{\text{imp}}, S^z] \propto [S^z, S^z] = 0 \tag{6.25}$$

and hence impurities magnetized along \hat{z} cannot relax Ω_z . $\beta_{y,y} = 0$ is less obvious, because Eq. (6.25) does not apply for spatially varying magnetic textures. We shall argue below that $\beta_{y,y}$ is unimportant in cases of interest.

The foregoing, seemingly artificial example becomes viable in the context of superconductivity. In order to show this, we begin by introducing a

¹⁹ $\alpha_{z,y}$ and $\alpha_{y,z}$ can be absorbed in the gyromagnetic factor.

particle-hole transformation:[130]

$$\begin{aligned} c_{\mathbf{k},\uparrow} &\rightarrow \tilde{c}_{\mathbf{k},\uparrow} \\ c_{-\mathbf{k},\downarrow}^\dagger &\rightarrow \tilde{c}_{\mathbf{k},\downarrow}, \end{aligned} \quad (6.26)$$

where $c_{\mathbf{k},\sigma}$ ($\tilde{c}_{\mathbf{k},\sigma}$) is the operator that annihilates a “real” (“pseudo”) electron with momentum \mathbf{k} and spin σ . The particle-hole transformation is a canonical transformation because the pseudoelectrons obey fermionic anticommutation relations. Eq. (6.26) maps charge operators into pseudospin operators:

$$\begin{aligned} \tilde{S}_{\mathbf{k}}^z &\equiv \tilde{c}_{\mathbf{k},\uparrow}^\dagger \tilde{c}_{\mathbf{k},\uparrow} - \tilde{c}_{\mathbf{k},\downarrow}^\dagger \tilde{c}_{\mathbf{k},\downarrow} = c_{\mathbf{k},\uparrow}^\dagger c_{\mathbf{k},\uparrow} - c_{-\mathbf{k},\downarrow} c_{-\mathbf{k},\downarrow}^\dagger \\ \tilde{S}_{\mathbf{k}}^x &\equiv \tilde{c}_{\mathbf{k},\uparrow}^\dagger \tilde{c}_{\mathbf{k},\downarrow} + \tilde{c}_{\mathbf{k},\downarrow}^\dagger \tilde{c}_{\mathbf{k},\uparrow} = c_{\mathbf{k},\uparrow}^\dagger c_{-\mathbf{k},\downarrow}^\dagger + c_{-\mathbf{k},\downarrow} c_{\mathbf{k},\uparrow} \\ \tilde{S}_{\mathbf{k}}^y &\equiv -i(\tilde{c}_{\mathbf{k},\uparrow}^\dagger \tilde{c}_{\mathbf{k},\downarrow} - \tilde{c}_{\mathbf{k},\downarrow}^\dagger \tilde{c}_{\mathbf{k},\uparrow}) = -i(c_{\mathbf{k},\uparrow}^\dagger c_{-\mathbf{k},\downarrow}^\dagger - c_{-\mathbf{k},\downarrow} c_{\mathbf{k},\uparrow}). \end{aligned} \quad (6.27)$$

On one hand, $\tilde{S}_{\mathbf{k}}^z$ is closely related to the charge density operator: one can ascribe a pseudospin along $+\hat{z}$ ($-\hat{z}$) to electrons (holes). On the other hand, $\tilde{S}_{\mathbf{k}}^x$ and $\tilde{S}_{\mathbf{k}}^y$ capture pairing correlations, which mix electrons and holes.

In this language, the BCS Hamiltonian for a superconductor in equilibrium can be expressed as

$$\mathcal{H}_{\text{BCS}} = \sum_{\mathbf{k}} (\tilde{c}_{\mathbf{k},\uparrow}^\dagger, \tilde{c}_{\mathbf{k},\downarrow}^\dagger) \begin{pmatrix} \xi_{\mathbf{k}} & \Delta \\ \Delta^* & -\xi_{\mathbf{k}} \end{pmatrix} \begin{pmatrix} \tilde{c}_{\mathbf{k},\uparrow} \\ \tilde{c}_{\mathbf{k},\downarrow} \end{pmatrix}, \quad (6.28)$$

where we have thrown away an infinite term $\sum_{\mathbf{k}} \xi_{\mathbf{k}}$ that is physically inconsequential.[6] Eq. (6.28) resembles the Hamiltonian of a parabolic-band ferromagnet with an exchange field $\mathbf{\Delta} = (\text{Re}(\Delta), \text{Im}(\Delta), 0)$, except for the fact that the dispersion relation for the spin-down electrons is reversed. This difference results in a gapped, semiconductor-like quasiparticle dispersion ($E_{\mathbf{k}} =$

$\pm\sqrt{\xi_{\mathbf{k}}^2 + \Delta^2}$) with the chemical potential in the middle of the gap. At zero temperature the “valence band” is full ²⁰ whereas the “conduction band” is empty. The ground state of Eq. (6.28) may be written as an antisymmetrized product of spinors that diagonalize the BCS Hamiltonian at each \mathbf{k} :

$$|\Psi_{\text{BCS}}\rangle = \prod_{\mathbf{k}} \left(u_{\mathbf{k}} \tilde{c}_{\mathbf{k},\uparrow}^\dagger + v_{\mathbf{k}} \tilde{c}_{\mathbf{k},\downarrow}^\dagger \right) |0\rangle, \quad (6.29)$$

where $|0\rangle$ is the vacuum and

$$\begin{aligned} u_{\mathbf{k}} &= \cos \frac{\theta_{\mathbf{k}}}{2} \\ v_{\mathbf{k}} &= e^{i\phi} \sin \frac{\theta_{\mathbf{k}}}{2} \end{aligned} \quad (6.30)$$

are the well-known BCS coherence factors, with $\cos \theta_{\mathbf{k}} = \xi_{\mathbf{k}}/E_{\mathbf{k}}$ and $\tan \phi = \text{Im}(\Delta)/\text{Re}(\Delta)$. Eq. (6.29) represents a domain wall in momentum space, where the pseudospins deep inside (far above) the Fermi sea are pointing along $+\hat{z}$ ($-\hat{z}$). The wall is tilted by an angle ϕ with respect to the xz plane.

In order to further realize the magnetic representation of superconductivity is instructive to evaluate the net pseudospin magnetization

$$\tilde{\mathbf{s}} = \sum_{\mathbf{k},a} \tilde{\mathbf{S}}_{\mathbf{k},a} f_{\mathbf{k},a}, \quad (6.31)$$

where $\tilde{\mathbf{S}}_{\mathbf{k},a} = \langle \Psi_{\mathbf{k},a} | \tilde{\mathbf{S}} | \Psi_{\mathbf{k},a} \rangle$ is the matrix element for the pseudospin operator

²⁰Consequently the ground state energy of \mathcal{H}_{BCS} diverges. Of course, the actual ground state energy of the superconductor becomes finite once we reinstate the infinite term ignored in Eq. (6.28).

and

$$\begin{aligned}\Psi_{\mathbf{k},0} &= (u_{\mathbf{k}}, v_{\mathbf{k}}) \\ \Psi_{\mathbf{k},1} &= (v_{\mathbf{k}}^*, -u_{\mathbf{k}}^*)\end{aligned}\tag{6.32}$$

are the eigenspinors at momentum \mathbf{k} corresponding to the valence and conduction bands, respectively. It follows that

$$\begin{aligned}\tilde{s}^x &= \sum_{\mathbf{k}} u_{\mathbf{k}} v_{\mathbf{k}}^* (f_{\mathbf{k},0} - f_{\mathbf{k},1}) + \text{c.c.} \\ \tilde{s}^y &= -\sum_{\mathbf{k}} i u_{\mathbf{k}} v_{\mathbf{k}}^* (f_{\mathbf{k},0} - f_{\mathbf{k},1}) + \text{c.c.} \\ \tilde{s}^z &= \sum_{\mathbf{k}} (|u_{\mathbf{k}}|^2 - |v_{\mathbf{k}}|^2) (f_{\mathbf{k},0} - f_{\mathbf{k},1}),\end{aligned}\tag{6.33}$$

where $f_{\mathbf{k},0}$ and $f_{\mathbf{k},1}$ are the occupation numbers for the “valence band” and “conduction band”, respectively.

\tilde{s}^x and \tilde{s}^y diverge logarithmically for an unrestricted momentum sum. This pathology can be remedied by introducing a cut-off $|\xi_{\mathbf{k}}| \leq \omega_D$ in the momentum integral, a procedure that is customary in the BCS theory. In fact, it can be readily shown that the first two lines of Eq. (6.33) are simply the BCS gap equation for an order parameter given by

$$\Delta \equiv (\text{Re}(\Delta), \text{Im}(\Delta)) = |\Delta|(\cos \phi, \sin \phi) = (g\tilde{s}^x, g\tilde{s}^y).\tag{6.34}$$

Eq. (6.34) can be verified by plugging the expressions for the coherence factors in Eq. (6.33), invoking particle-hole symmetry ($f_{\mathbf{k},0} = 1 - f_{\mathbf{k},1} \equiv 1 - f_{\mathbf{k}}$) and comparing the outcome with Eq. (6.2). Moreover, for a homogeneous

superconductor ϕ may be removed by a gauge transformation, which renders $\tilde{s}^y = 0$ in equilibrium.

The z -component of the pseudospin magnetization is related to the net charge density. From the third line of Eq. (6.33), we find that it too diverges in equilibrium. This is simply an artifice of the particle-hole transformation, which can be handled in two ways. One way is to restrict the momentum sum via $|\xi_{\mathbf{k}}| \leq \omega_D$; then $\tilde{s}^z = 0$ in equilibrium because $f_{\mathbf{k}}$ is even in $\xi_{\mathbf{k}}$ and $q_{\mathbf{k}} = e(|u_{\mathbf{k}}|^2 - |v_{\mathbf{k}}|^2)$ is odd in $\xi_{\mathbf{k}}$ (in other words in equilibrium there is no excess of electron-like or hole-like quasiparticles). Another way is to *define* the infinite \tilde{s}^z as zero; at any rate in equilibrium the electronic charge must be completely compensated by the ionic background at every point in time and space. For the sake of pedagogy we write down the expression for charge fluctuations, which is free of spurious divergences:

$$\begin{aligned}\delta\tilde{s}^z &= \sum_{\mathbf{k}} \delta q_{\mathbf{k}}(1 - 2f_{\mathbf{k}}) - 2 \sum_{\mathbf{k}} q_{\mathbf{k}} \delta f_{\mathbf{k}} \\ &\equiv \chi_{z,z} \mu_s,\end{aligned}\tag{6.35}$$

where μ_s is the condensate chemical potential (recall that $\mu_s \equiv 0$ in equilibrium) and

$$\begin{aligned}\chi_{z,z} &= -2 \sum_{\mathbf{k}} \frac{\partial(v_{\mathbf{k}}^2)}{\partial\mu_s}(1 - 2f_{\mathbf{k}}) - 2 \sum_{\mathbf{k}} q_{\mathbf{k}} \frac{\partial E_{\mathbf{k}}}{\partial\mu_s} \frac{\partial f_{\mathbf{k}}}{\partial E_{\mathbf{k}}} \\ &= -2 \sum_{\mathbf{k}} \frac{\Delta^2}{2E_{\mathbf{k}}^3}(1 - 2f_{\mathbf{k}}) + 2 \sum_{\mathbf{k}} q_{\mathbf{k}}^2 \frac{\partial f_{\mathbf{k}}}{\partial E_{\mathbf{k}}}.\end{aligned}\tag{6.36}$$

In the second line of Eq. (6.36) we have assumed that the amplitude of the superconducting gap remains immutable. $\chi_{z,z}$ characterizes the charge density

induced by a change in the chemical potential of the condensate and it agrees with the expression of Pethick and Smith in Ref. [10]. The first term in the expression for $\chi_{z,z}$ captures the changes in the coherence factors ²¹ and is sometimes referred to as the superfluid charge: indeed it vanishes at and above the critical temperature. The second term captures the changes in the occupation numbers ²² and is often called the quasiparticle charge: indeed it vanishes at zero temperature. If the external perturbation is static and uniform it follows that $\chi_{z,z} = -2N(0)$. ²³

The preceding discussion and digressions were designed to establish that a homogeneous superconductor in equilibrium is equivalent to a pseudospin ferromagnet magnetized along \hat{x} . Because of this equivalence, it is natural to propose a LLS equation for the low energy and long wavelength dynamics of the superconducting order parameter. We shall substantiate this guess by making contact with conventional microscopic theories of superconductivity.[133] The starting point of these theories is the partition function

$$Z = \text{Tr}e^{-\mathcal{H}/T}, \quad (6.37)$$

²¹As such it arises entirely from interband transitions (recall chapter 5).

²²Hence it originates from intraband transitions.

²³There is a subtlety here. If the external perturbation has a frequency ω and wavevector \mathbf{q} such that $\omega > qv_F$ it follows that the intraband contribution to $\chi_{z,z}$ (the “quasiparticle charge”) goes like $q^2v_F^2/\omega^2$ (see *e.g.* Ref.[131]), thus *vanishing* at $q = 0$. This observation is important for the study of collective modes in superconductors.[132]

where T is the temperature and

$$\begin{aligned} \mathcal{H} &= \int d\mathbf{r} \psi_\sigma^\dagger(\mathbf{r}) \left(-\frac{1}{2m} \nabla^2 - \mu \right) \psi_\sigma(\mathbf{r}) - g \int d\mathbf{r} \psi_\uparrow^\dagger(\mathbf{r}) \psi_\downarrow^\dagger(\mathbf{r}) \psi_\downarrow(\mathbf{r}) \psi_\uparrow(\mathbf{r}) \\ &+ \frac{1}{2} \int d\mathbf{r} d\mathbf{r}' \psi_\sigma^\dagger(\mathbf{r}) \psi_{\sigma'}^\dagger(\mathbf{r}') \frac{e^2}{|\mathbf{r} - \mathbf{r}'|} \psi_{\sigma'}(\mathbf{r}') \psi_\sigma(\mathbf{r}) \end{aligned} \quad (6.38)$$

is the full Hamiltonian for the interacting electrons.²⁴ Within the path integral formalism,[134] the quartic terms in Eq. (6.38) can be decoupled via two separate Hubbard-Stratonovich transformations. These transformations are accompanied by two auxiliary fields that may be identified with the complex pairing potential $\Delta = |\Delta|e^{i\phi}$ and the charge density n . In absence of equilibrium supercurrents, amplitude fluctuations decouple from charge and phase fluctuations.[132] In line with the LLS precepts we neglect amplitude fluctuations ($\delta|\Delta| = 0$) and adopt a Gaussian theory for phase and charge fluctuations around $\phi = 0$ and $n = 0$. Then, Eq. (6.37) may be expressed as

$$Z \simeq \int \mathcal{D}\phi \mathcal{D}n e^{-S_{\text{eff}}}, \quad (6.39)$$

where \mathcal{D} is the measure of the path integral and

$$S_{\text{eff}}[\phi, n] = \frac{i}{2} \int d\mathbf{r} d\tau (n \partial_\tau \phi - \phi \partial_\tau n) - \int d\mathbf{r} E[\phi, n] \quad (6.40)$$

is the low energy effective action in imaginary time τ . The first term in the effective action is the Berry phase, which indicates that the phase of the order parameter and the charge density are canonically conjugate variables.²⁵ The

²⁴The electron-electron interaction has been divided into an attractive and a repulsive channel. This is widespread practice, though it may raise concerns of overcounting.

²⁵Often the Berry phase is written as $S_B = i \int d\mathbf{r} d\tau n \partial_\tau \phi$. In Eq. (6.40) we have used $n \partial_\tau \phi = \frac{1}{2} (n \partial_\tau \phi - \phi \partial_\tau n + \partial_\tau (n\phi))$ and have taken advantage of the fact that n and ϕ are periodic in the imaginary time.

second term in the effective action describes the energy cost associated with phase and charge fluctuations. If as explained above we identify $\phi \rightarrow \tilde{s}^y$ and $n \rightarrow \tilde{s}^z$, the Berry phase may be rewritten as ²⁶

$$\begin{aligned} S_B &= \frac{i}{2} \int d\mathbf{r} d\tau (\tilde{s}^z \partial_\tau \tilde{s}^y - \tilde{s}^y \partial_\tau \tilde{s}^z) \\ &= \frac{i}{2} \hat{x} \cdot \left(\frac{\partial \tilde{\mathbf{s}}}{\partial \tau} \times \tilde{\mathbf{s}} \right). \end{aligned} \quad (6.41)$$

The first line of Eq. (6.41) is a reflection of the familiar spin commutation relations. The second line too has a well-known geometrical interpretation:[130, 133] it denotes the area spanned by a pseudospin coherent state in the unit sphere. The semiclassical equations of motion for the coupled charge and phase fluctuations can be extracted from the saddle point solution of the effective action; a little algebra then results in the Landau-Lifshitz equation for a pseudospin ferromagnet with an equilibrium orientation along \hat{x} :

$$\frac{\partial \hat{\Omega}}{\partial t} = \hat{x} \times \frac{\partial E}{\partial \hat{\Omega}}, \quad (6.42)$$

where $\hat{\Omega}$ denotes the direction of the pseudospin. The derivation of Eq. (6.42) offers a partial microscopic justification for the LLS approach to superconductivity. We stress that the LLS equation requires $\delta \tilde{s}^z, \delta \tilde{s}^y \ll \tilde{s}^x$, *i.e.* $\Omega_z \ll 1$ and $\Omega_y \ll 1$. ²⁷ Furthermore, by neglecting amplitude fluctuations of the

²⁶Note that \tilde{s}^z here is equivalent to $\delta \tilde{s}^z$ in Eq. (6.35). We can use both notations interchangeably because $\tilde{s}^z = 0$ in equilibrium. The same applies for \tilde{s}^y and $\delta \tilde{s}^y$.

²⁷We have chosen the equilibrium state to be uniform. We could have also started from a spiral (current carrying) superconducting state, for which the LLS equation would have to be slightly generalized.

order parameter the LLS equation becomes oblivious of thermal and quantum phase slips.²⁸

We now proceed with an evaluation of the effective magnetic field $\partial E/\partial\hat{\Omega}$. As pointed out in chapter 5, this effective field includes the anisotropy field. The energy functional for transverse pseudospin fluctuations is given by

$$E[\Omega_y, \Omega_z] = \int d\mathbf{r} \left[\frac{1}{2}K(\Omega^z)^2 + \frac{1}{2}\rho|\nabla\Omega^y|^2 - \hat{\Omega} \cdot \mathbf{V}^{\text{ext}} \right] \quad (6.43)$$

and bears a clear physical interpretation. The first term describes the energy cost of creating a net charge density.²⁹ The parameter K is directly related to the density-density response function ($K \propto \langle \tilde{s}^z \tilde{s}^z \rangle = \chi_{z,z}$), and plays the role of an easy-plane anisotropy constant in the pseudospin language. The second term in Eq. (6.43) captures the rigidity of the superconducting phase, or equivalently the kinetic energy cost of supercurrents. $\rho \propto \langle \tilde{s}^y \tilde{s}^y \rangle$ is proportional to the superfluid density. Note that for an isolated and uniform superconductor there is no anisotropy associated with the xy component of the order parameter because the global phase of the Cooper pair wave function is arbitrary and can always be gauged away. The third term captures the coupling of an external field \mathbf{V}^{ext} to the pseudospin operators. For an isolated superconductor there is no external (classical) perturbation that can couple directly to the order parameter, which means that $V_x^{\text{ext}} = V_y^{\text{ext}} = 0$ in practice.³⁰ From Eq.

²⁸Phase slips are fluctuation phenomena wherein the superconducting gap vanishes at a given region in time and space. Phase slips give rise to resistive effects in superconductors. See *e.g.* Refs. [129] and [135].

²⁹Owing to the spatial non-locality of the Coulomb interaction, one should in principle consider gradient terms in Ω_z . However, we will ignore these for the moment.

³⁰However, it is feasible to have $V_{x,y}^{\text{ext}} \neq 0$ by bringing *another superconductor* nearby.

(6.43) we reach

$$\begin{aligned} H_y &= -\frac{1}{2}\rho\nabla^2\Omega_y - V_y^{\text{ext}} \\ H_z &= K\Omega_z - V_z^{\text{ext}}. \end{aligned} \quad (6.44)$$

We now have all the necessary pieces to write a LLS equation for the superconducting order parameter in the Nambu-Gorkov representation; it reads

$$\begin{aligned} \Omega_x &\simeq \text{const} \\ \dot{\Omega}_y + \mathbf{v} \cdot \nabla\Omega_y &= -K\Omega_z + V_z^{\text{ext}} + \alpha_{z,z}\dot{\Omega}_z + \beta_{z,z}\mathbf{v} \cdot \nabla\Omega_z \\ \dot{\Omega}_z + \mathbf{v} \cdot \nabla\Omega_z &= -\frac{1}{2}\rho\nabla^2\Omega_y. \end{aligned} \quad (6.45)$$

Eq. (6.45) is one of the most salient results of this chapter. In its derivation we have allowed for charged but non-magnetic impurities, which implies $\alpha_{y,y} = 0$ because in the Nambu-Gorkov representation the potential due to those impurities couples to the z -pseudospin. We have also neglected $\beta_{y,y}$ because unlike $\beta_{z,z}$ it contains no intraband contributions,³¹ which are dominant in the cases of interest. We postpone the microscopic theory of the pseudospin magnetization damping to a subsequent section.

Though the form of Eq. (6.45) may be familiar for researchers working on spintronics, it requires renewed physical interpretation in the context of superconductivity. First, recall that Ω_z is a density fluctuation, Ω_y is the phase of the order parameter and $\rho\nabla\Omega_y$ describes the dissipationless flow of

³¹Recall Eq. (4.30) and use $\langle a, \mathbf{k} | \tilde{S}^y | a, \mathbf{k} \rangle = 0 \neq \langle a, \mathbf{k} | \tilde{S}^z | a, \mathbf{k} \rangle$.

Cooper pairs. If we take $\alpha_{z,z} = \beta_{z,z} = v = 0$, the second line of Eq. (6.45) states that the rate of change in the superconducting angle is governed by the applied electrostatic potential V_z^{ext} as well as by the chemical potential of the condensate $K\Omega_z$.³² This is nothing but the Josephson relation generalized[124] to account for quasiparticle charge imbalance.³³ Nonzero values of v , α or β point at new kinds of departures from the Josephson relation. In particular, the β term in the second line of Eq. (6.45) implies that in steady steady the electric field inside a superconductor is not simply proportional to the gradient of the superfluid chemical potential. On the other hand, the third line of Eq. (6.45) may be interpreted as a continuity equation for charge. It is for $\mathbf{v} = 0$ only that this equation agrees with the orthodox microscopic theory,[132] notwithstanding the lack of a relaxation term.³⁴

In view of the aforementioned peculiarities, it is interesting to search for new predictions of the LLS equations that may be experimentally testable in nonequilibrium superconductors. This search is the subject of the upcoming sections.

³²According to Eq. (6.35) the induced charge density is directly related to the change in the chemical potential of the condensate. In fact, $K\Omega_z$ corresponds to μ_s .

³³In our theory Ω_z stands for the total charge density rather than the quasiparticle charge density, with which it agrees near the transition temperature only.

³⁴In conventional theories, inelastic scattering (phonons) can relax the quasiparticle charge imbalance in homogeneous superconductors with an isotropic gap (see *e.g.* Ref. [5]). Yet our Ω_z stands for fluctuations in the *total* charge density.

6.4 Adiabatic Pseudospin Transfer Torques

Adiabatic spin transfer torques have important physical implications in conducting ferromagnets. In this section we discuss their counterparts in superconductors. Pseudospin transfer torques are characterized by a pseudospin velocity \mathbf{v} . The microscopic theory of \mathbf{v} consists on evaluating the transverse pseudospin response function under a perturbation that drives the quasiparticle population away from equilibrium. Adapting the formalism outlined in chapter 4, we write

$$\mathbf{v} \cdot \mathbf{q} = \frac{\Delta^2}{\tilde{s}} \sum_{\mathbf{k}, a, b} \frac{f_{\mathbf{k}, a} - f_{\mathbf{k}+\mathbf{q}, b}}{E_{\mathbf{k}+\mathbf{q}, b} - E_{\mathbf{k}, a}} \text{Im} \left[\langle a, \mathbf{k} | \tilde{S}^y | b, \mathbf{k} + \mathbf{q} \rangle \langle b, \mathbf{k} + \mathbf{q} | \tilde{S}^z | a, \mathbf{k} \rangle \right], \quad (6.46)$$

where $f_{\mathbf{k}} = f_0 + \delta f_{\mathbf{k}}$ denotes the nonequilibrium occupation number³⁵ of the quasiparticles and \mathbf{q} is the wavevector of the pseudospin magnons. Eq. (6.46) may be manipulated as

$$\begin{aligned} \mathbf{v} \cdot \mathbf{q} &= \frac{\Delta^2}{\tilde{s}} \sum_{\mathbf{k}, a, b} f_{\mathbf{k}, a} \left\{ \frac{\text{Im} \left[\langle a, \mathbf{k} | \tilde{S}^y | b, \mathbf{k} + \mathbf{q} \rangle \langle b, \mathbf{k} + \mathbf{q} | \tilde{S}^z | a, \mathbf{k} \rangle \right]}{E_{\mathbf{k}+\mathbf{q}, b} - E_{\mathbf{k}, a}} - (\mathbf{q} \rightarrow -\mathbf{q}) \right\} \\ &\simeq -\frac{1}{2\tilde{s}} \sum_{\mathbf{k}, a \neq b} f_{\mathbf{k}, a} \mathbf{v}_{\mathbf{k}, b} \cdot \mathbf{q} \text{Im} \left[\langle a, \mathbf{k} | \tilde{S}^y | b, \mathbf{k} \rangle \langle b, \mathbf{k} | \tilde{S}^z | a, \mathbf{k} \rangle \right]. \end{aligned} \quad (6.47)$$

In the second line of Eq. (6.47) we have assumed that $\langle a, \mathbf{k} | \tilde{S}^i | b, \mathbf{k} + \mathbf{q} \rangle \simeq \langle a, \mathbf{k} | \tilde{S}^i | b, \mathbf{k} \rangle$, which has lead us to ignore the contribution from intraband transitions³⁶ (because $\langle a, \mathbf{k} | \tilde{S}^y | a, \mathbf{k} \rangle = 0$). In addition, we have substituted

³⁵As in chapter 4, we incorporate the external perturbation simply by shifting the occupation numbers of the BCS quasiparticles. We neglect the changes in the coherence factors because they are presumably small in systems with long mean free paths.

³⁶In general the intraband contributions to v need not be negligible: our approximation sacrifices quantitative accuracy for analytical simplicity.

$E_{\mathbf{k},1} - E_{\mathbf{k},0} \simeq 2\Delta$ because the most important contributions stem from near the Fermi energy. Using $\text{Im}[\langle 0, \mathbf{k} | \tilde{S}^y | 1, \mathbf{k} \rangle \langle 1, \mathbf{k} | \tilde{S}^z | 0, \mathbf{k} \rangle] = \sin \theta_{\mathbf{k}}$, we arrive at

$$\begin{aligned} \mathbf{v} \cdot \mathbf{q} &\simeq -\frac{\Delta}{2\tilde{s}} \sum_{\mathbf{k}} \left(\frac{\delta f_{\mathbf{k},0} \mathbf{v}_{\mathbf{k},1} \cdot \mathbf{q}}{E_{\mathbf{k},1}} + \frac{\delta f_{\mathbf{k},1} \mathbf{v}_{\mathbf{k},0} \cdot \mathbf{q}}{E_{\mathbf{k},0}} \right) \\ &= -\frac{\Delta}{2\tilde{s}} \sum_{\mathbf{k}} \frac{\mathbf{v}_{\mathbf{k}} \cdot \mathbf{q}}{E_{\mathbf{k}}} (\delta f_{\mathbf{k},0} + \delta f_{\mathbf{k},1}). \end{aligned} \quad (6.48)$$

In the first line of Eq. (6.48) we have taken advantage of the fact that \mathbf{v} vanishes in equilibrium. In the second line of Eq. (6.48) we have used $E_{\mathbf{k},1} = \sqrt{\xi_{\mathbf{k}}^2 + \Delta^2} = -E_{\mathbf{k},0} \equiv E_{\mathbf{k}}$ and $\mathbf{v}_{\mathbf{k},1} = -\mathbf{v}_{\mathbf{k},0} \equiv \mathbf{v}_{\mathbf{k}} = \partial E_{\mathbf{k}} / \partial \mathbf{k}$. A crucial observation is that since $\mathbf{v}_{\mathbf{k}}$ is odd in $\xi_{\mathbf{k}}$ and $E_{\mathbf{k}}$ is even, only transverse perturbations (with $\delta f_{\mathbf{k},a}(\xi_{\mathbf{k}}) = -\delta f_{\mathbf{k},a}(-\xi_{\mathbf{k}})$) are able produce a pseudospin transfer torque.³⁷ In particular, this indicates that neither a uniform electric field nor a supercurrent can exert a pseudospin transfer torque.

In contrast, a uniform temperature gradient concerns

$$\delta f_{\mathbf{k},0} = \delta f_{\mathbf{k},1} = \mathbf{v}_{\mathbf{k}} \cdot \nabla T \frac{E_{\mathbf{k}}}{T} \frac{\partial f_{\mathbf{k}}}{\partial E_{\mathbf{k}}} \tau_{\mathbf{k}}, \quad (6.49)$$

which is *odd* in $\xi_{\mathbf{k}}$ and thus leads to a nonzero pseudospin velocity:³⁸

$$\mathbf{v} \propto \frac{\nabla T}{T} g v_F^2 N(0) \tau \int_{-\infty}^{+\infty} d\xi \left(\frac{\xi}{E} \right)^2 \frac{\partial f}{\partial E}, \quad (6.50)$$

where $g = \Delta / \tilde{s}$ and we have omitted a factor of order one that arises from the angular integration. Due to the spatial isotropy of the BCS Hamiltonian, the

³⁷We have verified that this “symmetry argument” holds true even for intraband transitions as well as for interband transitions involving the derivatives of the eigenspinors with respect to momentum.

³⁸In contrast, both electric and thermal currents can induce spin transfer torques in ordinary ferromagnets.

pseudospin velocity is parallel to the temperature gradient. The presence of the coupling constant g proves that pseudospin torques disappear in normal metals. Besides, the value of the integral in Eq. (6.50) is such that the pseudospin transfer torque drops exponentially as the temperature goes to zero. Likewise, short mean free paths deplete \mathbf{v} .

We now comment on the physical significance of the thermally induced torque. Let us first focus on the steady state of the LLS equations, where

$$\mathbf{v} \cdot \nabla \Omega_z = -\frac{1}{2} \rho \nabla^2 \Omega_y. \quad (6.51)$$

Eq. (6.51) indicates that in absence of temperature gradients the supercurrent will be uniform in space. Moreover, it describes the conversion between supercurrents and some kind of thermal quasiparticle currents. Admittedly, Eq. (6.45) does not capture the conversion between supercurrents and quasiparticle charge currents that takes place *e.g.* near superconductor-normal metal interfaces. This apparent limitation of our theory may be overcome by adding[136] a non-Gilbert type of damping term ($\propto \partial_x^2 \Omega_z$) to the equation of motion for Ω_z .

Second, we look for a steady state solution with uniform supercurrent ($\nabla^2 \Omega_y = 0$) and $V_z^{\text{ext}} = 0$:

$$\Omega_z = -\frac{1}{K} \mathbf{v} \cdot \nabla \Omega_y, \quad (6.52)$$

which means that in a current-carrying superconductor ($\nabla \Omega_y = \text{const} \neq 0$) a temperature gradient will induce a uniform charge density. This effect is

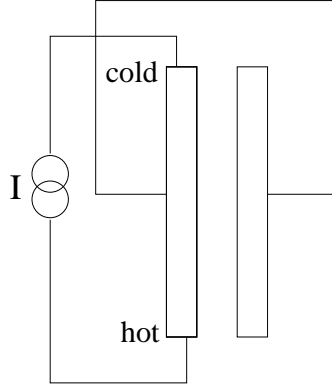


Figure 6.1: Two superconducting wires are separated by a thin insulating layer. One of the wires is placed under a uniform temperature gradient. According to Eq. (6.53), biasing this wire with a current I is akin to applying an electrochemical potential difference between the two wires, which will spearhead *ac* Josephson currents between them.

reminiscent to the one discovered by Pethick and Smith.³⁹

Third, let us seek solutions of the LLS equations in which the charge fluctuations vanish everywhere in the superconductor ($\Omega_z = 0$ for $\forall \mathbf{x}, t$). This enforces $\nabla^2 \Omega_y = 0$ and

$$\dot{\Omega}_y = -\mathbf{v} \cdot \nabla \Omega_y, \quad (6.53)$$

which suggests that in presence of a temperature gradient the superconducting phase changes in time (at the same rate in every point). This precession is of course inconsequential in isolated superconductors, but could have experimental repercussions in Josephson junction[137] type geometries. For definiteness, consider the setup displayed in Fig. (6.1). Two superconducting wires are

³⁹See *e.g.* chapter 15 in Ref. [10].

placed in close proximity and separated by an insulating layer, with one of the wires having a uniform temperature *gradient*. In steady state, the superconducting phases of the two wires are locked to each other and consequently no current flows *between* the wires.⁴⁰ If a current bias is applied to the wire with the thermal gradient, the global superconducting phase of that wire will begin to precess and an *ac* Josephson effect will ensue between the two superconductors. The frequency of the Josephson oscillations should be proportional to the product of the current bias and the temperature gradient. To the best of our knowledge this effect has not been experimentally measured.⁴¹

Finally, pseudospin torques can modify the dispersion of collective modes in superconductors; we defer this discussion until Sec. VII.

6.5 Pseudospin Relaxation in Superconductors

Attempts to determine the relaxation rate of the order parameter in nonequilibrium superconductors date back to the first days of the time-dependent Ginzburg-Landau theory.[139] Several subsequent studies[140, 141] have fo-

⁴⁰There could be a time-independent supercurrent in the wire with temperature gradient, which would cancel out the normal thermoelectric current. This phenomenon is known as the fountain effect.[138] However, the electrochemical potential difference between the two superconductors would still be zero.

⁴¹A potential challenge for the observation of this effect is that the superconductor with the temperature gradient could develop a charge imbalance quantified by Eq. (6.52), thereby reaching a steady state ($\dot{\Omega}_y = 0$) without an interwire *ac* Josephson effect. Amusingly, one might extend this concern to the traditional *ac* Josephson effect with a voltage difference across the junction: should an appropriate charge imbalance develop on each superconductor, a steady state would be achieved where the phase difference would be static even in presence of an external voltage bias.

cused on the particle-hole (Landau) damping and have emphasized the fact that Landau terms are singular at the origin of the energy-momentum space.⁴² The origin of such singularities appears to reside on the neglect of impurities, which renders infinitely long-lived BCS quasiparticles. Nevertheless, disorder should be expected to play a crucial role in the order parameter relaxation of a superconductor, much like it does in ordinary ferromagnets. In this section we transfer our theory of the Gilbert damping from magnetism to superconductivity.⁴³

In chapters 2-4 we learned that in conducting ferromagnets nonequilibrium magnons decay into particle-hole excitations at the Fermi energy. Since pseudospin ferromagnets have no states available at the Fermi energy, the Gilbert damping of pseudospin waves fades away at zero temperature.⁴⁴ Another consequence of the energy gap is that the analytical structure of the disorder self energy is more complicated in superconductors than in ordinary ferromagnets (Fig. (6.2b)).

With these caveats in mind, we evaluate the transverse pseudospin

⁴²They are proportional to ω/q , where (ω, \mathbf{q}) denotes the frequency and wavevector of the external perturbation. For an evaluation of Landau damping in normal metals see *e.g.* Ref. [131].

⁴³We limit ourselves to temperatures well below the transition temperature. Consequently our results may not be immediately comparable to recent work (see Ref.[142] and references therein) on dissipation near superconductor-insulator or superconductor-normal metal quantum critical points.

⁴⁴From a band structure point of view, pseudospin ferromagnets are more akin to *insulating* ferromagnets. In insulating ferromagnets the particle-hole channel is often superseded by other relaxation mechanisms such as two-magnon scattering (see *e.g.* Ref. [103]). It is not unlikely that the latter be dominant in pseudospin ferromagnets at low temperatures.

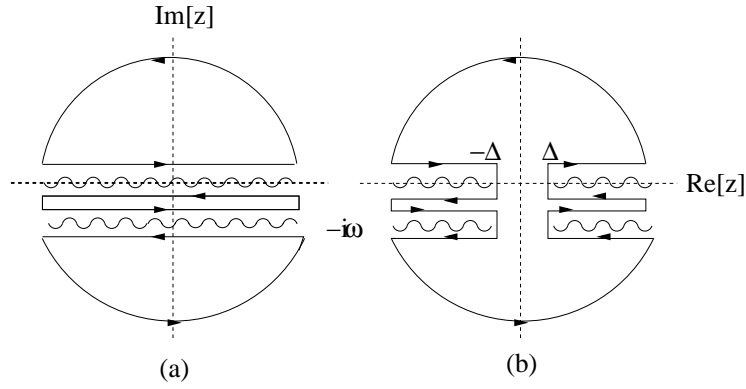


Figure 6.2: Integration contours in the complex plane for the Matsubara summations required by the microscopic evaluation of transverse spin response functions. In normal metals (a), the disorder self energy is given by $i/(2\tau)\text{Im}[z]$, where z stand for the complex frequency. This leads to a branch cut for $\text{Im}[z] = 0$ (there is an additional cut at $\text{Im}[z] = -i\omega$ where ω is the frequency of the external perturbation). In a superconductor (b), the disorder self energy has an additional factor of $1/\sqrt{z^2 - \Delta^2}$, which alters the structure of the branches.

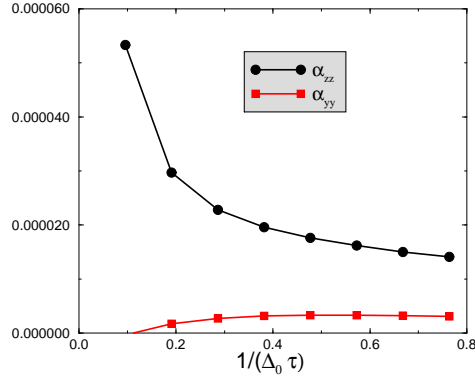


Figure 6.3: Gilbert damping for a pseudospin ferromagnet as a function of the non-magnetic impurity scattering rate. We take a temperature that is a third of the superconducting gap, and for simplicity we consider a one-dimensional superconductor. For $\alpha_{z,z}$, we find breathing-Fermi-surface type behavior with the damping decreasing monotonically as disorder becomes more pronounced. While we expect $\alpha_{y,y} = 0$ on physical grounds, our numerical results show that $\alpha_{y,y}$ has a residual nonzero value that originates from interband transitions (it is easy to see that intraband contributions vanish); these residual terms remain even when we include impurity vertex corrections. We thus associate the numerical value of $\alpha_{y,y}$ with the uncertainty/error of our calculation.

response function following the process outlined in chapter 3. We arrive at

$$\alpha_{z,z} = \frac{\Delta^2}{2\pi\tilde{s}} \text{Re}(P^{A,R} - P^{R,R}), \quad (6.54)$$

where

$$P^{A(R),R} = \int_{|\epsilon|>\Delta} d\epsilon \frac{\partial f}{\partial \epsilon} \sum_{a,b} \int_{\mathbf{k}} \Lambda_{a,b}^{A(R),R}(\mathbf{k}, \epsilon) G_b^R(\mathbf{k}, \epsilon) \tilde{S}_{b,a}^z(\mathbf{k}) G_a^{A(R)}(\mathbf{k}, \epsilon). \quad (6.55)$$

In Eq. (6.55) we have defined $\Lambda = \tilde{S}^z +$ impurity vertex corrections, and the retarded (advanced) Green's functions for the BCS quasiparticles are

$$G_a^{R(A)}(\mathbf{k}, \epsilon) = \frac{1}{\epsilon - E_{\mathbf{k},a} + (-)\Sigma_{\text{imp},a}}, \quad (6.56)$$

where

$$\Sigma_{\text{imp},a} = \frac{i}{2\tau_{\mathbf{k},a}} \frac{1}{\sqrt{\epsilon^2 - \Delta^2}} \left(\epsilon + \frac{\Delta^2}{E_{\mathbf{k},a}} \right) \quad (6.57)$$

is the disorder self energy that reduces to the customary normal-metal expression in the $\Delta \rightarrow 0$ limit.⁴⁵

As expected, Eq. (6.55) yields $\alpha_{z,z} = 0$ for a BCS superconductor⁴⁶ at zero temperature. By virtue of Anderson's theorem, this observation remains true in presence of non-magnetic disorder. At low temperatures the Gilbert damping coefficient scales as $\exp(-\Delta/T)$.

In Fig. (6.5) we plot $\alpha_{z,z}$ as a function of disorder. We find that damping is most noticeable in clean superconductors where the mean free path

⁴⁵In the derivation of Eq. (6.57) we have made use of the chapter written by V. Ambegaokar in Ref. [143].

⁴⁶For a superconducting gap with nodes there could be damping even at zero temperature.

exceeds the coherence length, i.e. $\Delta\tau > 1$. This indicates a prominence of intraband transitions, which we now interpret within a pseudospin version of the breathing Fermi surface model.

In a homogeneous superconductor the global phase Ω_y of the Cooper pairs is irrelevant, and hence the energy of the quasiparticles does not depend on it. Indeed this is why $\alpha_{y,y}$ vanishes within the breathing Fermi surface model.⁴⁷ In contrast, $\partial E_{\mathbf{k},a}/\partial\Omega_z \neq 0$. Therefore, out-of-plane excursions of the pseudospin magnetization alter the band structure, leading to instantaneous quasiparticle populations that are out of equilibrium.⁴⁸ Interestingly, nonequilibrium distributions occur at nonzero temperatures only: at zero temperature the lower (upper) quasiparticle band is completely full (empty) and the Pauli exclusion principle freezes their occupation numbers regardless of band deformations.⁴⁹

Elastic and inelastic impurities provide a medium for the quasiparticles to reorganize back into a Fermi distribution, but this process takes up a time τ . Such time lag is responsible for damping, and accordingly $\alpha_{z,z} \propto \tau \neq 0$ at

⁴⁷However, in our numerical calculations $\alpha_{y,y}$ is not precisely zero. This error comes from interband transitions, for which the breathing Fermi surface arguments presented above do not apply. In any event, these interband contributions too ought to vanish after treating disorder exactly, which means that our evaluation of impurity vertex corrections may not be quantitatively precise.

⁴⁸Changing Ω_z is akin to *horizontally* shifting the quasiparticle bands in momentum space. At nonzero temperatures this results in both longitudinal (energy) and transverse (charge imbalance) perturbations of the quasiparticle population.

⁴⁹We assume that fluctuations are small enough so that the magnitude of the superconducting gap remains nonzero.

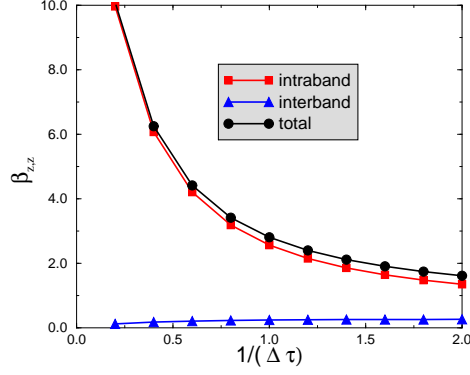


Figure 6.4: Non-adiabatic pseudospin transfer torque coefficient as a function of disorder. We take $T = \Delta/3$. The intraband contributions dominate over interband contributions and accordingly β grows linearly with the quasiparticle lifetime. We find that β is several orders of magnitude larger than α .

nonzero temperatures.⁵⁰

6.6 Non-Adiabatic Pseudospin Transfer Torque

The microscopic theory of the β term in superconductors parallels the one exposed in chapter 4. Like in the case of the Gilbert damping, we find that $\beta_{z,z}$ decays monotonically with disorder (Fig. (6.4)). Unlike the Gilbert damping, the non-adiabatic pseudospin transfer torque alters the *steady state* solution of the LLS equations. So as to gain some physical intuition, we consider a one-dimensional superconductor under a uniform temperature gradient and assume the applied electric field to be zero ($V_z^{\text{ext}} = 0$). Under these con-

⁵⁰In our numerical calculations $\alpha_{z,z}$ appears to have a sublinear dependence on τ ; more work is needed to elucidate this issue.

ditions Eq. (6.45) yields the following steady state solution:

$$\partial_x \Omega_z = -\frac{\beta v}{K} \partial_x^2 \Omega_z. \quad (6.58)$$

For $\beta = 0$ and/or $v = 0$, Ω_z and accordingly the superfluid chemical potential are uniform. In contrast, for $\beta \neq 0$, $\partial_x \Omega_z$ and accordingly the supercurrent vary exponentially in space with a characteristic lengthscale $\beta v/K$, which remarkably depends on the magnitude of the temperature gradient. This result may have observable implications at superconductor-normal metal interfaces. The conventional lore[144, 145] states that when a uniform temperature gradient is applied along such interface, mutually cancelling supercurrents and quasiparticle currents will arise in the superconducting side. These currents are uniform only deep into the superconductor; close to the interface they have an exponential dependence in space and consequently a measurable voltage difference appears there. Since conventional theories predict a characteristic lengthscale that is independent of the temperature gradient, they are in apparent disagreement with our result.

6.7 Thermal Doppler Shift of Pseudospin Waves

The importance of collective oscillations in the theory of superconductivity became obvious soon after the inception of the BCS theory. The original theory had given a correct account of the Meissner effect only in the Coulomb gauge, where $\nabla \cdot \mathbf{A} = 0$. This insufficiency was found to arise from the fact that only quasiparticle excitations had been included among the excited states.

Thereafter Anderson[125] demonstrated that a vector potential with nonzero divergence couples to a collective density fluctuation mode; the inclusion of this mode leads to a gauge invariant, current conserving theory.

In spite of their theoretical importance, collective modes in superconductors tend to be experimentally irrelevant.⁵¹ For instance, in an uncharged fermionic superfluid a gapless (Goldstone) mode exists, known as the Bogoliubov-Anderson mode, in which the phase of the order parameter varies periodically in space and time. However, in charged superconductors phase fluctuations couple to density fluctuations and subsequently the frequency of the Bogoliubov-Anderson mode is shifted to the plasma frequency, which is typically much higher than any superconducting energy scale (but see below).⁵² Thus the change of the ordinary plasmon under a superfluid transition is experimentally inappreciable. Similarly, the charged analogues of the first and fourth sound in superfluid Helium-4 are driven to the plasma frequency because they involve⁵³ density oscillations.

The first experimental demonstration⁵⁴ of the existence of a collective mode with an acoustic dispersion in a superconductor was given by Carlson and Goldman in 1973. The Carlson-Goldman mode exists only in a narrow window

⁵¹For an early account see *e.g.* chapter 7 of Ref. [143]. For a more modern review see *e.g.* G. Schon's chapter in Ref. [11].

⁵²Goldstone's theorem on the existence of gapless collective excitations is rendered inconclusive in presence of long-ranged Coulomb interactions.

⁵³The counterpart of the second sound could in principle be observable in a superconductor, yet it turns out to be strongly damped for almost all cases of interest.

⁵⁴For a review by one of the original authors see chapter 17 of Ref. [10].

near the transition temperature and consists of oscillations of the quasiparticle charge imbalance, which in turn trigger oscillations of the phase of the order parameter. Throughout this process the quasiparticle and the condensate currents cancel each other and since the total charge density does not oscillate the Carlson-Goldman mode is not driven up to the plasma frequency. The damping of this mode has its origins in the Ohmic losses of the normal current, and is small only near the transition temperature. From a microscopic point of view[132] the procedure to evaluate the Carlson-Goldman mode is no different from that to evaluate the ordinary plasmon.

In reduced dimensions the Coulomb interaction is altered in such manner that low-energy collective modes may arise even at low temperatures. In thin superconducting films, gapless plasmons have been observed with a square-root dispersion law.[146] Additionally, Mooij and Schon[147] proposed a propagating and weakly-damped mode for one-dimensional superconductors, which has been recently detected.[148]

These coupled phase and charge collective modes are readily accessible within the LLS formalism. For this purpose it is convenient to write the LLS equation in the momentum and frequency domain:

$$\begin{pmatrix} V_z^{\text{ext}} \\ V_y^{\text{ext}} \end{pmatrix} = \begin{pmatrix} K + i\omega\alpha - i\mathbf{q} \cdot \mathbf{v}\beta & -i\omega + i\mathbf{q} \cdot \mathbf{v} \\ i\omega - i\mathbf{q} \cdot \mathbf{v} & \rho q^2/2 \end{pmatrix} \begin{pmatrix} \Omega_z \\ \Omega_y \end{pmatrix}, \quad (6.59)$$

where q and ω are the wavevector and frequency of the external potential V^{ext} . The dispersion relation of the pseudospin waves can be determined from the zeros of the determinant of the response matrix in Eq. (6.59). For the sake of

transparency we neglect damping terms and therefore

$$\omega = \mathbf{q} \cdot \mathbf{v} \pm \sqrt{K\rho q^2/2}. \quad (6.60)$$

Let us assume $\mathbf{v} = 0$ for the moment. In bulk and at low temperatures Coulomb interactions dictate $K = 4\pi e^2/q^2$, which leads to $\omega = \omega_P \sqrt{\rho_s/n_e}$. ω_P is the frequency of the ordinary plasmon, $\rho_s = m\rho/2$ is the superfluid density and n_e is the total electron density. For conventional superconductors $\rho_s \simeq n_e$ at low temperatures, unless the system is highly disordered or granular.[132] Hence $\omega_P \sqrt{\rho_s/n_e}$ is often a large frequency, for which the LLS equation is inapplicable to begin with. In contrast, near the critical temperature K is given by a different expression[132] and consequently the gapless Carlson-Goldman mode emerges.⁵⁵ In reduced dimensions, low-frequency pseudospin waves occur even at low temperatures. In two-dimensional superconductors $K \propto 1/q$ and therefore $\omega \propto q^{1/2}$. In one-dimensional superconductors $K \propto \log(1/q)$ and hence $\omega \propto q\sqrt{\log(1/q)}$.

When $\mathbf{v} \neq 0$, these collective modes may be stiffened or softened depending on the relative orientation between the temperature gradient and the wavevector of the mode. This effect is akin to the Doppler shift realized in the spin wave spectrum of metallic ferromagnets.[62] In one-dimensional wires, there exists a critical pseudospin velocity $v_c = \sqrt{K\rho/2}$ for which the collective mode frequency becomes zero at all wavevectors. However, the accessibility of

⁵⁵While the LLS equation ignores amplitude fluctuations, it can still describe the Carlson-Goldman mode because the phase and charge oscillations are decoupled from amplitude fluctuations.

this critical velocity appears doubtful as in experiments conducted so far the phase velocity of the Mooij-Schon mode is comparable to the Fermi velocity, which is probably much larger than the characteristic pseudospin velocity. In two-dimensional films, the thermal Doppler shift may manifest itself through a crossover between square-root and linear dispersions. In bulk superconductors, the phase velocity of the Carlson-Goldman mode (which is typically much smaller than that of the Mooij-Schon mode) is likewise expected to vary under a thermal gradient.

In sum, we predict that a constant and uniform thermal gradient will modify the phase velocity of the propagating collective modes in superconductors. This prediction awaits experimental verification (or falsification).

6.8 Thermal Pseudospin-Galvanic Effects

Hitherto we have been inspecting superconductors that have a uniform order parameter *in equilibrium*. In this section we consider an equilibrium pseudospin configuration that forms an spiral in the xy plane of the particle-hole space:

$$\Delta(\mathbf{x}) = \Delta_0 e^{i\mathbf{Q}\cdot\mathbf{x}}, \quad (6.61)$$

where we take Δ_0 to be a real number without loss of generality. This configuration sustains a uniform supercurrent

$$\mathbf{j} \propto -i\Delta^*(\mathbf{x})\nabla\Delta(\mathbf{x}) + \text{c.c.} = \Delta_0^2\mathbf{Q}. \quad (6.62)$$

Because the spiral order parameter breaks inversion symmetry, we anticipate phenomena analogous to the inverse spin-galvanic effect analyzed in chapter 5. As a preliminary, we write the Hamiltonian for this system in the $(c_{\mathbf{k}+\mathbf{Q},\uparrow}, c_{-\mathbf{k}+\mathbf{Q},\downarrow}^\dagger)$ representation:

$$\mathcal{H} = \begin{pmatrix} \xi_{\mathbf{k}+\mathbf{Q}} & \Delta_0 \\ \Delta_0 & -\xi_{\mathbf{k}-\mathbf{Q}} \end{pmatrix}, \quad (6.63)$$

which exhibits the following quasiparticle spectrum:

$$\begin{aligned} E_{\mathbf{k}} &= \frac{\xi_{\mathbf{k}+\mathbf{Q}} - \xi_{\mathbf{k}-\mathbf{Q}}}{2} \pm \sqrt{\left(\frac{\xi_{\mathbf{k}+\mathbf{Q}} + \xi_{\mathbf{k}-\mathbf{Q}}}{2}\right)^2 + \Delta_0^2} \\ &\simeq \mathbf{Q} \cdot \frac{\partial \xi_{\mathbf{k}}}{\partial \mathbf{k}} \pm \sqrt{\xi_{\mathbf{k}}^2 + \Delta_0^2} + O(Q^2). \end{aligned} \quad (6.64)$$

Notice that $E_{\mathbf{k}} \neq E_{-\mathbf{k}}$ for $Q \neq 0$; this is a consequence of broken inversion symmetry. Moreover, the fact that $E_{\mathbf{k}}$ is an even function of $\xi_{\mathbf{k}}$ will play an important role in our considerations below.⁵⁶ The eigenspinors at momentum \mathbf{k} are $\Psi_{\mathbf{k},0} = (\cos(\theta_{\mathbf{k}}/2), \sin(\theta_{\mathbf{k}}/2))$ and $\Psi_{\mathbf{k},1} = (-\sin(\theta_{\mathbf{k}}/2), \cos(\theta_{\mathbf{k}}/2))$, where $\cos \theta_{\mathbf{k}} \simeq \xi_{\mathbf{k}} / \sqrt{\xi_{\mathbf{k}}^2 + \Delta_0^2}$.

With the above information we can readily derive the equilibrium pseudospin magnetization:

$$\begin{aligned} \tilde{s}^x &\simeq \sum_{\mathbf{k}} \frac{\Delta_0}{\sqrt{\xi_{\mathbf{k}}^2 + \Delta_0^2}} (f_{\mathbf{k},0} - f_{\mathbf{k},1}) \\ \tilde{s}^y &= 0 \\ \tilde{s}^z &\simeq \sum_{\mathbf{k}} \frac{\xi_{\mathbf{k}}}{\sqrt{\xi_{\mathbf{k}}^2 + \Delta_0^2}} (f_{\mathbf{k},0} - f_{\mathbf{k},1}) \simeq 0. \end{aligned} \quad (6.65)$$

⁵⁶While $\xi_{\mathbf{k}}$ is certainly odd around the Fermi energy, $\frac{\partial \xi_{\mathbf{k}}}{\partial \mathbf{k}}$ is even.

The equation for \tilde{s}^x is simply the BCS gap equation for a current-carrying superconductor.⁵⁷ $\tilde{s}^y = 0$ because we have taken the global phase of the spiral to be zero (it can always be gauged away). $s^z = 0$ follows from the fact that the term inside $\sum_{\mathbf{k}}$ is odd in $\xi_{\mathbf{k}}$.

Next, we focus on the influence of a uniform temperature gradient on the pseudospin density, encoded in⁵⁸

$$\delta\tilde{s}^i = \chi^{i,j} \frac{\nabla^j T}{T}, \quad (6.66)$$

where

$$\chi^{i,j} = \frac{1}{2\pi} \text{Re} \int_{|\epsilon + \mathbf{k}_F \cdot \mathbf{Q}| > \Delta_0} \frac{\partial f}{\partial \epsilon} \int_{\mathbf{k}} \tilde{S}_{a,b}^i \frac{\{\mathcal{H}, v^j\}_{b,a}}{2} (G_a^R(\mathbf{k}, \epsilon) G_b^A(\mathbf{k}, \epsilon) - G_a^A(\mathbf{k}, \epsilon) G_b^R(\mathbf{k}, \epsilon)) \quad (6.67)$$

is the pseudospin-caloric response function, and $\{, \}$ stands for an anticommutator.⁵⁹ Unlike its spin counterpart, the pseudospin magnetization is *invariant* under time-reversal. This can be verified by recalling that (i) the order parameter of a (conventional) BCS superconductor does not break time-reversal symmetry and (ii) the charge density is even under time reversal. This

⁵⁷Since we are neglecting $O(Q^2)$ terms, the magnitude of the superconducting gap is actually the same as for a uniform ($Q = 0$) superconductor.

⁵⁸Unlike in chapter 5 we consider a thermal current rather than an electric current.

⁵⁹We define the “thermal velocity” through an anticommutator between the Hamiltonian and the velocity operator, which is partly inspired by the customary definition of “spin velocities” in terms of anticommutators between the Hamiltonian and the spin operator. Our definition converges with the conventional expression (see *e.g.* Ref. [39]) for thermal currents in single-band models, and includes interband transitions on the same footing as intraband transitions in multiband models. As it turns out[123] the definition of thermal currents is altogether subtle; however, these uncertainties do not change the results of the present section qualitatively.

observation implies that $\chi^{i,j}$ must be even under time-reversal, because so is $\nabla T/T$. As we shall demonstrate next, this symmetry requirement is fulfilled via $\chi^{i,j} \propto Q^j \tau$.

We begin with $\delta \tilde{s}^x$, which depicts the change in the *magnitude* of the spiral order parameter. It is easy to verify that $\tilde{S}_{a \neq b}^x$ is odd in $\xi_{\mathbf{k}}$ and that $v_{a \neq b}^i$ is even in $\xi_{\mathbf{k}}$. Therefore, interband contributions vanish after integrating over momenta. In contrast, intraband contributions are nonvanishing. In order to see this, we note that $S_{a,a}^x$ is even in $\xi_{\mathbf{k}}$ while $v_{a,a}^i$ has a piece that is even in $\xi_{\mathbf{k}}$ and a piece that is odd. Since $E_{\mathbf{k}}$ is even in $\xi_{\mathbf{k}}$, only the part of $v_{a,a}^i$ that is even in $\xi_{\mathbf{k}}$ will survive the momentum integral. This part is Q^i/m , which is already linear in the spiral wavevector; consequently, we can set $Q = 0$ in the matrix elements of the pseudospin operator as well as in the energy eigenvalues. As a result, we write

$$\delta \tilde{s}^x = \frac{1}{2\pi} \frac{\nabla^i T}{T} \int_{|\epsilon| > \Delta_0} \frac{\partial f}{\partial \epsilon} \int_{\mathbf{k}} \tilde{S}_{a,a}^x(\mathbf{k}) v_{a,a}^i(\mathbf{k}, \mathbf{Q}) E_{\mathbf{k},a} A_a^2(\epsilon, \mathbf{k}), \quad (6.68)$$

where A is the spectral function defined in Eq. (4.14). Eq. (6.68) may be unfolded as

$$\begin{aligned} \delta \tilde{s}^x &= \frac{\mathbf{Q} \cdot \nabla T}{2\pi m T} \int_{|\epsilon| > \Delta_0} \frac{\partial f}{\partial \epsilon} \int_{\mathbf{k}} \frac{\Delta_0}{E_{\mathbf{k}}} (A_0^2 E_{\mathbf{k},0} - A_1^2 E_{\mathbf{k},1}) \\ &= -\frac{\mathbf{Q} \cdot \nabla T}{2\pi m T} \Delta_0 \int_{|\epsilon| > \Delta_0} \frac{\partial f}{\partial \epsilon} \int_{\mathbf{k}} (A_0^2 + A_1^2) \\ &\sim -\frac{\mathbf{Q} \cdot \nabla T}{m T} \Delta_0 N(0) \tau \int_{|\epsilon| > \Delta_0} \frac{\partial f}{\partial \epsilon} \\ &= -\frac{\mathbf{Q} \cdot \nabla T}{m T} \Delta_0 N(0) \tau [f(-\Delta_0) - f(\Delta_0) - 1] \\ &\propto \frac{\mathbf{Q} \cdot \nabla T}{m T} \Delta_0 N(0) \tau f(\Delta_0). \end{aligned} \quad (6.69)$$

In the derivation of the third line above we have performed the integrals over the spectral functions as though they were those of a normal metal; otherwise we would have not been able to present analytical results.⁶⁰ The corrections due to pairing are likely to be small at larger temperatures and/or dirtier samples. Likewise, we have ignored miscellaneous factors of order unity throughout.

In sum, a thermal gradient can enhance or deplete the superconducting gap of a current carrying superconductor, depending on the relative orientation between the supercurrent and the temperature gradient. This effect vanishes at zero temperature, and is most pronounced in clean superconductors. While microwave absorption, phonon injection and tunneling currents are well-established methods[10] to change the magnitude of the superconducting gap, we are not aware of any discussions⁶¹ concerning the influence of temperature gradients. We can envisage an experiment which would consist of applying a current-bias to a clean superconducting wire placed under a temperature gradient. If our prediction is correct, the magnitude of the energy gap should show an asymmetry with respect to the direction of the applied current.

Next, let us look at $\delta\tilde{s}^y$. The global phase of a an isolated superconductor should have no preferred value regardless of the external perturbation, which suggests that $\delta\tilde{s}^y = 0$. Our calculation verifies this claim; the cancel-

⁶⁰The disorder self energy for a superconductor is even more complicated in presence of a nonzero pairing momentum.

⁶¹Modulo the superconducting fountain effect, which nonetheless cannot explain a thermal *enhancement* of the gap.

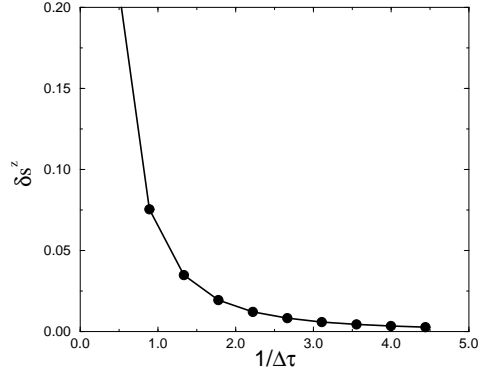


Figure 6.5: Quasiparticle charge imbalance induced by a temperature gradient in a current-carrying superconductor, as a function of the scattering rate from impurities.

lation between the contributions from $\epsilon > \Delta_0$ and $\epsilon < -\Delta_0$ turns out to be key.

Lastly, we turn our attention to $\delta\tilde{s}^z$, which is the thermally-induced charge density. We have already highlighted this phenomenon in Sec. IV; here we complement it with a numerical calculation based on Eq. (6.66); see Fig. (6.5). As expected, the induced charge imbalance grows monotonically with the quasiparticle lifetime.⁶²

6.9 “Quasiparticle Spin Imbalance” in Spiral Magnets

Thus far we have drawn from the theory of magnetism in order to propose potentially novel effects in nonequilibrium superconductivity. Here we

⁶²However, the relationship appears to be superlinear. Further reality checks appear to be necessary in order increase confidence in our numerical results.

embark on the opposite enterprise: based on our knowledge of nonequilibrium superconductivity, we shall prove that a spin-unpolarized transport current can induce a nonequilibrium transverse spin density in a spiral ferromagnet. This effect is the magnetic counterpart of the thermally-induced quasiparticle charge discussed above.

In a xy spiral ferromagnet, the exchange field is given by

$$\Delta = \Delta_0 (\cos(\mathbf{Q} \cdot \mathbf{x}), \sin(\mathbf{Q} \cdot \mathbf{x}), 0), \quad (6.70)$$

where \mathbf{Q} is the spiral wavevector. The Hamiltonian of this system is

$$\mathcal{H} \simeq \xi_{\mathbf{k}1} + \mathbf{Q} \cdot \frac{\partial \xi_{\mathbf{k}}}{\partial \mathbf{k}} S^z + \Delta_0 S^x + O(Q^2), \quad (6.71)$$

written in the $(c_{\mathbf{k}+\mathbf{Q},\uparrow}, c_{\mathbf{k}-\mathbf{Q},\downarrow})$ basis. Correspondingly, the eigenstates at momentum \mathbf{k} are $\Psi_{\mathbf{k},0} = (\cos(\theta_{\mathbf{k}}/2), \sin(\theta_{\mathbf{k}}/2))$ and $\Psi_{\mathbf{k},1} = (-\sin(\theta_{\mathbf{k}}/2), \cos(\theta_{\mathbf{k}}/2))$, where $\cos \theta_{\mathbf{k}} \simeq (\mathbf{Q} \cdot \partial \xi_{\mathbf{k}} / \partial \mathbf{k}) / \Delta_0$.

In equilibrium the magnetization along \hat{z} is zero. In presence of a transport current, it changes into

$$\delta s^z = \sum_{\mathbf{k}} \frac{\mathbf{Q} \cdot \partial \xi_{\mathbf{k}} / \partial \mathbf{k}}{\Delta_0} (\delta f_{\mathbf{k},0} - \delta f_{\mathbf{k},1}), \quad (6.72)$$

where as usual "0" ("1") labels the quasiparticle band that is lowest (highest) in energy and $\delta f_{\mathbf{k}}$ denotes the deviation of the quasiparticle occupation numbers from equilibrium. If transport is driven by an electric current, we get

$$\delta s^z = e \sum_{\mathbf{k}} \frac{\mathbf{Q} \cdot \partial \xi_{\mathbf{k}} / \partial \mathbf{k}}{\Delta_0} \left(\mathbf{v}_{\mathbf{k},0} \cdot \mathbf{E} \tau_{\mathbf{k},0} \frac{\partial f_{\mathbf{k},0}}{\partial E_{\mathbf{k},0}} - \mathbf{v}_{\mathbf{k},1} \cdot \mathbf{E} \tau_{\mathbf{k},1} \frac{\partial f_{\mathbf{k},1}}{\partial E_{\mathbf{k},1}} \right). \quad (6.73)$$

Without further calculations, Eq. (6.73) may be rewritten as

$$\delta s^z \propto \frac{\mathbf{Q} \cdot \mathbf{E}}{e\Delta_0}(\sigma_0 - \sigma_1) + O(Q^2), \quad (6.74)$$

where σ_0 and σ_1 are the zero-frequency and zero-wavevector electrical conductivities corresponding to the two quasiparticle bands. For $\Delta_0 \neq 0$ one finds $\sigma_0 \neq \sigma_1$ because the density of states of the two bands differ at the Fermi surface. Therefore, an electric current induces a *uniform* out-of-plane magnetization in a ferromagnet with in-plane spiral order. This result agrees in part with a recent prediction of Goto, Katsura and Nagaosa.[149] Goto *et al.* further state that the sign of the current-spin density will depend on α/β and that the spiral wavevector will be modified by an electric current.

In a similar fashion, a thermal gradient leads to $s^z \neq 0$; in this case we write

$$\delta s^z \propto \frac{\mathbf{Q} \cdot \nabla T}{T\Delta_0}(\kappa_0 - \kappa_1), \quad (6.75)$$

where $\kappa = T\alpha_S\sigma/e$ and α_S stands for the Seebeck coefficient.[150]

Finally, one can easily verify that neither electric nor thermal currents change the in-plane components of the magnetization. This differs strikingly from the result of the previous section, which showed that \tilde{s}^x can be changed by mediation of a thermal gradient. This lack of correspondence between the pseudospin-spiral and spin-spiral orders originates from the distinct symmetry of the respective Hamiltonians under the parity transformation: $E_{\mathbf{k}} \neq E_{-\mathbf{k}}$ in a current-carrying superconductor whereas $E_{\mathbf{k}} = E_{-\mathbf{k}}$ in a spiral ferromagnet.

6.10 Summary and Conclusions

In this chapter we have analyzed nonequilibrium superconductivity borrowing techniques from nonequilibrium magnetism. Within the Nambu-Gorkov representation, a superconductor may be described as an easy-plane *pseudospin* ferromagnet with an out-of-plane anisotropy governed by repulsive Coulomb interactions. In this representation the Landau-Lifshitz-Slonczewski equation epitomizes the low-energy and long-wavelength transverse fluctuations of the order parameter. What is more, the LLS equation embodies a new way of looking at nonequilibrium superconductivity and suggests a number of interesting analogies with nonequilibrium magnetism. In fact, we have predicted possibly new thermal effects that may be experimentally testable in superconductors.

One drawback of the LLS approach is that it is unable to describe amplitude fluctuations of the order parameter. These fluctuations fall into thermal or quantum phase slips, and there is ample evidence to believe that they may be responsible for the resistive effects that proliferate in low dimensional superconductors. However, thermal phase slips are negligible at low temperatures and quantum phase slips are suppressed[129] in superconductors with long mean free paths. It may thus be the case that the LLS approach will be accurate in clean superconductors away from the critical temperature.

Future work will consist of consolidating the predictions made in this chapter, building new ones, carrying out a much more exhaustive comparison between the conventional and the novel approaches, and deriving the full LLS

equation from the microscopic BCS theory. Another potentially interesting avenue to pursue is the simulation of superconducting wires using atomistic LLS equations.[151]

Chapter 7

Conclusions

Now this is not the end. It is not even the beginning of the end. But it is, perhaps, the end of the beginning. (Winston Churchill)

The original work reported in this thesis has extended the microscopic theory of the Landau-Lifshitz-Slonczewski equation in a number of ways.

First, we have carefully analyzed the role of disorder on magnetization relaxation in electric equilibrium. Disorder is indeed a crucial ingredient, yet present electronic structure calculations are able to include it only approximately. Our evaluation of impurity vertex corrections, carried out for simple but physically relevant models, predicts that state-of-the-art *ab-initio* calculations of the Gilbert damping may not be quantitatively accurate in strongly spin-orbit coupled ferromagnets such as (Ga,Mn)As.

Second, we have studied magnetization relaxation in presence of an electric current. We have demonstrated that the change in magnetic damping due to the electric current is directly related to the non-adiabatic spin transfer torque parameter, which plays an important role in the dynamics of magnetic domain walls. Concurrently we have arrived at the first analytical expression for the non-adiabatic torque that is valid for arbitrary band struc-

tures. Calculations based on this formula will soon lead to reasonably accurate predictions in real materials. In particular it may be interesting to find or design systems where the Gilbert damping coefficient and the non-adiabatic spin transfer torque coefficient have the opposite sign.

Third, we have explored a new type of current-induced spin torque that does not require inhomogeneous magnetization. We have referred to this torque as the ferromagnetic inverse spin-galvanic effect (ISGE), and have shown that it arises in bulk ferromagnets that are chiral and noncentrosymmetric. Thereafter we have linked the ferromagnetic ISGE with the change in magnetic anisotropy due to an electric current, and have derived a formula that can be applied to real materials. Once again, computer calculations based on our formula will determine the technological impact of this novel spin torque. More generally, our work may provide a starting point for future research on how electric currents influence the genesis and morphology of magnetic spirals and domain walls.

Fourth, we have applied the Landau-Lifshitz-Slonczewski equation to evaluate the low energy and long wavelength dynamics of the *superconducting* order parameter. Since superconductors are easy-plane ferromagnets in the particle-hole space, they may in principle be approached from the viewpoint of nonequilibrium magnetism. While nonequilibrium magnetism and nonequilibrium superconductivity have traditionally been studied as separate disciplines, we believe that many of their phenomena are connected. By exploiting these analogies, we have suggested potentially new effects involving

temperature gradients. A more careful theoretical effort will be instrumental in order to corroborate and expand our preliminary results; such effort is currently underway.

Appendices

Appendix A

Quadratic Spin Response to an Electric and Magnetic Field

Consider a system that is perturbed from equilibrium by a time-dependent perturbation $\mathcal{V}(t)$. The change in the expectation value of an operator $O(t)$ under the influence of $\mathcal{V}(t)$ can be formally expressed as

$$\delta\langle O(t)\rangle = \langle\Psi_0|U^\dagger(t)O(t)U(t)|\Psi_0\rangle - \langle\Psi_0|O(t)|\Psi_0\rangle \quad (\text{A.1})$$

where $|\Psi_0\rangle$ is the unperturbed state of the system,

$$U(t) = T \exp \left[-i \int_{-\infty}^t \mathcal{V}(t') dt' \right] \quad (\text{A.2})$$

is the time-evolution operator in the interaction representation and T stands for time ordering. Expanding the exponentials up to second order in \mathcal{V} we arrive at

$$\delta\langle O(t)\rangle = i \int_{-\infty}^t dt' \langle [O(t), \mathcal{V}(t')] \rangle - \frac{1}{2} \int_{-\infty}^t dt' dt'' \langle [[O(t), \mathcal{V}(t')], \mathcal{V}(t'')] \rangle. \quad (\text{A.3})$$

For the present work, $O(t) \rightarrow S^a$ ($a = x, y, z$) and

$$\mathcal{V}(t) = - \int d\mathbf{r} \mathbf{j} \cdot \mathbf{A}(\mathbf{r}, t) + \int d\mathbf{r} \mathbf{S} \cdot \mathcal{H}_{\text{ext}}(\mathbf{r}, t), \quad (\text{A.4})$$

where \mathbf{A} is the vector potential, \mathcal{H}_{ext} is the external magnetic field, and \mathbf{j} is the current operator. Plugging Eq. (A.4) into Eq. (A.3) and neglecting

$O(A^2)$, $O(\mathcal{H}_{\text{ext}}^2)$ terms we obtain

$$\delta S^a(x) = \sum_b \int dx' \chi_{S,j}^{a,b} A^b(x') + \sum_b \int dx' \chi_{S,S}^{a,b} \mathcal{H}_{\text{ext}}^b(x') + \sum_{b,c} \int dx' dx'' \chi_{S,S,j}^{a,b,c} A^b(x') \mathcal{H}_{\text{ext}}^c(x''), \quad (\text{A.5})$$

where $x \equiv (\mathbf{r}, t)$ and $\int dx' \equiv \int_{-\infty}^{\infty} dt' \int d\mathbf{r}'$. The linear and quadratic response functions introduced above are defined as

$$\begin{aligned} \chi_{S,j}^{a,b}(x, x') &= i \langle [S^a(x), j^b(x')] \rangle \Theta(t - t') \\ \chi_{S,S}^{a,b}(x, x') &= i \langle [S^a(x), S^b(x')] \rangle \Theta(t - t') \\ \chi_{S,S,j}^{a,b,c}(x, x', x'') &= \langle [[S^a(x), j^b(x')], S^c(x'')] \rangle \Theta(t - t') \Theta(t' - t'') \\ &\quad + \langle [[S^a(x), S^b(x'')], j^c(x')] \rangle \Theta(t - t'') \Theta(t' - t') \end{aligned} \quad (\text{A.6})$$

where we have used $T[F(t)G(t')] = F(t')G(t'')\Theta(t' - t'') + G(t'')F(t')\Theta(t'' - t')$, Θ being the step function. $\chi_{S,j}$ is the spin density induced by an electric field in a uniform ferromagnet, and it vanishes unless there is intrinsic spin-orbit interaction. $\chi_{S,S}$ is the spin density induced by an external magnetic field. $\chi_{S,S,j}$ is the spin density induced by the combined action of an electric and magnetic field (see Fig. (A.1) for a diagrammatic representation); this quantity is closely related to $(\mathbf{v}_s \cdot \mathbf{q})\chi^{(2)}$, introduced in Section II.

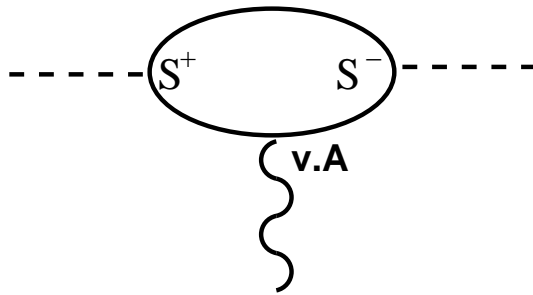


Figure A.1: Feynman diagram for $\chi_{S,S,j}$. The dashed lines correspond to magnons, whereas the wavy line represents a photon.

tions G and performing the Matsubara sum we get

$$\begin{aligned} \tilde{\chi}_{+,-}^{\text{QP,(1)}} &= -V \frac{\Delta_0^2}{2} \int_{\mathbf{k}, \mathbf{k}'} u^i 2 \operatorname{Re} [S_{a,b}^+ S_{b,b'}^i S_{b',a'}^- S_{a',a}^i] \int_{-\infty}^{\infty} \frac{d\epsilon_1 d\epsilon'_1 d\epsilon_2 d\epsilon'_2}{(2\pi)^4} A_a(\epsilon_1, \mathbf{k}) A_{a'}(\epsilon'_1, \mathbf{k}') \\ &\quad \times A_b(\epsilon_2, \mathbf{k} + \mathbf{q}) A_{b'}(\epsilon'_2, \mathbf{k}' + \mathbf{q}) \left[\frac{f(\epsilon_1)}{(\epsilon_1 - \epsilon'_1)(i\omega + \epsilon_1 - \epsilon_2)(i\omega + \epsilon_1 - \epsilon'_2)} \right. \\ &\quad \left. + \left(\begin{array}{c} \epsilon_1 \leftrightarrow \epsilon_2, \epsilon'_1 \leftrightarrow \epsilon'_2, \\ \omega \leftrightarrow -\omega \end{array} \right) \right] \end{aligned} \quad (\text{B.2})$$

where twice the real part arose after absorbing two of the terms coming from the Matsubara sum. Next, we apply $i\omega \rightarrow \omega + i0^+$ and take the imaginary part:

$$\begin{aligned} \tilde{\chi}_{+,-}^{\text{QP,(1)}} &= V \frac{\Delta_0^2}{2} 2\pi \int_{\mathbf{k}, \mathbf{k}'} u^i \operatorname{Re} [S_{a,b}^+ S_{b,b'}^i S_{b',a'}^- S_{a',a}^i] \\ &\quad \times \int_{-\infty}^{\infty} \frac{d\epsilon_1 d\epsilon'_1 d\epsilon_2 d\epsilon'_2}{(2\pi)^4} A_a(\epsilon_1, \mathbf{k}) A_{a'}(\epsilon'_1, \mathbf{k}') A_b(\epsilon_2, \mathbf{k} + \mathbf{q}) A_{b'}(\epsilon'_2, \mathbf{k}' + \mathbf{q}) \\ &\quad \times \frac{f(\epsilon_1)}{\epsilon_1 - \epsilon'_1} \left[\frac{\delta(\omega + \epsilon_1 - \epsilon_2)}{\omega + \epsilon_1 - \epsilon'_2} + \frac{\delta(\omega + \epsilon_1 - \epsilon'_2)}{\omega + \epsilon_1 - \epsilon_2} - \left(\begin{array}{c} \omega \rightarrow -\omega, \\ \mathbf{q} \rightarrow -\mathbf{q} \end{array} \right) \right] \end{aligned} \quad (\text{B.3})$$

where we used $1/(x - i\eta) = PV(1/x) + i\pi\delta(x)$, and invoked spin-rotational invariance to claim that terms with $S_{a,b}^x S_{b,b'}^i S_{b',a'}^y S_{a',a}^i$ will vanish. Integrating the delta functions we arrive at

$$\begin{aligned} \tilde{\chi}_{+,-}^{\text{QP,(1)}} &= V \frac{\Delta_0^2}{2} \int_{\mathbf{k}, \mathbf{k}'} u^i \operatorname{Re} [\dots] \int_{-\infty}^{\infty} \frac{d\epsilon'_1 d\epsilon_2 d\epsilon'_2}{(2\pi)^3} \frac{f(\epsilon_2) A_a(\epsilon_2, \mathbf{k}) A_{a'}(\epsilon'_1, \mathbf{k}')}{(\epsilon_2 - \epsilon'_2)(\epsilon_2 - \epsilon'_1)} \\ &\quad \times [A_b(\epsilon_2 + \omega, \mathbf{k} + \mathbf{q}) A_{b'}(\epsilon'_2 + \omega, \mathbf{k}' + \mathbf{q}) + A_b(\epsilon'_2 + \omega, \mathbf{k} + \mathbf{q}) A_{b'}(\epsilon_2 + \omega, \mathbf{k}' + \mathbf{q})] \\ &\quad - \left(\begin{array}{c} \omega \rightarrow -\omega, \\ \mathbf{q} \rightarrow -\mathbf{q} \end{array} \right) \end{aligned} \quad (\text{B.4})$$

The next step is to do the ϵ'_1 and ϵ'_2 integrals, taking advantage of the fact that for weak disorder the spectral functions are sharply peaked

Lorentzians (in fact at the present order of approximation one can take regard them as Dirac delta functions). The result reads

$$\begin{aligned}
\tilde{\chi}_{+,-}^{\text{QP},(1)} &= V \frac{\Delta_0^2}{2} \int_{\mathbf{k}, \mathbf{k}'} u^i \text{Re} [\dots] \\
&\times \int_{-\infty}^{\infty} \frac{d\epsilon_2}{2\pi} \frac{f(\epsilon_2) A_a(\epsilon_2, \mathbf{k})}{\epsilon_2 - \epsilon_{\mathbf{k}', a'}} \left[\frac{A_b(\epsilon_2 + \omega, \mathbf{k} + \mathbf{q})}{\epsilon_2 + \omega - \epsilon_{\mathbf{k}'+\mathbf{q}, b'}} + \frac{A_{b'}(\epsilon_2 + \omega, \mathbf{k}' + \mathbf{q})}{\epsilon_2 + \omega - \epsilon_{\mathbf{k}+\mathbf{q}, b}} \right] \\
&- (\omega \rightarrow -\omega, \mathbf{q} \rightarrow -\mathbf{q}) \tag{B.5}
\end{aligned}$$

By making further changes of variables, this equation can be rewritten as

$$\begin{aligned}
\tilde{\chi}_{+,-}^{\text{QP},(1)} &= V \frac{\Delta_0^2}{2} \int_{\mathbf{k}, \mathbf{k}'} u^i \text{Re} [\dots] \int_{-\infty}^{\infty} \frac{d\epsilon_2}{2\pi} \frac{(f(\epsilon_2) - f(\epsilon_2 + \omega)) A_a(\epsilon_2, \mathbf{k})}{\epsilon_2 - \epsilon_{\mathbf{k}', a'}} \\
&\times \left[\frac{A_b(\epsilon_2 + \omega, \mathbf{k} + \mathbf{q})}{\epsilon_2 + \omega - \epsilon_{\mathbf{k}'+\mathbf{q}, b'}} + \frac{A_{b'}(\epsilon_2 + \omega, \mathbf{k}' + \mathbf{q})}{\epsilon_2 + \omega - \epsilon_{\mathbf{k}+\mathbf{q}, b}} \right] \tag{B.6}
\end{aligned}$$

This is the first order vertex correction for the Gilbert damping. In order to obtain an analogous correction for the non-adiabatic STT, it suffices to shift the Fermi factors in Eq. (B.6) as indicated in the main text. This immediately results in Eq. (4.21).

Appendix C

Derivation of Eq. (4.26)

Let us first focus on the first term of Eq. (4.17), namely

$$E_i q_j \int_{\mathbf{k}} [|\langle a, \mathbf{k} | S^+ | b, \mathbf{k} \rangle|^2 + |\langle a, \mathbf{k} | S^- | b, \mathbf{k} \rangle|^2] A_a A'_b v_{\mathbf{k},a}^i v_{\mathbf{k},b}^j \tau_{\mathbf{k},a} \quad (\text{C.1})$$

We shall start with the azimuthal integral. It is easy to show that the entire angle dependence comes from $v^i v^j \propto k_i k_j$, from which the azimuthal integral vanishes unless $i = j$.

Regarding the $|k|$ integral, we assume that $\lambda k_F, \Delta_0, 1/\tau \ll \epsilon_F$; otherwise the analytical calculation is complicated and must be tackled numerically. Such assumption allows us to use $\int_{\mathbf{k}} \rightarrow N_{2D} \int_{-\infty}^{\infty} d\epsilon$. For inter-band transitions ($a \neq b$), $A_a A'_b$ contributes mainly thru the pole at $\epsilon_{F,a}$, thus all the slowly varying factors in the integrand may be set at the Fermi energy. For intra-band transitions ($a = b$), $A_a A'_a$ has no peak at the Fermi energy; hence it is best to keep the slowly varying factors inside the integrand.

The above observations lead straightforwardly to the following result:

$$\begin{aligned} & E_i q_j \int_{\mathbf{k}} [|\langle a, \mathbf{k} | S^+ | b, \mathbf{k} \rangle|^2 + |\langle a, \mathbf{k} | S^- | b, \mathbf{k} \rangle|^2] A_a A'_b v_{\mathbf{k},a}^i v_{\mathbf{k},b}^j \tau_{\mathbf{k},a} \\ \simeq & \mathbf{E} \cdot \mathbf{q} \frac{m^2}{8m_+ m_-} \left(1 + \frac{\Delta_0^2}{b^2}\right) \frac{(\epsilon_{F,-} \tau_- \Gamma_+ - \epsilon_{F,+} \tau_+ \Gamma_-)}{b^3} \\ - & \mathbf{E} \cdot \mathbf{q} \left[\frac{m^2}{m_+^2} \frac{1}{2} \frac{\lambda^2 k_F^2}{b^2} \left(1 + \frac{\Delta_0^2}{b^2}\right) \tau_+^2 + \frac{m^2}{m_-^2} \frac{1}{2} \frac{\lambda^2 k_F^2}{b^2} \left(1 + \frac{\Delta_0^2}{b^2}\right) \tau_-^2 \right] \quad (\text{C.2}) \end{aligned}$$

The second and third line in Eq. (C.2) come from inter-band and intra-band transitions, respectively. The latter vanishes in absence of spin-orbit interaction, leading to a 2D version of Eq. (4.20). Since the band-splitting is much smaller than the Fermi energy, one can further simplify the above equation via $\tau_+ \simeq \tau_- \rightarrow \tau$.

Let us now move on the second term of Eq. (4.17), namely

$$E_i q_j \int_{\mathbf{k}} \text{Re} [\langle b, \mathbf{k} | S^- | a, \mathbf{k} \rangle \langle a, \mathbf{k} | S^+ \partial_{k_j} | b, \mathbf{k} \rangle + (S^+ \leftrightarrow S^-)] A_a A_b v_{\mathbf{k},a}^i \tau_{\mathbf{k},a} \quad (\text{C.3})$$

Most of the observations made above apply for this case as well. For instance, the azimuthal integral vanishes unless $i = j$. This follows from a careful evaluation of the derivatives of the eigenstates with respect to momentum; $\partial_{k_j} \theta = \sin(\theta) \cos(\theta) k_j / k^2$ ($0 \leq \theta \leq \pi/2$) is a useful relation in this regards, while $\partial_{k_j} \phi$ plays no role. As for the $|k|$ integral, we no longer have the derivative of a spectral function, but rather a product of two spectral functions; the resulting integrals may be easily evaluated using the method of residues. The final result reads

$$\begin{aligned} & E_i q_j \int_{\mathbf{k}} \text{Re} [\langle b, \mathbf{k} | S^- | a, \mathbf{k} \rangle \langle a, \mathbf{k} | S^+ \partial_{k_j} | b, \mathbf{k} \rangle + (S^+ \leftrightarrow S^-)] A_a A_b v_{\mathbf{k},a}^i \tau_{\mathbf{k},a} \\ \simeq & -\mathbf{E} \cdot \mathbf{q} \left[\frac{m}{32m_-} \frac{\lambda^2 k_F^2 \Delta_0^2}{b^6} \left(1 + \frac{\tau_-}{\tau_+} \right) + \frac{m}{32m_+} \frac{\lambda^2 k_F^2 \Delta_0^2}{b^6} \left(1 + \frac{\tau_+}{\tau_-} \right) \right] \\ & + \mathbf{E} \cdot \mathbf{q} \left[\frac{m}{4m_+} \frac{\lambda^2 k_F^2 \Delta_0^2}{b^4} \tau_+^2 + \frac{m}{4m_-} \frac{\lambda^2 k_F^2 \Delta_0^2}{b^4} \tau_-^2 \right] \end{aligned} \quad (\text{C.4})$$

The first line in Eq. (C.4) stems from inter-band transitions, whereas the second comes from intra-band transitions; *both* vanish in absence of spin-orbit

interaction. Once again we can take $\tau_+ \simeq \tau_- \rightarrow \tau$. Combining Eqs. (C.2) and (C.4) one can immediately reach Eq. (4.26).

Bibliography

- [1] D. Pines. *Elementary Excitations in Solids*. Benjamin (New York), 1963.
- [2] G.R. Stewart. *Rev. Mod. Phys.*, 73:79, 2001.
- [3] G.T. Rado and H. Suhl (eds.). *Magnetism*. Academic Press (New York), 1963.
- [4] K. Baberschke, M. Donath, and W. Nolting (eds.). *Band-Ferromagnetism*. Springer-Verlag (Berlin), 2001.
- [5] M. Tinkham. *Introduction to Superconductivity (2nd ed.)*. Dover Publications (New York), 1996.
- [6] M. Tinkham. *Theory of Superconductivity (revised printing)*. Perseus Books (Reading, Massachusetts), 1999.
- [7] P.G. de Gennes. *Superconductivity of Metals and Alloys (3rd ed.)*. Perseus Books (Reading, Massachusetts), 1999.
- [8] S. Maekawa (ed.). *Concepts in Spin Electronics*. Oxford University Press (New York), 2006.
- [9] J.A.C. Bland and B. Heinrich (eds.). *Ultrathin Magnetic Structures III: Fundamentals of Nanomagnetism*. Springer-Verlag (Berlin), 2005.

- [10] K.E. Gray (ed.). *Nonequilibrium Superconductivity, Phonons and Kapitza Boundaries*. Plenum Press (New York), 1981.
- [11] D.N Langenberg and A.I. Larkin (eds.). *Nonequilibrium Superconductivity*. North Holland (New York), 1986.
- [12] M.Devoret, A. Wallraff, and J.M. Martinis. *arXiv*, 0411174, 2004.
- [13] T.L. Gilbert. *IEEE Trans. Magn.*, 40:3443, 2004.
- [14] D.C. Ralph and M.D. Stiles. *J. Magn. Magn. Mater.*, 320:1190, 2008.
- [15] V. Korenman and R.E. Prange. *Phys. Rev. B*, 6:2769, 1972.
- [16] V. Kambersky. *Czech J. Phys. B*, 26:2769, 1976.
- [17] Y. Tserkovnyak, G.A. Fiete, and B.I. Halperin. *Appl. Phys. Lett.*, 84:5234, 2004.
- [18] E.M. Hankiewicz, G. Vignale, and Y. Tserkovnyak. *Phys. Rev. B*, 75:174434, 2007.
- [19] Y. Tserkovnyak, H.J. Skadsem, A. Brataas, and G.E.W. Bauer. *Phys. Rev. B*, 74:144405, 2006.
- [20] H.J. Skadsem, Y. Tserkovnyak, A. Brataas, and G.E.W. Bauer. *Phys. Rev. B*, 75:094416, 2007.
- [21] H. Kohno, G. Tataru, and J. Shibata. *J. Phys. Soc. Japan*, 75:113706, 2006.

- [22] R.A. Duine, A.S. Nunez, J. Sinova, and A.H. MacDonald. *Phys. Rev. B*, 75:214420, 2007.
- [23] Y. Tserkovnyak, A. Brataas, and G.E.W. Bauer. *J. Magn. Magn. Mater.*, 320:1282, 2008.
- [24] D. Steiauf and M. Fahnle. *Phys. Rev. B*, 72:064450, 2005.
- [25] D. Steiauf, J. Seib, and M. Fahnle. *Phys. Rev. B*, 78:020410, 2008.
- [26] K. Gilmore, Y.U. Idzerda, and M.D. Stiles. *Phys. Rev. Lett.*, 99:27204, 2007.
- [27] V. Kambarsky. *Phys. Rev. B*, 76:134416, 2007.
- [28] O. Gunnarsson. *J. Phys. F*, 6:587, 1976.
- [29] Z. Qian and G. Vignale. *Phys. Rev. Lett.*, 88:056404, 2002.
- [30] K. Capelle and B.L. Gyorffy. *Europhys. Lett.*, 61:354, 2003.
- [31] J. Shi, G. Vignale, D. Xiao, and Q. Niu. *Phys. Rev. Lett.*, 99:197202, 2007.
- [32] I. Souza and D. Vanderbilt. *Phys. Rev. B*, 77:054438, 2008.
- [33] A.C. Jenkins and W.M. Temmerman. *Phys. Rev. B*, 60:10233, 1999.
- [34] I. Garate and A.H. MacDonald. *Phys. Rev. B*, 79:064404, 2009.

- [35] J. Sinova, T. Jungwirth, X. Liu, Y. Sasaki, J.K. Furdyna, W.A. Atkinson, and A.H. MacDonald. *Phys. Rev. B*, 69:85209, 2004.
- [36] I. Garate and A.H. MacDonald. *Phys. Rev. B*, 79:064403, 2009.
- [37] T. Jungwirth, J. Sinova, J. Masek, J. Kucera, and A.H. MacDonald. *Rev. Mod. Phys.*, 78:809, 2006.
- [38] A.H. MacDonald, P. Schiffer, and N. Samarth. *Nat. Materials*, 4:195, 2005.
- [39] G.D. Mahan. *Many-Particle Physics (3rd ed.)*. Kluwer Academic/Plenum Publishers (New York), 2000.
- [40] For a possible exception see A. Bove, F.A. Altomare, N.B. Kundtz, A.M. Chang, Y.J. Cho, X. Liu, and J. Furdyna. *arXiv*, 0802.3871, 2008.
- [41] J.J. Sakurai (ed. S.F. Tuan). *Modern Quantum Mechanics (revised edition)*. Addison-Wesley (New York), 1994.
- [42] P. Yu and M. Cardona. *Fundamentals of Semiconductors (3rd ed.)*. Springer (New York), 2005.
- [43] L. Berger. *J. Appl. Phys.*, 49:2156, 1978.
- [44] L. Berger. *J. Appl. Phys.*, 50:2137, 1979.
- [45] L. Berger. *Phys. Rev. B*, 54:9353, 1996.
- [46] J.C. Slonczewski. *J. Magn. Magn. Mater.*, 159:L1, 1996.

- [47] H. Kubota, A. Fukushima, Y. Ootani, S. Yuasa, K. Ando, H. Maehara, K. Tsunekawa, D.D. Djayaprawira, N. Watanabe, and Y. Suzuki. *Jap. J. of Appl. Phys.*, 44:L1237, 2005.
- [48] J. Hayakawa, S. Ikeda, Y.M. Lee, R. Sasaki, T. Meguro, F. Matsukura, H. Takahashi, and H. Ohno. *Jap. J. of Appl. Phys.*, 44:L1267, 2005.
- [49] J.A. Katine and E.E. Fullerton. *J. Magn. Magn. Mater.*, 320:1217, 2008.
- [50] M.D. Stiles and J. Miltat. *Top. Appl. Phys.*, 101:225, 2006.
- [51] P.M. Haney, R.A. Duine, A.S. Nunez, and A.H. MacDonald. *J. Magn. Magn. Mater.*, 320:1300, 2008.
- [52] G. Tatara, H. Ohno, and J. Shibata. *Phys. Rep.*, 468:213, 2008.
- [53] M.D. Stiles and A. Zangwill. *Phys. Rev. B*, 66:14407, 2002.
- [54] A. Shapiro, P.M. Levy, and S. Zhang. *Phys. Rev. B*, 66:104430, 2003.
- [55] J. Xiao, A. Zangwill, and M.D. Stiles. *Phys. Rev. B*, 70:172405, 2004.
- [56] A. Brataas, G.E.W. Bauer, and P.J. Kelly. *Phys. Rep.*, 427:157, 2006.
- [57] A.S. Nunez and A.H. MacDonald. *Solid State Comm.*, 139:31, 2006.
- [58] S. Zhang and Z. Li. *Phys. Rev. Lett.*, 93:127204, 2004.
- [59] J. Xiao, A. Zangwill, and M.D. Stiles. *Phys. Rev. B*, 73:054428, 2006.

- [60] M. Yamanouchi, D. Chiba, F. Matsukura, and H. Ohno. *Phys. Rev. Lett.*, 96:113706, 2006.
- [61] See for instance J. Kunes and V. Kambersky. *Phys. Rev. B*, 65:212411, 2002.
- [62] J. Fernandez-Rossier, M. Braun, A.S. Nunez, and A.H. MacDonald. *Phys. Rev. B*, 69:174412, 2004.
- [63] G. Tatara and P. Entel. *Phys. Rev. B*, 78:064429, 2008.
- [64] K. Obata and G. Tatara. *Phys. Rev. B*, 77:214429, 2008.
- [65] S.E. Barnes and S. Maekawa. *Phys. Rev. Lett.*, 95:107204, 2005.
- [66] K.M.D. Hals, A.K. Nguyen, and A. Brataas. *arXiv*, 0811.2235, 2008.
- [67] K. Gilmore, Y.U. Idzerda, and M.D. Stiles. *J. Appl. Phys.*, 103:07D303, 2008.
- [68] A. Manchon and Zhang S. *Phys. Rev. B*, 78:212405, 2008.
- [69] A. Manchon and S. Zhang. *Phys. Rev. B*, 79:094422, 2009.
- [70] A. Chernyshov, M. Overby, X. Liu, J.K. Furdyna, and L.P. Rokhinson. *arXiv*, 0812.3160, 2009.
- [71] I. Garate and A.H. MacDonald. *APS March Meeting*, Pittsburgh, 2009.
- [72] A.S. Nunez, R.A. Duine, P.M. Haney, and A.H. MacDonald. *Phys. Rev. B*, 73:214426, 2006.

- [73] Z. Wei, A. Sharma, A.S. Nunez, P.M. Haney, R.A. Duine, J. Bass, A.H. MacDonald, and M. Tsoi. *Phys. Rev. Lett.*, 98:116603, 2007.
- [74] M.I. Dyakonov and V.I. Perel. *Phys. Lett.*, 35A:459, 1971.
- [75] E.L. Ivchenko and G.E. Pikus. *JETP Lett.*, 27:604, 1978.
- [76] E.L. Ivchenko, G.E. Pikus, I.I. Farbstein, V.A. Shalygin, and A.V. Sturbin. *JETP Lett.*, 29:441, 1979.
- [77] A.G. Aronov and Y.B. Lyanda-Geller. *JETP Lett.*, 50:431, 1989.
- [78] V. Edelstein. *Solid State Comm.*, 73:233, 1990.
- [79] A.G. Aronov, Y.B. Lyanda-Geller, and G.E. Pikus. *Sov. Phys. JETP*, 73:537, 1991.
- [80] E.L. Ivchenko and S. Ganichev. *Spin Physics in Semiconductors (ed. M.I. Dyakhonov)*. Springer, New York, 2008.
- [81] M. Ranvah, Y. Melikhov, D.C. Jiles, J.E. Snyder, A.J. Moses, P.I. Williams, and S.H. Song. *J. Appl. Phys.*, 103:07E506, 2008.
- [82] D. Chiba, M. Sawicki, Y. Nishitani, Y. Nakatani, F. Matsukura, and H. Ohno. *Nature*, 455:515, 2009.
- [83] T. Maruyama, Y. Shiota, T. Nozaki, K. Ohta, N. Toda, M. Mizuguchi, A.A. Tulakurpar, and Y. Suzuki. *Nature Nanotechnology*, 4:158, 2009.

- [84] M. Weiler, A. Brandlmaier, S. Gepreags, M. Althammer, M. Opel, G. Bihler, H. Huebl, M.S. Brandt, R. Gross, and S.T.B. Goennenwein. *New J. Phys.*, 11:013021, 2009.
- [85] B. Botters, F. Giesen, J. Podbielski, P. Bach, G. Schmidt, L.W. Molenkamp, and D. Grundler. *Appl. Phys. Lett.*, 89:242505, 2006.
- [86] A. Lemaitre, A. Miard, L. Travers, O. Mauguin, L. Largeau, C. Gourdon, and V. Jeudy. *Appl. Phys. Lett.*, 93:021123, 2009.
- [87] P. Gambardella, S. Stepanow, A. Dmitriev, J. Honolka, F.M.F. de Groot, M. Lingenfelder, S.S. Gupta, D.D. Sarma, P. Bencok, S. Stanescu, S. Clair, S. Pons, N. Lin, A.P. Steitsonen, H. Brune, J.V. Barth, and K. Kern. *Nat. Materials*, 8:189, 2009.
- [88] A.Y. Silov, P.A. Blajnov, J.H. Wolter, R. Hey, K.H. Ploog, and N.S. Averkiev. *Appl. Phys. Lett.*, 85:5929, 2004.
- [89] Y. Kato, R.C. Myers, A.C. Gossard, and D.D. Awschalom. *Phys. Rev. Lett.*, 93:176601, 2004.
- [90] V. Shi, R.C. Myers, Y.K. Kato, W.H. Lau, A.C. Gossard, and D.D. Awschalom. *Nat. Phys.*, 1:31, 2005.
- [91] C.L. Yang, H.T. He, L. Ding, L.J. Cui, Y.P. Zeng, J.N. Wang, and W.K. Ge. *Phys. Rev. Lett.*, 96:186605, 2006.

- [92] S.D. Ganichev, S.N. Danilov, P. Schneider, V.V. Belkov, L.E. Golub, W. Wegscheider, D. Weiss, and W. Prettl. *J. Magn. Magn. Mater.*, 300:127, 2006.
- [93] A.A. Burkov, A.S. Nunez, and A.H. MacDonald. *Phys. Rev. B*, 70:155308, 2004.
- [94] O. Bleibaum. *Phys. Rev. B*, 73:035322, 2006.
- [95] M. Trushin and J. Schliemann. *Phys. Rev. B*, 75:155323, 2007.
- [96] H.A. Engel, E.I. Rashba, and B.I. Halperin. *Phys. Rev. Lett.*, 98:036602, 2007.
- [97] J. Stohr. *Magnetism*. Springer (Berlin), 2006.
- [98] S.W. Cheong and M. Mostovoy. *Nat. Materials*, 6:13, 2007.
- [99] R. Ramesh and N.A. Spalding. *Nat. Materials*, 6:21, 2007.
- [100] C. Ederer and N.A. Spalding. *Phys. Rev. B*, 71:060401, 2005.
- [101] T. Zhao, A. Choll, F. Zavaliche, K. Lee, M. Barry, A. Doran, M.P. Cruz, Y.H. Chu, C. Ederer, N.A. Spaldin, R.R. Das, D.M. Kim, S.H. Baek, C.B. Eom, and R. Ramesh. *Nat. Materials*, 5:823, 2006.
- [102] C.X. Liu, B. Zhou, S.Q. Shen, and B.F. Zhu. *Phys. Rev. B*, 77:125345, 2008.

- [103] S.V. Vonsovskii (ed.). *Ferromagnetic Resonance*. Pergamon Press (Oxford), 1966.
- [104] P. Bruno. *Physical Origins and Theoretical Models of Magnetic Anisotropy*. Frerienkurse des Forschungszentrums Julich (Julich), 1993.
- [105] M.T. Johnson, P.J.H. Bloemen, F.J.A. den Broeder, and J.J. de Vries. *Rep. Prog. Phys.*, 59:1409, 1996.
- [106] J. Stohr. *J. Magn. Magn. Mater.*, 200:470, 1999.
- [107] A.I. Liechtenstein, M.I. Katsnelson, and V.A. Gubanov. *J. Phys. F*, 14:L125, 1984.
- [108] M. Weinert, R.E. Watson, and J.W. Davenport. *Phys. Rev. B*, 32:2115, 1985.
- [109] G.H.O. Daalderop, P.J. Kelly, and M.F.H. Schuurmans. *Phys. Rev. B*, 41:11919, 1990.
- [110] M. Springford (ed.). *Electrons at the Fermi Surface*. Cambridge University Press (Cambridge), 1980.
- [111] J. Wunderlich, T. Jungwirth, B. Kaestner, A.C. Irvine, K.Y. Wang, N. Stone, U. Rana, A.D. Gidings, A.B. Shick, C.T. Foxon, R.P. Campion, D.A. Williams, and B.L. Gallagher. *Phys. Rev. Lett.*, 97:077201, 2006.
- [112] X. Wang, R. Wu, D.S. Wang, and A.J. Freeman. *Phys. Rev. B*, 54:61, 1996.

- [113] N. Nagaosa, J. Sinova, S. Onoda, A.H. MacDonald, and N.P. Ong. *arXiv*, 0904.4154, 2009.
- [114] I. Stolichnov, S.W.E. Riester, H.J. Trodahl, N. Setter, A.W. Rushforth, K.W. Edmonds, R.P. Campion, C.T. Foxon, and B.L. Gallagher. *Mat. Materials*, 7:464, 2008.
- [115] Ohno H and T. Dietl. *J. Magn. Magn. Mater.*, 320:1293, 2008.
- [116] M. Abolfath, T. Jungwirth, J. Brum, and A.H. MacDonald. *Phys. Rev. B*, 63:054418, 2001.
- [117] T. Dietl, H. Ohno, and F. Matsukura. *Phys. Rev. B*, 63:195205, 2001.
- [118] J. Zemen, J. Kucera, K. Olejnik, and T. Jungwirth. *arXiv*, 0904.0993, 2009.
- [119] M. Silver, W. Batty, A. Ghiti, and E.P. O'Reilly. *Phys. Rev. B*, 46:6781, 1992.
- [120] R. Winkler. *Spin-Orbit Coupling Effects in Two-Dimensional Electron and Hole Systems*. Springer (Berlin), 2003.
- [121] J. Stohr, H.C. Siegmann, A. Kashuba, and S.J. Gamble. *Appl. Phys. Lett.*, 94:072504, 2009.
- [122] O. Krupin, G. Bihlmayer, K. Starke, S. Gorovikov, J.E. Prieto, K. Do-
brich, S. Blugel, and G. Kaindl. *Phys. Rev. B*, 71:201403(R), 2005.

- [123] A. Larkin and A. Varlamov. *Theory of Fluctuations in Superconductors*. Clarendon Press (Oxford), 2005.
- [124] N. Kopnin. *Theory of Nonequilibrium Superconductivity*. Oxford University Press (Oxford), 2001.
- [125] P.W. Anderson. *Phys. Rev.*, 112:1900, 1958.
- [126] L.P. Gorkov. *Soviet Phys. JETP*, 7:505, 1958.
- [127] Y. Nambu. *Phys. Rev.*, 117:648, 1960.
- [128] K. Moon, H. Mori, K. Yang, S.M. Girvin, A.H. MacDonald, L. Zheng, D. Yoshioka, and S.C. Zhang. *Phys. Rev. B*, 51:5138, 1995.
- [129] K.Y. Arutyunov, D.S. Golubev, and A.D. Zaikin. *Phys. Rep.*, 464:1, 2008.
- [130] A. Auerbach. *Interacting Electrons and Quantum Magnetism*. Springer-Verlag (New York), 1994.
- [131] A.L Fetter and J.D. Walecka. *Quantum Theory of Many-Particle Systems (reprint)*. Dover Publications (New York), 2003.
- [132] I.O. Kulik, O. Entil-Wohlman, and R. Orbach. *J. Low Temp. Phys.*, 43:591, 1981.
- [133] N. Nagaosa. *Quantum Field Theory in Condensed Matter Physics*. Springer-Verlag (Berlin), 1999.

- [134] J.W. Negele and H. Orland. *Quantum Many-Particle Systems*. Perseus Books (Reading, Massachusetts), 2003.
- [135] R. Tidecks. *Nonequilibrium Phenomena in Quasi-One-Dimensional Superconductors*. Springer (Berlin), 1990.
- [136] A.H. MacDonald, A.A Burkov, Y.N. Joglekar, and E. Rossi. *ICPS 2002 Conference Proceedings*, 171:29, 2002.
- [137] K.K. Likharev. *Dynamics of Josephson Junctions and Circuits*. Gordon and Breach Science Publishers (Amsterdam), 1986.
- [138] J. Clarke and S.M. Freake. *Phys. Rev. Lett.*, 29:588, 1972.
- [139] E. Abrahams and T. Tsuneto. *Phys. Rev.*, 152:416, 1966.
- [140] I.J.R. Aitchison, G. Metikas, and D.J. Lee. *Phys. Rev. B*, 62:6638, 2000.
- [141] S.G. Sharapov, H. Beck, and V.M. Loktev. *Phys. Rev. B*, 64:134519, 2001.
- [142] A. Del Maestro, B. Rosenow, and S. Sachdev. *Annals of Physics*, 324:523, 2009.
- [143] R.D. Parks (ed.). *Superconductivity (vols. 1 and 2)*. Marcel Dekker Inc. (New York), 1969.
- [144] G. Schon. *Festkorperprobleme*, 21:341, 1981.

- [145] S.N. Artemenko and A.F. Volkov. *Sov. Phys. JETP*, 43:548, 1976.
- [146] O. Buisson, P. Xavier, and J. Richard. *Phys. Rev. Lett.*, 73:3153, 1994.
- [147] J.E. Mooij and G. Schon. *Phys. Rev. Lett.*, 55:114, 1985.
- [148] B. Camarota, F. Parage, F. Balestro, P. Delsing, and O. Buisson. *Phys. Rev. Lett.*, 86:480, 2001.
- [149] K. Goto, H. Katsura, and N. Nagaosa. *arXiv*, 0807.2901, 2008.
- [150] M. Marder. *Condensed Matter Physics (corrected printing)*. John Wiley and Sons (New York), 2000.
- [151] P.M. Haney and M.D. Stiles. *arXiv*, 0906.2423, 2009.

Vita

Ion Garate Aranberri was born in Elgoibar, Basque Country on 12 May 1980, the son of Ignacio Garate and Maritxu Aranberri. He received the Bachelor of Science degree in Physics from the University of the Basque Country in June 2003. During the 2002-2003 academic year he was a TASSEP exchange student at the University of Texas at Austin. He entered the Graduate School of the University of Texas at Austin in August of 2003.

Permanent address: 1906 Pearl Street
Austin, Texas 78705

This dissertation was typeset with L^AT_EX[†] by the author.

[†]L^AT_EX is a document preparation system developed by Leslie Lamport as a special version of Donald Knuth's T_EX Program.